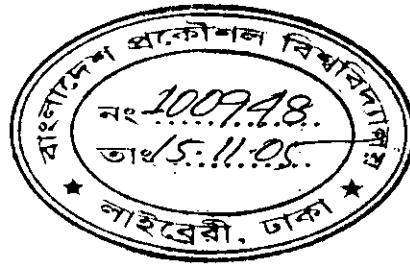# Deposition and Characterization of Carbon Thin Films by Electroplating

A thesis submitted to
the department of Electrical and Electronic Engineering
of
Bangladesh University of Engineering and Technology
in partial fulfillment of the requirement
for the degree of
MASTER OF SCIENCE IN ELECTRICAL AND ELECTRONIC ENGINEERING

by

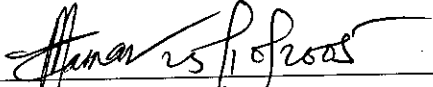## Muhammad Athar Uddin

#100948#

DEPARTMENT OF ELECTRICAL AND ELECTRONIC ENGINEERING
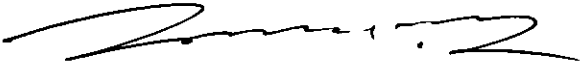
BANGLADESH UNIVERSITY OF ENGINEERING AND TECHNOLOGY

2005

i

The thesis entitled **"Deposition and Characterization of Carbon Thin Films by Electroplating"** submitted by Muhammad Athar Uddin, Roll no.: 100006203P, Session: October 2000 has been accepted as satisfactory in partial fulfillment of the requirement for the degree of MASTER OF SCIENCE IN ELECTRICAL AND ELECTRONIC ENGINEERING on October 25, 2005.
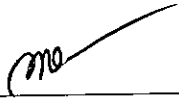
BOARD OF EXAMINERS

1. _____

   Dr. Sharif Mohammad Mominuzzaman
   Associate Professor
   Department of Electrical and Electronic Engineering
   BUET, Dhaka-1000, Bangladesh

   Chairman
   (Supervisor)

2. _____

   Dr. S. Shahnawaz Ahmed
   Professor and Head
   Department of Electrical and Electronic Engineering
   BUET, Dhaka-1000, Bangladesh

   Member
   (Ex-Officio)

3. _____

   Dr. Mohammad Jahangir Alam
   Associate Professor
   Department of Electrical and Electronic Engineering
   BUET, Dhaka-1000, Bangladesh

   Member

4. _____

   Dr. Md. Abu Hashan Bhuiyan
   Professor
   Department of Physics
   BUET, Dhaka-1000, Bangladesh

   Member
   (Exterual)

Declaration

It is hereby declared that this thesis or any part of it has not been submitted elsewhere for the award of any degree or diploma.

Signature of the candidate

Muhammad Athar Uddin
25/10/05
_____
(Muhammad Athar Uddin)

Dedication

To My Parents

Contents

List of Figures

List of Tables

Acknowledgements

I wish to offer my heartiest gratitude and profound respect to my thesis supervisor Dr. Sharif Mohammad Mominuzzaman, Associate Professor, Department of Electrical and Electronic Engineering (EEE), Bangladesh University of Engineering and Technology (BUET), Bangladesh, for giving me the opportunity to work with him and for his continuous guidance, suggestions and wholehearted supervision throughout the progress of this work. I am indebted to him for acquainting me with the world of advanced research.

I am grateful to the Head of the Department of EEE, BUET, who provided all the research facilities of the Department accessible all the time and encouraged me completing the work.

I am also grateful to Dr. Mohammad Ali Choudhury, Professor, Department of EEE for his encouraging advice to complete the thesis.

I thank Dr. M. M. Shahidul Hassan, Professor Department of EEE for his proper guidance and instruction to complete my M.S.

I thank Dr. Md. Wahab Khan, Professor, Department of Chemistry, for his helpful advice to take FTIR spectroscopy of samples in the Department of Chemistry. I thank Mr. M. Nurul Islam, Assistant Professor Department of Chemistry for his helpful advice to measure the P^H of electrolytes in the Department of Chemistry. I thank Dr. Nazrul Islam, Professor and Head, Department of Chemistry for giving me available facilities of his Department necessary for my thesis.

I thank Dr. A. S. M. A. Haseeb and Dr. Qumrul Ahsan, Professors, Department of Materials and Metallurgical Engineering for their helpful advice to take SEM micrograph of samples in the Department of Materials and Metallurgical Engineering. I thank the technical persons involved in SEM analysis and optical

Abstract

Carbon thin films were deposited on Aluminum (Al), Copper (Cu) and Silicon (Si) substrates by electrolysis of methanol. The effect of camphor ($C_{10} H_{16}O$) — a natural source, incorporation with methanol is investigated. Camphor with varying amount (1%, 2%, 3%, 4%, 5%, 6% 7% and 8%) was mixed in methanol solvent to prepare the electrolytes. Aluminum, copper and silicon substrates were mounted on the negative electrode. Remarkable change in the variation of current density as a function of applied potential was observed with camphor content. Thin films were deposited on Al, Cu and Si substrates for different percentage of camphor and were compared. Current density was observed to vary with substrate. For Al and Cu substrates current density was highest for the 2% camphor in methanol solution whereas for Si substrate current density was highest for the 6% camphor in methanol solution. The maximum current density with camphor content was different for Al, Cu and Si substrates. P^H of various solutions before and after deposition has been analyzed. Camphor has an influence on P^H. The films were characterized by Optical Microscopy, Scanning Electron Microscopy (SEM), Electron Dispersion Spectroscopy (EDS), Fourier transform of infrared (FTIR) spectroscopy, Transmittance/reflectance Spectroscopy (UV-VIS-NIR region). From optical microscopy and SEM micrograph we got sharp differences between pure and deposited substrates. Changes in the pictures are found with camphor incorporation in methanol solution, and there are certain indications of formation of films on different substrates. EDS analysis shows that carbon films are deposited on the above three types of substrate. But percentage of carbon content in the film is maximum for Si than Al and Cu substrate; therefore Si shows higher affinity to carbon than the other two. From the FTIR spectroscopy we got sp^2 and sp^3 C-H stretch and existence of amorphous carbon bonding for Si. But Al and Cu do not show such type of properties. In case of Si substrate the ratio of sp^3/sp^2 is maximum (0.66) for 6% camphor in methanol and is less for any other range of camphor percentage (0.45 for 0% camphor in methanol and 0.56 for 8% camphor in methanol). From the measurement of transmittance/reflectance of two electro deposited thin film of Si (one for 0% camphor and another for 6% camphor) by UV-VIS-NIR it was found that, the two films have different optical properties. It was found that the optical band gap for the electrodeposited film of 0% camphor is 1.1 eV but that for 6% camphor is 1.2 eV.

Chapter 1
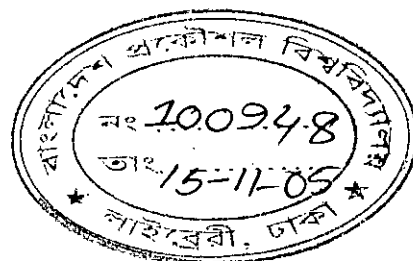
Introduction

Silicon (Si) and some compound semiconductor based materials are prevalent in the field of semiconductor industry for many years. In search of alternative low cost materials, carbon has attracted attention of the researchers and engineers for its applications in electronic device fabrication and solar cells because of its wide range of structural, mechanical, optical and electrical properties. Carbon is available in the nature in wide varieties of forms, from graphite to diamond, whose behaviors are wide apart from each other. Besides these, carbon is found in the nature in numerous amorphous forms. These amorphous forms of carbon have now received a great interest of the device researchers. These forms of carbon show outstanding electrical, physical and optical properties and all these properties can be varied over a wide range by changing the optical gap of the material. So, scientists are now trying to use these forms of carbon for device fabrication purposes. Properties of carbon films depend on the growth condition, deposition method, electrolytes used, substrate materials etc. And here this is our main objective to study. Chapter one covers the background along with the objectives of the work. The organization of the thesis is also presented at the end of this chapter.

1.1 Background

There have recently been two important advances in the science of crystalline carbon, the discovery that diamond can be readily grown by vapour deposition and the discovery of a third allotrope of carbon, a molecular crystal of the fullerene molecule, 'buckyball' C_{60} [1]. There has been a parallel advance in effort in disordered carbons. The range of disordered carbons is wide covering soots, chars, carbon fibres, glassy carbon and evaporated amorphous carbon. These carbons are basically sp^2 bonded. A range of new preparation methods has produced forms of amorphous carbon (a-C) and hydrogenated amorphous carbon (a-C: H), which is mechanically hard, infrared transparent and chemically inert. They are finding immediate applications as hard coating materials for magnetic disc drives or as antireflective coatings for infrared windows. Their beneficial properties arise from the sp^3 component of their bonding and these carbons are frequently called diamond like carbon (DLC). In general, such carbons can be fully amorphous or contain crystalline inclusions. This field of non-crystalline carbons is of interest both technologically to materials scientists' and also at a more fundamental level to solid-state chemists and physicists.

Precursors and method of deposition of carbon films are the two dominating factors that dictate the optical and electrical properties of the film. And hence these two factors are strongly considered in order to obtain desired carbon thin film having certain optical and electrical properties required for application in various opto-electronic devices. Therefore, researches on finding alternative precursor materials and simple method of deposition have been getting priority all the time. In connection with this research, camphor ($C_{10}H_{16}O$) has been found as an alternative precursor material because it has some advantages over graphite [2].

Graphite is purely sp^3 hybridized whereas camphor consists of both sp^2 and sp^3 hybridized carbon in its structure. Hydrogen in a-C films modifies the properties of the films and introduces many sp^3 sites. Hydrogen passivates the dangling bond in the gap states and also tailors the optoelectronic properties of the film. So while

using graphite as the precursor, additional hydrogen gas / ions have to be supplied but camphor has hydrogen abundantly in its structure. Furthermore, the presence of sp^3-hybridized bonds in camphor molecule plays a beneficial role in the deposition of carbon films especially for diamond like carbon (DLC) films.

1.2 Objectives of the Work

Interest in depositing of Carbon Thin Film has been motivated by properties of this material and the demand of modern technologies, especially those associated with development in the electronic industry. These properties include extreme hardness, chemical inertness, high electrical resistively, high dielectric strength, optical transparency and high thermal conductivity has made these films extremely useful in a variety of applications. Deposition techniques that may provide advantages in these applications are of considerable interest.

Many studies have been reported on the preparation of carbon thin films. These include chemical vapour [3, 4] deposition, microwave plasma decomposition [5] of hydrocarbon gas, physical vapour deposition i.e. ion-beam [6], pulsed laser [2, 7] etc. All the above methods are vapour deposition techniques. Using these techniques, high quality films and rapid growth rates have been achieved. However, a deposition of DLC films in the liquid phase is seldom reported.

There is experimental evidence that most materials that can be deposited from the vapor phase can also be deposited in the liquid phase using electroplating techniques and vice versa [8]. Enlightened by this conclusion, Namba [9] first attempted to grow diamond phase carbon films in the liquid phase with the aid of an organic solution such as ethanol at a temperature less than 70^0C. In his article, however, only X ray photoemission spectroscopy (XPS) results had been shown for the existence of carbon films, or DLC films had been obtained but the choice of a suitable solution was limited. Among the electrolytes ethanol gave an interesting result. Suzuki *et al.* [10] recently made an attempt to deposit carbon films by electrolysis of a water-ethylene glycol solution. Graphite carbon had been obtained according to their result.

Nevertheless, ethylene glycol is a viscous solution, which will cause some difficulty in cleaning the substrate after deposition. Since DLC films synthesized in the liquid phase have significant scientific and technological implications, it is worth pursuing research with electrodes. Then Hao Wang et al. [11] deposited film by using methanol solution. Methanol is selected because its polarizability and conductivity are stronger than those of ethanol and the structure of methanol is even closer to that of diamond.

Recent study shows that Mominuzaman et al. succeeded to deposit carbon thin film by simple ion beam sputtering (IBS) [6] and pulsed laser ablation [12, 13] of camphoric carbon, obtained from camphor, a natural source. Based on the observations of camphor carbon films they suggested that camphor and camphor like other precursors might be best-suited candidates as starting materials for semiconducting carbon films for electronics applications.

In the present article, a film deposition is attempted by the techniques of electrolysis. Methanol (CH_3OH), 1% camphoric solution in methanol, 2% camphoric solution in methanol, 3% camphoric solution in methanol, 4% camphoric solution in methanol, 5% camphoric solution in methanol, 6% camphoric solution in methanol, 7% camphoric solution in methanol 8% camphoric solution in methanol are used as electrolytes. Aluminum (Al), copper (Cu) and silicon (Si) are used as substrates.

Our objectives are to observe the role of substrates on thin film deposition, control the current density by camphor incorporation in methanol solution, study the character of deposited films and role of camphor on film character and try to vary the optical band gap of electrodeposited thin films by changing the sp^3/sp^2 ratio through camphor incorporation in methanol solution.

1.3 Thesis Layout

Organization of the thesis includes four chapters

Chapter one gives background and objective of the work.

Chapter two deals with the review of the carbon materials, various forms of carbon, present status of carbon research, the review of the thin film, history of thin film technology, thin film application. This chapter will also provide different type of deposition methods (such as ion beam methods, sputtering, plasma deposition, electroplating).

Chapter three deals with the experimental details of carbon thin films, results and discussions on the deposition process, properties of the methanol as electrolytes, role of camphor in methanol solution as starting materials for semiconducting carbon films, some characteristics of carbon thin films by electrolysis of organic solutions. The experimental data obtained from our experiment has been analyzed. P^H of various solutions before and after deposition has been analyzed. The morphology of the films deposited in various solutions was observed by optical microscopy, SEM micrograph, EDS analysis, FTIR spectroscopy and measurement of transmittance/reflectance using UV-VIS-NIR technique.

Conclusive discussions and remarks are in chapter four. Some suggestions leading to future scope of work are also presented here.

Chapter 2

Review of carbon research and introduction to camphoric carbon films

2.1 Carbon Material

Carbon occurs widely in its elemental form as crystalline and amorphous solids. Diamond and graphite are the two crystalline allotropes of carbon. The diamond crystal structure is face centered cubic with inter atomic distances of 0.15mm. Each atom is covalently bonded to four other carbon atoms (sp^3 tetragonal bonds). The structure of graphite is described as layers of carbon atoms with strong trigonal bonds (sp^2) with inter-atomic distance of 0.1415nm in the basal plane. The fourth electron in the outer shell forms a weak bond of the Vander Walls type between planes and accounts for such properties of graphite as good electrical conductivity, lubricity, lower density, a grayish black appearance and softness, which are in contrast to the properties of diamond.

Under ambient conditions, the graphite phase with strong in plane trigonal bonding is a stable state. Under high pressure and temperature graphite can be converted into diamond and when exposed to irradiation or heat, diamond will quickly transform back to the more stable graphite phase. During the formation of thin film of diamond,

it is observed that under a very special condition diamond structure is formed, otherwise graphite structure dominates.

Interest in depositing thin films of carbon (especially diamond like carbon) has been motivated by the unique properties of this material and the demand of modern technologies, especially those associated with the developments in the electronics industry. These properties include extreme hardness, chemical inertness, high electrical resistivity, high dielectric strength, optical transparency and thermal conductivity. These are various techniques used to obtain high quality diamond like carbon (DLC) thin films. In this chapter, various forms of carbon are described and also present status of amorphous and diamond like carbon researches are reviewed.

2.2 Various Form of Carbon

Carbon has atomic number of 6 and is classified in-group IV of the second period of the periodic table and $1s^2 2s^2 2p_x^1 2p_y^1$ electronic ground state configuration. The four electrons in outer orbital may arrange themselves in different combinations of sub orbital (s, P_x, P_z) of outer shell and hence form different hybridized bonding configurations (sp^1, sp^2, sp^3) as in figure 2.1 Graphite or diamond structure is dictated by the trigonal (sp^2) or tetrahedral (sp^3) configurations.

Other than graphite and diamond forms of carbon, there also exists in numerous forms which can be characterized as imperfect diamond structure, i.e. the layer are not orientated with respect to their common axis, the angular displacement of layers is random and the layers overlap one another irregularity.
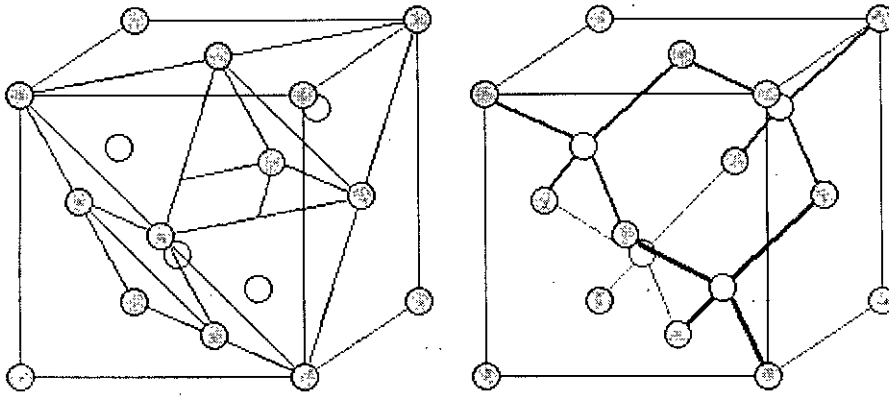
Figure 2.1: The ideal diamond structure

Some important forms of carbon (DLC), amorphous carbon (a-C) or hydrogenated amorphous carbon (a-C:H) have mixture of sp^2 and sp^3 bonded carbon of different fractions. Soon after the discovery of fooleries family in 1985 research on carbon and carbon related materials mainly a-C or a-C: H entered into a new era and scientists all over the world are working on this remarkable element, carbon, for its use in optoelectronic devices.

2.3 Presents Status of Carbon Research

Amorphous carbon refers to a carbon network that has both sp^2 and sp^3 bonding structures and almost no sp1 bond. Recently, many researchers have shown much interest in developing microelectronic devices from diamond like carbon (DLC) and a-C film. As carbon has many outstanding properties of DLC, a-C or a-C: H, it can be varied over an unusual wide range from semi-metallic graphite (0.0 eV) to that of insulating diamond (5.5 eV). These properties depend on growth conditions, methods of deposition and precursor materials. Various methods are employed to prepare a-C or a-C:H films such as pulsed laser deposition (PLD) ion beam deposition, sputtering, chemical vapor deposition (CVD), radio frequency (r. f.) / microwave plasma CVD etc. Table 2.1 summarizes some characteristic properties of a-C films prepared from various methods and using different precursor materials.

Table 2.1: Properties of various forms of carbon

	Density ($gmcm^{-3}$)	Hardness G pa	% sp^3	at % H	Gap (eV)	Ref.
Diamond	3.515	100	100		5.5	14
Graphite	2.267		0		-0.04	15
C_{60}			0	0	1.8	16
Glassy C	1.3-1.55	2-3	0		0.01	17
a-C, evap	1.9-2.0	2-5	1		0.4-0.7	18
a-C, MSIB	3.0	30-130	90-15	9	0.5-1.5	19
Pd a:H Hard	1.6-2.2	10-20	30-60	10-40	0.8-1.7	20
PD a-C:H, Soft	0.9-1.6	<5	50-80	40-65	1.6-4	20
Polyethylene	0.92	0.01	100	67	6	21

It is found from the study that the semiconducting carbon films can be either intrinsic or they can be doped during or after the growth to make them extrinsic semiconductors. Carbon based hetero structures such as metal insulator semiconductor (MIS) diodes, scottky diodes, metal insulator semiconductor field effect transistor, hetero junction diodes, thin film transistor (TFT) and solar cell on silicon have already been reported and thereby demonstrate the potentiality of carbon materials in electronic devices.

Method of deposition of carbon films and precursor are the two dominating factors that dictate the optical and electrical properties of the film. And hence these two factors are strongly considered in order to obtain desired carbon thin film having certain optical and electrical properties required for application in various optoelectronic devices. Therefore, researches on finding alternative precursor materials and simple method of deposition have been getting priority all the time. In connection with this research, camphor ($C_{10}H_{16}O$) has been found as an alternative precursor material because it has some advantages over graphite.

Graphite is purely sp^3 hybridized whereas camphor consists of both sp^2 and sp^3 hybridized carbon in its structure. Hydrogen in a-C films modifies the properties of the films and introduces many sp^3 sites. Hydrogen passivates the dangling bond in the gap states and also tailors the optoelectronic properties of the film. So while using graphite as the precursor, additional hydrogen gas/ions have to be supplied but camphor has hydrogen abundantly in its structure. Furthermore, the presence of sp^3-hybridized bonds in camphor molecule plays a beneficial role in the deposition of carbon films especially for diamond like carbon (DLC) films.

Recent study shows that Mominuzaman et al. [6] succeeded to deposit carbon thin film by simple ion beam sputtering (IBS) of camphoric carbon, obtained from camphor, a natural source. They also studied various opto-electrical properties and the effects of annealing on these properties, in light of the semi conducting nature of these films, through the electrical conduction mechanism. They reported the optoelectronic characteristics of carbon thin films deposited by ion beam sputtering of a camphoric carbon target without any H$_2$ gas precursor observed to be similar to those of hydrogenated a-C films. The optical absorption coefficient of a deposited film is in the order of 10^4-10^5 cm^{-1} and its optical gap is 0.5 eV.

The optical and electrical properties of these films remain almost stable while annealed up to 400^{0}C but suffer abrupt changes at annealing temperature greater than 400^{0}C. The room temperature conductivity of a deposited film is found in the order of 10^{-1} (ohm-cm)$^{-1}$ and upon annealing up to 800^{0}C, it shows a graphitic nature and the conductivity is increased and reached at the order of 10^1 (ohm-cm)$^{-1}$.

Inspired with the previous results, Mominuzzaman et al. [2] proceeded to use camphor as precursor material in the deposition methods other than IBS and succeeded. They were the first to use camphor as precursor in pulsed laser deposition (PLD) method. Along with the preparation of un-doped camphoric carbon (CC) film, they also succeeded in preparing phosphorus (P) incorporated CC films. Various opto-electrical properties of these films and the variation of these properties due to phosphorus incorporation were also studied [22]. It was reported that the optical gap

of un-doped CC film is about 0.85 eV and remains relatively unchanged for the films deposited using targets containing up to 5% P. However, for the films deposited from the target containing 7% P, the gap decreases to 0.75 eV. This decline in optical gap indicates an increase in the sp^2 fraction due to graphitization of the CC film, which is induced by high percentage of phosphorus content. The resistivity of the un-doped CC films are approximately $2x-10^4$ ohm-cm and increased to $3.7x10^4$ ohm-cm for the film deposited from the target containing 1% P. But for the films deposited from the target containing higher percentage of P, the resistivity decreases sharply at first and gradually thereafter.

Based on these observations of camphor carbon films they suggested that camphor and camphor like other precursors might be best-suited candidates as starting materials for semiconducting carbon films for electronics applications.

2.4 Basic Knowledge of Thin Film

A thin film is a liquid or solid such that one of its linear dimensions is very small in comparison with the other two dimensions. Usually one classifies thin films (arbitrarily) into:

- Thick films (D>1 micrometer, D: film thickness)
- Thin films (D<1 micrometer);

This thesis work discusses mainly the systems of a (solid) film on a (solid) substrate (backed films) rather than unsupported films (foils). They (solid substrate) imply a production process in the form of film growth by sustaining an atomic or molecular flux to the surface of the substrate and subsequently by growing of the film. Film growths will either involve chemical reaction of a gas or liquid with substrate surface; or physical processes such as evaporation from a source and sputtering from a target, then condensation onto the substrate.

2.5 The History of Thin Film Technology

- In 1650 A. D. interference colors of thin liquid film on a liquid surface (oil on water) were observed by R. Boyle, R. Hooke, and I Newton.
- In 1850 A. D. electro-deposition (by M. Faraday) chemical reduction deposition, film formation during glow discharge (by W. Grove) and evaporation of metallic wires by current were discovered.

Solid films produced by the first two methods received early recognition for their technical importance as anticorrosive films or films for mirrors, whereas those prepared by the later methods lacked reproducibility for a long time. Only since the improvements of vacuum equipment for film preparation as well as for investigation (electron microscopy, LEED, other surface analytical techniques) reproducible and useful films were readily obtained. Since 1950 a vigorous development arose by production of films for optical, electronic, mechanical, and protective applications. In 1965 semiconductor electronics made use of thin film methods, which reveal two major merits mass fabrication by printing techniques and miniaturization by integration (integration density: elements / mm^2).

2.6 Main Fields of Application

- Computer electronics, commercial electronics, medical electronics, space technology, and energy conversation (solar cells).
- Optical applications of metal and dielectric films:
    * Filters
    * Reflection coatings
    * Optical wave-guide for optoelectronic communications of
  semiconducting films
- IR-sensors and thin film laser diodes
- Magnetic and super conducting films for memory and logical devices.

Basic scientific interest is focused on film formation processes in order to obtain an insight into the mechanisms leading to special structure properties: Island, labyrinth,

continuous films (macrostructure) amorphous, polycrystalline, single crystal films (microstructure) on film stability (the mobility of atoms in the films enable relaxation and hereto diffusion)

2.7 Thin Film Deposition Methods

2.7.1 Ion Beam Method

A wide variety of deposition methods have been used to prepare diamond like carbon. A common feature of each method is exposure of the growing film to bombardment by ions of medium energy, 20-500 V, which appears to promote sp^3 bonding [20, 23, 24]. The various methods and their growth rates are summarized in Table 2.2.

The first ion beam device of Aisenberg [25] generated carbon ions by sputtering carbon sectrodes in an Ar atmosphere in magnetically confined plasma. A bias voltage extracts the ions and directs them at the substrate. Higher growth rates were found to be possible if the ions are generated from a hydrocarbon source gas. The resulting films may have contained both a-C and diamond micro crystallites. Speneer *et al.* [26], and Vora and Moravec [27] confirmed the results, while Mori and Namba [16] investigated the dependence of film properties on deposition conditions. A very popular ion source is shown in figure 2.2 that due to Kayfmann [28]. In this source, electrons from a thermion cathode are used with an axial magnetic field to generate plasma. This gives high ionization rates in a source gas such as methane. Positive ions are extracted from the source by a bias electrode and are directed at a substrate. A further increase in deposition rate is achieved by using a cascade source. Highly ionized thermal plasma of methane and Ar is created in the pumping conditions and designs are such that the plasma expands supersonically into a high vacuum towards the substrate. This expansion causes a high degree of ionization of the plasma.
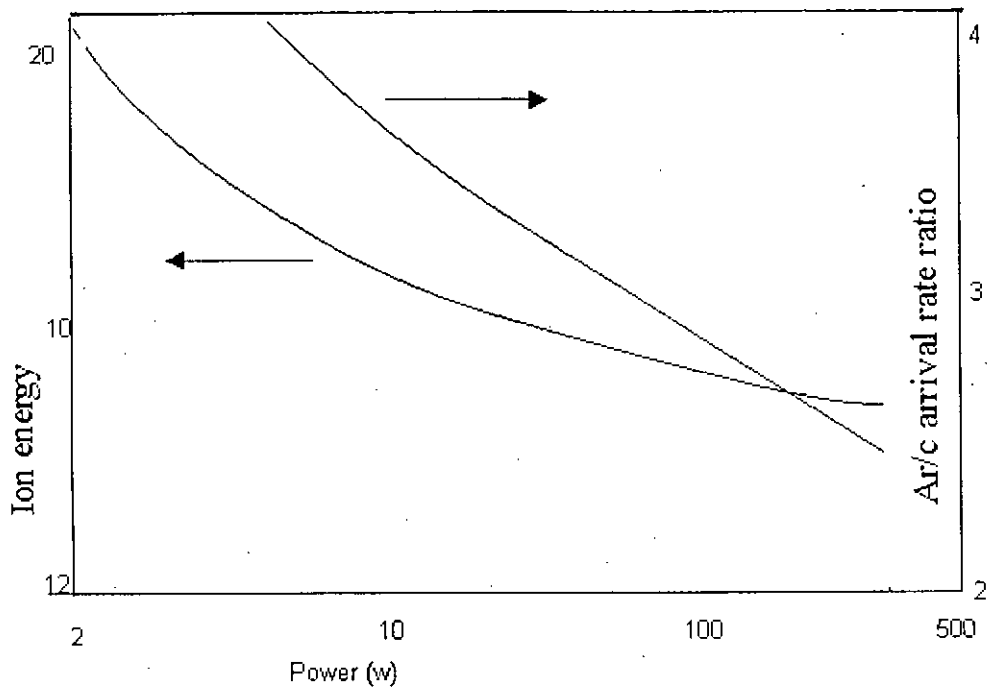
Figure 2.2 Variation of Ar+ and C atom arrival rates with sputtering power for
magnetron sputtering

Deposition of a single ion species is possible if the ion beam is passed through a
magnetic mass analyzer for c/m selection. The analyzer filters neutrals, clusters
species, graphitic fragments and impurities from the beam and allows only a pure
beam of C+ (or C-) ions to reach the substrate. Structural studies summarized later
indicating that the resulting material is fully amorphous with the highest fraction of
sp^3 bonding of those from any present deposition process. The deposition rates for
using the carbon can maximize this method are as an ion source (figure 2.2).
Typically rates are now 400A/min. They are confined magnetically for stability. The
main practical problem with this method is the high compressive stress in the films
the films, which limits their adhesion and thereby the maximum stable film
thickness.

Table 2.2: Methods for the deposition of Diamond like Carbon

	Precursor	Typical Growth Rate, A/sec.	Ref.
Ion beam	Graphite	1.3	25
Ion beam	Methane	2	28
PD	Methane	1	20
PD	Benzene	15	20
Ar beam sputtering	Graphite	3	29
Magnetron sputtering	Graphite	3	42
Ion plating	Benzene	10	33
Laser Plasma	Graphite	<3	43
Cascade are	Ar/methane	300	44
Mass selected ion beam	Graphite	0.1-6	45

2.7.2 Sputtering

Various sputtering methods can be used to produce hard carbons. In ion beam sputtering, a beam of typically 1 kV Ar ions is directed at a graphite target [29, 30]. An angle of incidence of $30\text{-}45^0$ is used to maximize the yield. The sputtered carbon is condensed onto a nearby substrate. A second Ar ion beam can be directed at the substrate to provide the ion bombardment of the growing film. A disadvantage of ion beam sputtering is its low deposition rates due to the low sputtering rate of graphite.

Higher deposition rates can be achieved by magnetron sputtering. Here Ar plasma is used to both sputter from the target and bombard the growing film, as shown in figure 2.2. Growth rates vary linearly with rf. power and are typically 3A/sec [16]. Ion energies are of order 20 eV and decline slowly with increasing power or gas

pressure. A mixture of Ar and carbon ions and atoms reaches the substrate. Savvides [31] noted that the ion/atom ratio in the beam increases with decreasing sputtering power because the ion yield decreases less quickly than the neutral atom flux as in figure 2.2.

This is the opposite dependence to that in plasma deposition where ion bombardment effectively increases with plasma power. A dc bias can be applied separately to the substrate if it is desired to raise the mean ion energy. The general advantage of sputtering methods is their good process control and their ability to be scaled up for manufacturing. A disadvantage is that the hardest films seem to be prepared under conditions of low power and low gas pressure, where deposition rates are lower.

2.7.3   Plasma Deposition

The most popular deposition method involves the rf. plasma decomposition of a hydrocarbon source gas onto negatively self-biased substrates. Plasma deposition (PD) or strictly plasma-assisted chemical vapour deposition (PACVD) Holland and Ojha [32], and it pioneered for a-C: H is also widely used to deposit a-ST. Self-biasing is preferred to dc biasing for a-C: H because the films are insulating. In this method, shown in figure 2.3, the rf. power is capacitively coupled to the substrate electrode and the counter electrode is either a second electrode or just the grounded walls of the deposition chamber.

This gives a large difference between the electrode sizes. If the rf. frequency is greater than the ion plasma frequency, of order 2-5 MHz, the electrons can follow the rf. voltage but the ions cannot. The large difference in electrode size and also in the electron and ion mobility produces a negative dc. Self-bias on the powered electrode makes it cathode. The ion current is now largely dc while the compensating electron current flows in short bursts each rf. cycle (figure 2.3).

The discharge now consists of a glow region, in which the ions are generated by collisions with electrons, and a space charge region or ion-sheath, across which the

ions are accelerated to reach the cathode. The equivalent electrical circuit for the plasma is a resistance for the plasma glow in series with a capacitance for the sheath. The dc bias is largely dropped across the sheath (figure 2.4).
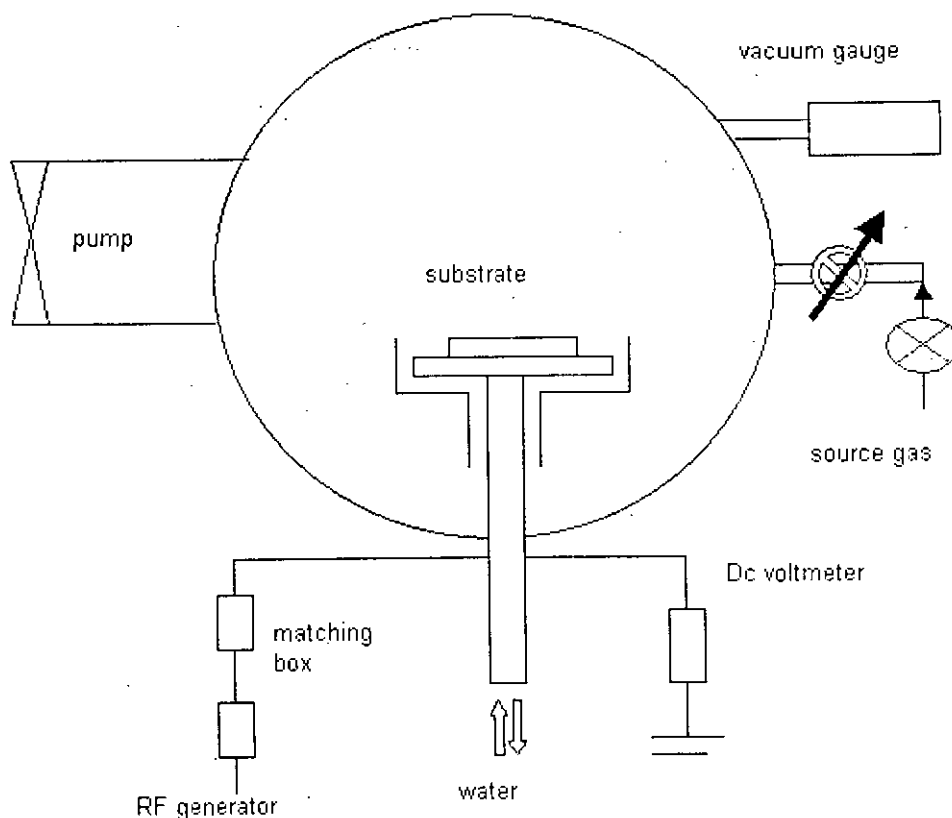
Figure 2.3: Schematic of capacitively coupled Rf plasma deposition apparatus with substrate attached to the powered electrode

The bias voltage, - V_b varies with rf. power W and operating pressure P as

$$V_b = k \ (W/P)^{\frac{1}{2}} \quad \text{.................................... [2.1]}$$

Where k depends on factors such as the electrode areas. Catherine and Couderc have shown that this is the dependence expected for ohmic plasma and a sheath thickness proportional to $P^{-1/2}$. The ion energy E_i depends on V and the ion mean free path in the sheath at low pressures in the absence of collisions.

$$E_1 = eV_b \ldots\ldots\ldots\ldots\ldots\ldots\ldots\ldots\ldots\ldots\ldots\ldots\ldots\ldots \text{[2.2]}$$

While at higher, typical operating pressures there is a spectrum of ion energies with a mean value of

$$E_1 = k/V_t/p^{1/2} \ldots\ldots\ldots\ldots\ldots\ldots\ldots\ldots\ldots\ldots\ldots\ldots \text{[2.3]}$$

Or about $E_1 = 0.6V_b$ for typical pressure of 3 Pa *Koidl et al.* [20] have measured ion energy spectrum for Ar discharges.
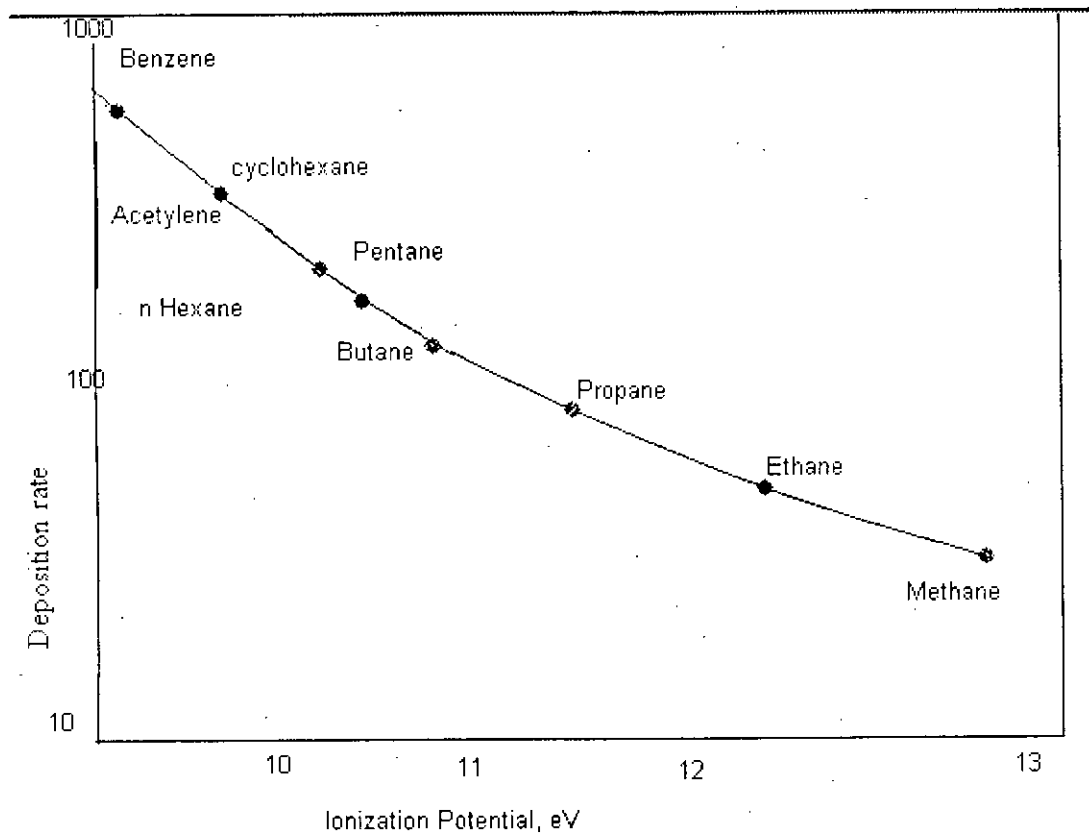
Figure 2.4: Plasma deposition rates versus ionization potential of precursor gas, for a gas pressure of 3 Pa and a self-bias voltage of 400v.

The deposition rate varies with the ionization potential and molecular weight of the source gas as shown in figure 2.4, with low ionization potentials and large molecular

weights giving higher growth rates. The deposition rate v for a given gas has been found to vary with bias voltage and gas pressure as

$$v = k \, V_b \, P \quad \text{..} \quad [2.4]$$

By Koidl et al. [20], for various different source gases (methane, acetylene and benzene). The deposition rate can saturate or decline for biases over 1.2-1.5 kV as the incoming ions begin to sputter the film. The total deposition flux again consists of both ions and neutral species from un-ionized background gas. Some of the neutral species can be energetic, as they are formed by charge exchange reactions with energetic ions. Catherine found the ion/neutral flux ratio to be 0.1-0.2 for methane plasmas on the basis of ion flux measurements. The advantage of plasma-deposition is its simplicity and high deposition rates with the appropriate gases.

A problem with PD is in the scaling up to larger systems as film properties depend mainly on bias voltage and thereby electrode areas rather than directly on process parameters like RF power and gas pressure. The properties of PD a-C: H depends strongly on the ion energies. Low ion energies only weakly dissociate the source gas and give a highly hydrogenated or polymeric from of a-C:H. This regime is similar to that of plasma polymerization. Plasma deposition is also a popular method of preparing a-Si:H and polycrystalline diamond, but the conditions are considerably different in each case, as summarized in table 2.3. Hard a-C: H is obtained if there is ion bombardment during deposition, and these conditions are favored by a cathodic substrate (to receive positive ions), a high RI: power (for a high bias voltage), low gas pressure (for high ionization) and low substrate temperatures (to minimize self-annealing).

Table 2.3: Conditions for plasma deposition of a-C: H electronic grade a-Si: H and polycrystalline diamond.

	a-C:H	a-Si:H	Diamond
RF power density, W/cm^2	1	0.01	10
Gas pressure, Pa	3	10	3
Substrate electrode	Cathode	Anode	
T_0, ^0C	25	2.50	800
Dilution			$H_2/CH_4=100$

Electronic grade a-Si:H is deposited from saline plasmas under conditions, which minimize the concentration of defect states due to Si dangling bonds. Sufficient hydrogen must be retained to passivate the dangling bonds but not so much that polymeric SiH_2 groups are common. This requires gentle conditions of low RF power density, a moderate gas pressure, an anodic substrate (to minimize ion bombardment) and a substrate temperature of about 250^0C to give optimum self-annealing. Diamond growth is favored by using hydrogen-diluted source gases, a high power density and a higher substrate temperature. These conditions generate atomic hydrogen, which suppresses the deposition of graphite and a-C by various mechanisms such as preferential etching. There are also a variety of hybrid deposition methods such as ion plating in which the plasma is created by RF plasma and then a separate field accelerates the ions from a grid electrode to the substrate [33].

Using microwave discharges more highly ionized plasmas can be produced, particularly if operated at the electron cyclotron resonance. This method produces high ion densities even at low gas pressures. The absence of electrodes and ability to control the shape and position of the plasma make this method technically attractive. Control of both ionization and ion energy can be achieved by using a microwave ion source and a rf. self-biasing accelerator.

2.7.4 Laser Methods

Carbon ion plasma can also be produced by the laser ablation of graphite, figure 2.5. The resulting plasma probably resembles that formed by a catholic are. The resulting a-C is found to have a diamond-like character if the laser power density exceeds a threshold value.

LASER INPUT

rotation

substrate

witness pole

limit of useful deposition

to HV electrode

Graphite
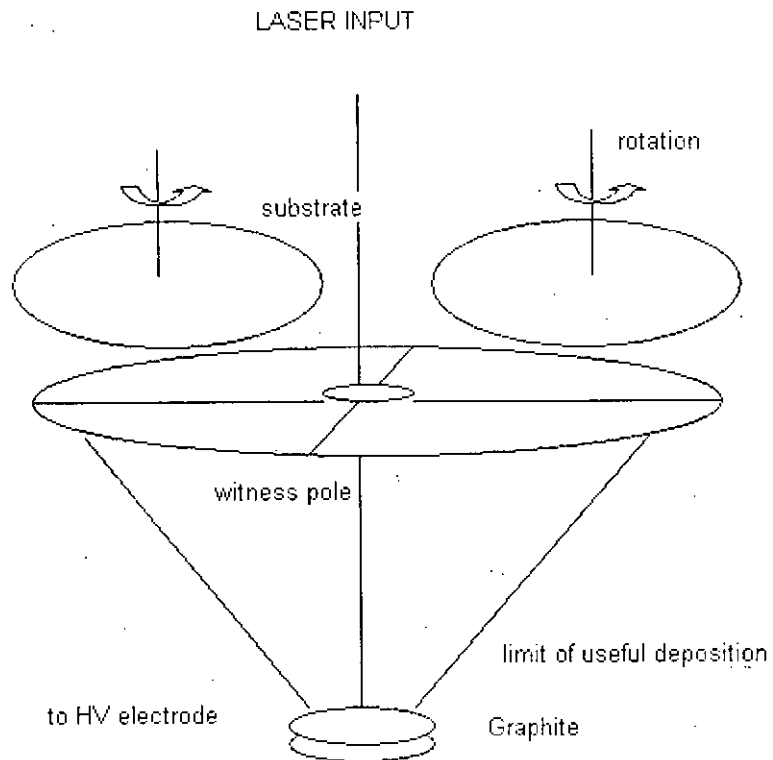
Figure 2.5: Laser-plasma deposition apparatus

2.7.5   Chemical Methods

2.7.5.1   Electroplating

This method is suitable only for deposition of metal and alloys on electrically conducting substrates. The film material is present in the form of positive ions in the electrolyte (mostly an aqueous solution of an ionic compound). The number of ions discharged at the cathode and hence Faraday's law gives the mass of deposit.

$$m/A = jt \, M\alpha/n \, F \quad \text{...} [2.5]$$

Where m/A denotes mass per area, j denotes current density time. M. molecular weight, n = valance, F = 96490 As/g equivalent, α = current efficiency = 1-0.5.

Among the 70 metallic elements there are 33, which can be electrodeposited, but only 14 of them are deposited routinely:

Al, Ag, Au, Cd, Cu, Cr, Fe, Ni, Pb, Pt, Rh, Sn, Zn.

For physicists, the elementary process of discharge and film formation is of interest: Ions (of both types) are accelerated towards the oppositely charged electrode, where they form a double layer screening the bulk electrolyte from the main part of the electric field. The voltage drops in the double layer (about 30nm, thick) leading to fairly high field strengths (107 V cm-1). In an aqueous system the positive ions undergo several reactions before being incorporated in the films:

- Dehydration
- Discharges
- Surface diffusion
- Nucleation, Crystallization

In general polycrystalline deposits but in special cases epitaxial growth on a single crystal cathode is possible, e.g., Ni on Cu.

Table 2.4: Summary of film properties prepared by ion beam and sputter deposition

Deposition Conditions				Properties of hard a-C films			
Condensation of carbons (ion beam deposition)	Source of carbon	Ion energy (eV)	Density (g/em)	Electrical resistivity (* cm)	Optical proprieties	Hardness (kg/mm²) (HV or HK)	Chemical meartness
	Carbon in rf plasma	40-100		$\sim 10^{10}$	Refractive index. F=2.0	> Glass	Resist HF for 40 hi 10-20 yr archive lifetime
	Carbon in nrc[h]	50-100		$>10^{12}$	n~2		
	Carbon in de plasma	50-100		Dielectric constant ~6 (diamond = 5.7)	n = 2.3 nt λ = 5 wn	185 QHK (diamond 7000 HK)	
Sputtering deposition	Carbon target in rf. plasma	Rf power = 2.25 and 75W	10^{-2}-10^{3}	Optical gap E_0~08cV			
	Carbon Sputtered by Ar beam	1-20	2.1-2.2	$>10^{11}$	Reflectance 0.2 Absorplance 0.7 Absorption coefficient α=6.7x10^{4} cm^{-1} transmittance 0.1		
	Dc Magnetron Sputtering of a graphite target	Sputtering power density W cm^{-2})		(At 300K)	n (at λ = 1μm)	E_n (eV)	HV
		0.25	2.1-2.2	2.5x10^{4}	2.4	0.74	2400
		2.5	1.9	1.0	2.73	0.50	2095
		25	1.6	0.2	2.95	0.04	740

* Reference 21 * Reference 32 * Reference 34 * Reference 35 * Reference 36 * Reference 37

For alloys deposition one must account for different electrochemical potentials governing the ratio of discharged ions of the components at a certain voltage. Suitable chemical complexing of ions may adjust the particular discharge reactions. Special feature of electrode position is the high growth rates $D=dD/dt=1\mu s^{-1}$ at a current density $j=1\ Acm^{-1}$.

2.7.5.2 Electroless Plating (Chemical-Reduction Plating)

In some special cases electrochemical reactions may occur without an external field, e.g., silvering of mirrors by $AgNO_3$ solutions with formaldehyde or sugar as a mild reducing agent. This reaction takes at any surface submersed in the bath. Sometimes the reaction is only on special surfaces:

$NiCl$+ sodium hypophosphite $\rightarrow$ Ni deposit only on Ni, CO, Fe and Al surfaces
.... [2.6]

2.7.5.3 Chemical Vapor Deposition (CVD)

Such methods [38] that are making use of a gas transport reaction and very important in semiconductor device fabrication.

The film material is usually one of the components in a volatile compound, which decomposes at the substrate in the form of a heterogeneous reaction. Elevated temperatures are usually required, thus enabling the growth of single crystal films on a suitable substrate, very often iso-epitaxial growth of Si on single crystal.

2.7.5.4 Anodization

The reacting partner is atomic oxygen and hence a very reactive state is produced by the decomposition of H_2O next to the anode of an aqueous electrolytic system. The reactions is

a: $M + nH_2O \rightarrow MO_n + 2nH^+ + 2ne$... [2.7]

c: $2ne + 2nH_2O \rightarrow nH_2 + 2nOH$ .... [2.8]

2.7.5.5 Thermal Growth

It is known that a reactive material surface such as that Pb and Al already forms an oxide layer at room temperature when exposed to atmosphere. The process is very important one in semiconductor technology where oxidized in water vapor at high temperatures (about 1000^0C). The SiO_2 thus formed has excellent insulating and protecting properties. Ni-tridization is possible as well if NH_3 is the reactive gas. Temperature can be generally reduced if reactive plasma is created and the ions are accelerated towards the substrate. The growth relation is parabolic one.

2.8 Un-doped Camphoric Carbon (CC) Films

Since the carbon thin films possess some outstanding properties [39] and these properties can be tailored over an unusual wide range, the filed of research on carbon thin films is attracting much more attracting of the researchers. However, the properties of these films strongly depend on the precursor material and method of deposition. Hydrogen in a-C thin films modifies the properties of the films and introduces many sp^3 sites, causing an increase in the band gap. Graphite had been being commonly used as a target material since long. Graphite consists of only sp^2-hybridized carbon in its structure (figure 2.6). The existence of sp^3 bond assists in depositing diamond like carbon (DLC) films, which possess improved version of thin films quality. Again when the film is hydrogenated to modify the properties, additional hydrogen to be added is case of using graphite but camphor molecule has abundant hydrogen in its own structure. Because of having these advantages over graphite, camphor $(C_{10}H_{16}O)$ has been introduced as an alternative precursor material for the deposition of carbon thin films. Now the experimental details of the

deposition of thin film from camphor target and some properties of these films will be discussed in the following subsections in table 2.5
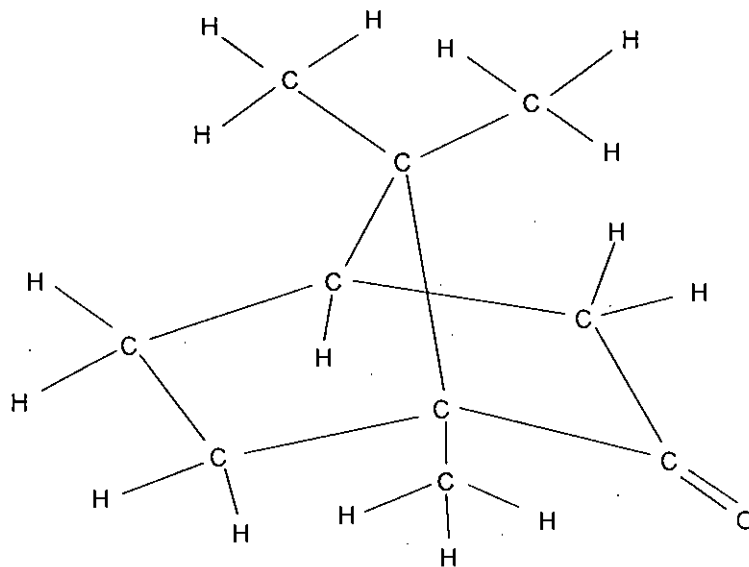
Figure 2.6: chemical structure of camphor

Table 2.5: Summary of ways of preparing thin films

Method	Deposition Rate As^{-1}	Rate Control	Type*	Advantages	Limitations
Electro-Plating	10^2-104	Current density	M	Simple apparatus	Metallic Substrate
Chemical Reduction	10	Solution temp, p^{11}	M	Simple apparatus	Limited number of materials
Vapor	1-10^3	Pressure, temperature	M, S, I	Single crystal, Clean films	High substrate temperature, low pressure
Anodization	10	Current density	I	Simple apparatus, Thin amorphous Films	Metallic substrate limited no. of metals, limited thickness
Thermal	1	Pressure, Temp	M, S, I	Simple apparatus	Metallic substrate, Limited thickness Limited no. of Metals
Evaporation	10-103	Source Temp.	M, S, I	Large range of materials and substrates	Vacuum apparatus, Some materials Decompose on heating
Sputtering	10	Current potential	M, S, I	High adhesion, very large range of materials	Suitable targets, Vacuum apparatus

Chapter 3

THIN FILM DEPOSITION, RESULTS AND DISCUSSIONS

3.1 Carbon thin film deposition by electroplating

Thin films of carbon have recently attracted much interest for its potential use as hard; wear resistance films, and optical coatings. The methods known for depositing carbon thin film, such as chemical vapor deposition, pulsed-laser deposition, and ion-beam sputtering, are all vapor deposition techniques.

There is experimental evidence that most materials, which can be deposited from the vapor phase, can also be deposited in liquid phase using electroplating techniques and vice versa. In our laboratory we used methanol solution for electroplating purpose. Methanol is selected because its polarizability and conductivity are stronger than those of ethanol and the structure of methanol is even closer to that of diamond.

Precursors and method of deposition of carbon films are the two dominating factors that dictate the optical and electrical properties of the film. In connection with this research, camphor ($C_{10}H_{16}O$) has been found as an alternative precursor material because it has some advantages over graphite. Graphite is purely sp^3 hybridized whereas camphor consists of both sp^2 and sp^3 hybridized carbon in its structure. Furthermore, the presence of sp^3-hybridized bonds in camphor molecule plays a beneficial role in the deposition of carbon films especially for diamond like carbon

(DLC) films. Naturally, we are interested to use camphor as precursor material in the deposition methods. In the present article, a film deposition is attempted by the technique of electrolysis. Methanol (CH_3OH) and different percentages of camphor (1%, 2%, 3%, 4%, 5%, 6%, 7% and 8%) in methanol are used as electrolytes respectively.

3.2 Experimental Details

A schematic diagram of the system is shown in fig. 3.2 Copper, aluminum or Silicon substrate with a size of $3.2\times1.5\times0.1$ cm^3, have mounted on the negative electrode in this electroplating technique. The pure water, CH_3COCH_3 solution and CH_3OH layout solution clean the substrates successively. The distance between the substrate and positive electrode was set to 1.5 cm. The potential applied to the substrate could be changed from 0 to 2500 V.
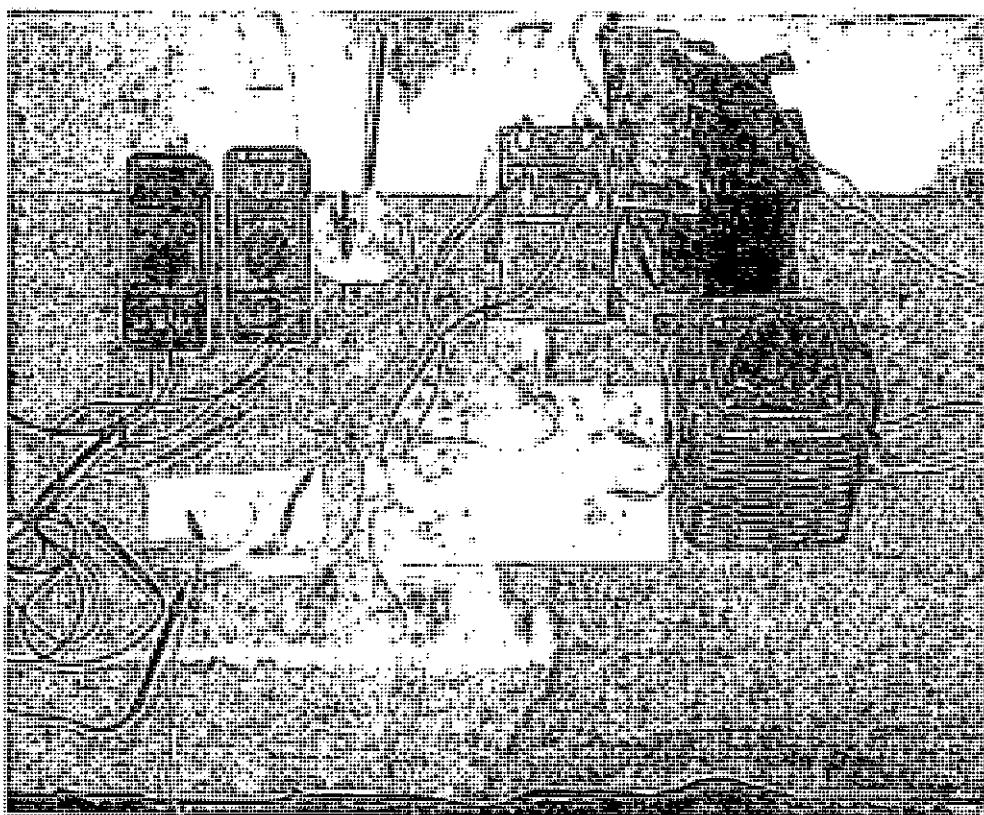
Figure 3.1: Photograph of experimental layout

A thermometer is adjusted to the system to measure the temperature of solution during the deposition occurs. Carbon thin films were deposited on Aluminum (Al), Copper (Cu) and Silicon (Si) substrates by electrolysis of methanol. The effect of camphor (C_{10} $H_{16}O$) — a natural source, incorporation with methanol is investigated. Remarkable change in the variation of current density as a function of applied potential was observed with different percentage of camphor content. Thin films were deposited on Al, Cu and Si substrates for different percentage of camphor and are compared. Current density is observed to vary with substrate. For Al and Cu substrates current density was highest for the 2% camphor in methanol solution whereas for Si substrate current density was highest for the 6% camphor in methanol solution. The maximum current density with camphor content was different for Al, Cu and Si substrates. Films were produced by electro deposition on Al, Cu and Si in methanol solution using several percentage of camphor. P^H of various solutions before and after deposition has been analyzed. Then the films were characterized by optical microscopy, SEM micrograph, EDS analysis, FTIR spectroscopy for investigation and transmittance/reflectance measurement using UV-VIS-NIR.
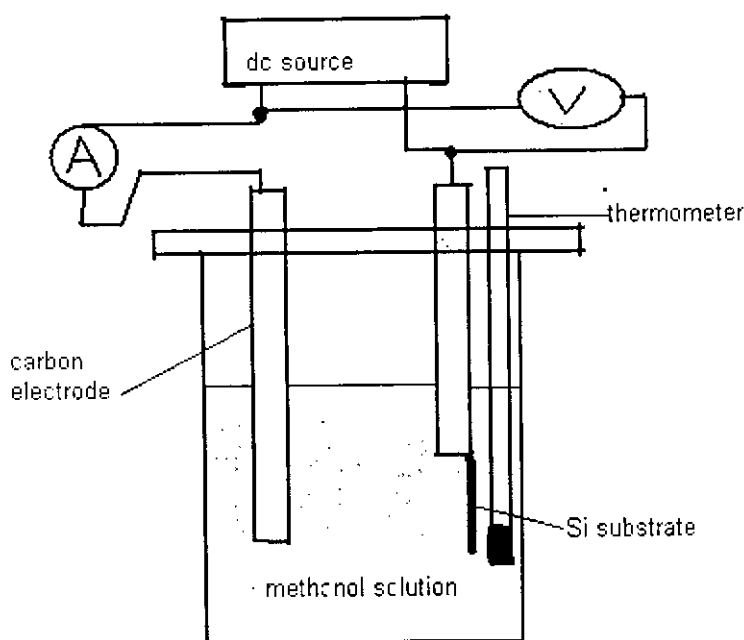
Figure 3.2: Schematic diagram of the deposition system

3.3 Results and Discussions

3.3.1 Analyses of Current Density-Voltage (J-V) Characteristics

The substrate current plays an important role in film formation from an organic solution. Higher current density indicates more ionized charge particles move from solution to electrode, which may have some effect on the growth rate of film. Current densities are measured for various applied voltages with respect to different electrolytes. Various applied potential and corresponding current densities for aluminum, copper and silicon substrates are shown in the following tables. The relationships are also shown graphically. For both Al and Cu substrates current densities against various applied potentials are measured for 0%, 1%, 2%, 4% and 7% of camphor. For Si substrate current densities are measured for 0%, 2%, 4%, 6% and 8% of camphor.

Table 3.1: Methanol with 0% camphor and aluminum substrate

Applied Voltage (Volts)	Current Density (mA/cm^2)	Temperature (^{0}C)
120.0	0.8	22
300.0	2.1	24
483.0	3.3	24
597.0	4.1	28
751.0	5.4	40
895.0	6.8	41
1038.0	8.3	45
1193.0	9.7	51
1491.0	12.0	55
1789.0	14.8	60
2087.0	19.5	65
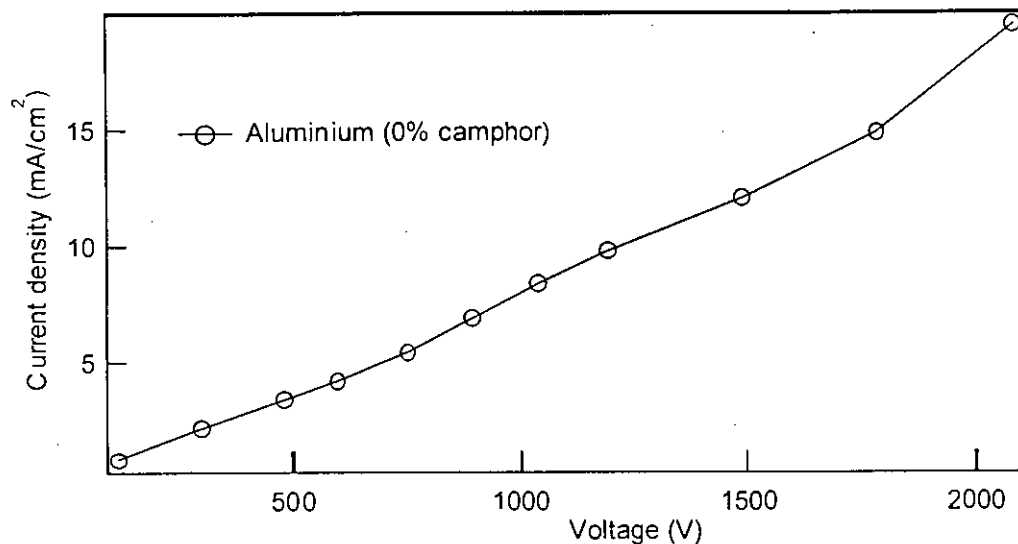
Figure 3.3: Current density of the aluminum substrate as a function of applied potential with respect to methanol with 0% camphor solution.

The data of table 3.1 in case of 0% camphor on Al substrate is plotted in figure 3.3 and it is found that, by changing voltage from 0 V to 2087 V current density changes from 0 mA to 19.5 mA.

Table 3.2: Methanol with 1% camphor solution and Al substrate

Applied Voltage (Volts)	Current Density (mA/cm^2)	Temperature (^{0}C)
158.4	0.8	22
288.4	1.6	22
446.4	2.4	25
584.6	3.0	26
725.7	4.0	31
884.1	5.2	32
1000.0	6.2	45
1154.8	7.4	45
1307.5	8.4	46
1454.4	9.6	61
1584.0	10.4	66
1771.2	12.0	66
1909.4	13.6	67
2016.0	14.9	67
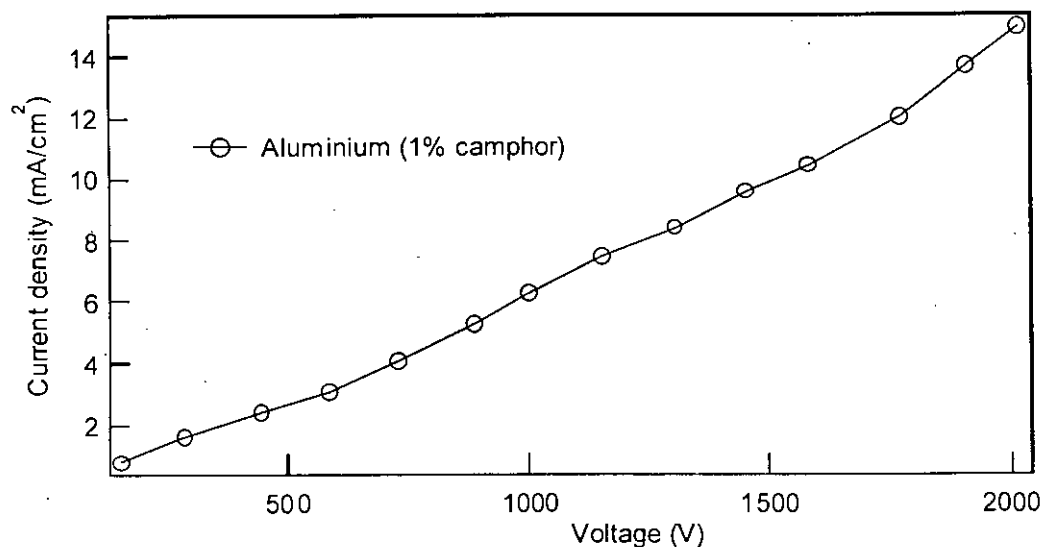
Figure 3.4: Current density of the aluminum substrate as a function of applied potential with respect to methanol with 1% camphor solution.

The data of table 3.2 in case of 1% camphor on Al substrate is plotted in figure 3.4 and it is found that, by changing voltage from 0 V to 2016 V current density changes from 0 mA to 14.9 mA.

Table 3.3: Methanol with 2% camphor solution and Al substrate

| Applied Voltage (Volts)	Current Density (mA/cm^2)	Temperature (^{0}C)
172.8	2.0	44
308.1	4.2	40
437.7	6.0	38
596.1	8.4	39
734.4	10.4	41
887.0	11.3	42
996.4	13.6	42
1154.8	15.5	42
1301.7	17.3	42
1440.0	18.6	43
1592.6	21.3	43
1728.0	23.3	47
1906.5	24.6	55
2030.4	28.0	55
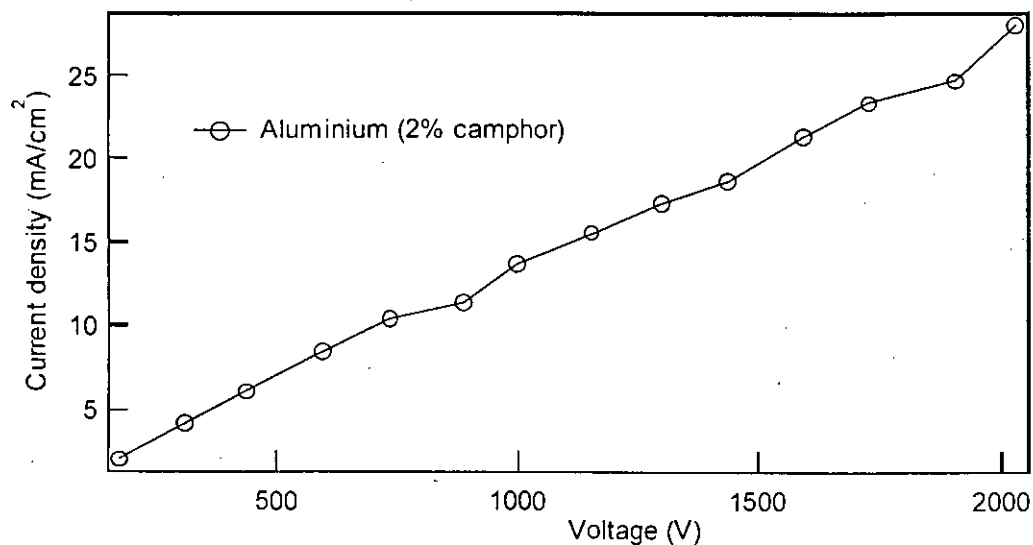
Figure 3.5: Current density of the aluminum substrate as a function of applied potential with respect to methanol with 2% camphor

The data of table 3.3 in case of 2% camphor on Al substrate is plotted in figure 3.5 and it is found that, by changing voltage from 0 V to 2030.4 V current density changes from 0 mA to 28 mA.

Table 3.4: Methanol with 4% camphor solution and Al substrate

| Applied Voltage (Volts)	Current Density (mA/cm^2)	Temperature (^{0}C)
158.4	1.4	24
319.6	2.9	32
452.1	4.0	36
578.8	5.1	38
745.9	7.0	38
866.8	8.4	38
1000.0	9.8	58
1177.9	11.5	58
1307.5	12.7	56
1460.1	14.8	56
1584.0	16.3	55
1733.7	18.0	56
1872.0	19.6	55
2033.2	21.7	55

Figure 3.6: Current density of the Al substrate as a function of applied potential with respect to methanol with 4% camphor

The data of table 3.4 in case of 4% camphor on Al substrate is plotted in figure 3.6 and it is found that, by changing voltage from 0 V to 2033.2 V current density changes from 0 mA to 21.7 mA.

Table 3.5: Methanol with 7% camphor solution and Al substrate

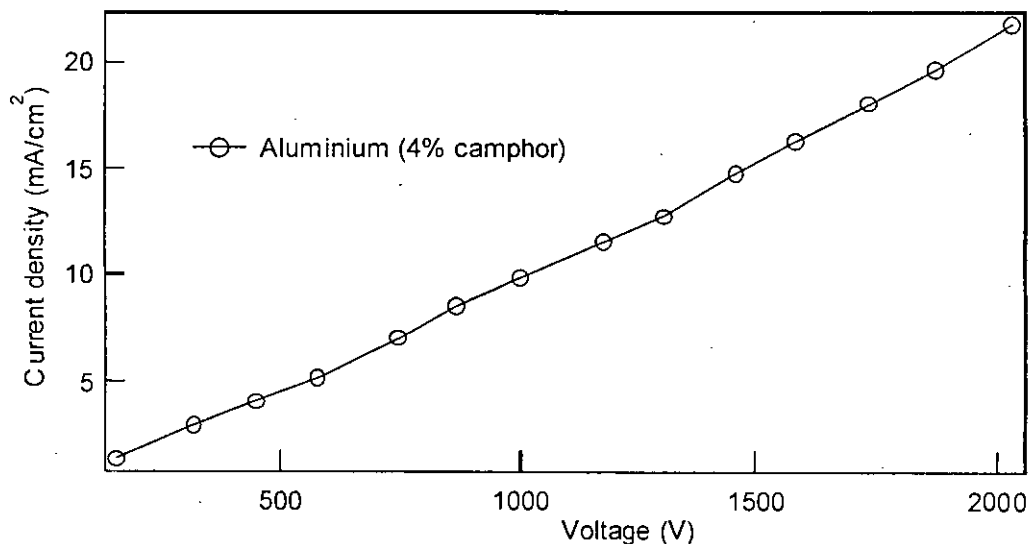| Applied Voltage (Volts)	Current Density (mA/cm^2)	Temperature (^{0}C)
150.0	0.7	25
339.8	1.6	26
446.4	2.1	30
622.0	2.8	31
748.8	3.6	35
884.1	4.5	40
1000.0	.5.6	42
1154.8	6.2	45
1316.1	7.2	46
1451.5	8.2	47
1598.4	8.8	58
1733.7	9.9	61
1874.8	10.8	65
2018.8	11.8	66

Figure 3.7: Current density of the aluminum substrate as a function of applied potential with respect to methanol with 7% camphor

The data of table 3.5 in case of 7% camphor on Al substrate is plotted in figure 3.8 and it is found that, by changing voltage from 0 V to 2018.8 V current density changes from 0 mA to 11.8 mA.

The optimum amount of camphor in methanol solution was measured for Al for maximum current density. The experiment was done for 0%, 1%, 2%, 4% and 7% of camphor. Change in current density for different % of camphor was analyzed. Current density as a function of applied voltage for different percentage of camphor in methanol solution was compared in figure 3.8 for aluminum substrate. For 0% camphor content (only methanol solution) a moderate current density pattern was found. By adding little camphor (1%) in the solution the current density is decreased from that of only methanol solution. With increase of camphor content (2%) the current density increased and reached to a maximum value. For further increase of camphor content, the current density is decreased. For the methanol containing 4% camphor. the current density was in between that of 2% and 0%. For 7% camphor content. the current density decreased further and dropped to a value less than that of 1% camphor and indicated the saturation of camphor into the solution.
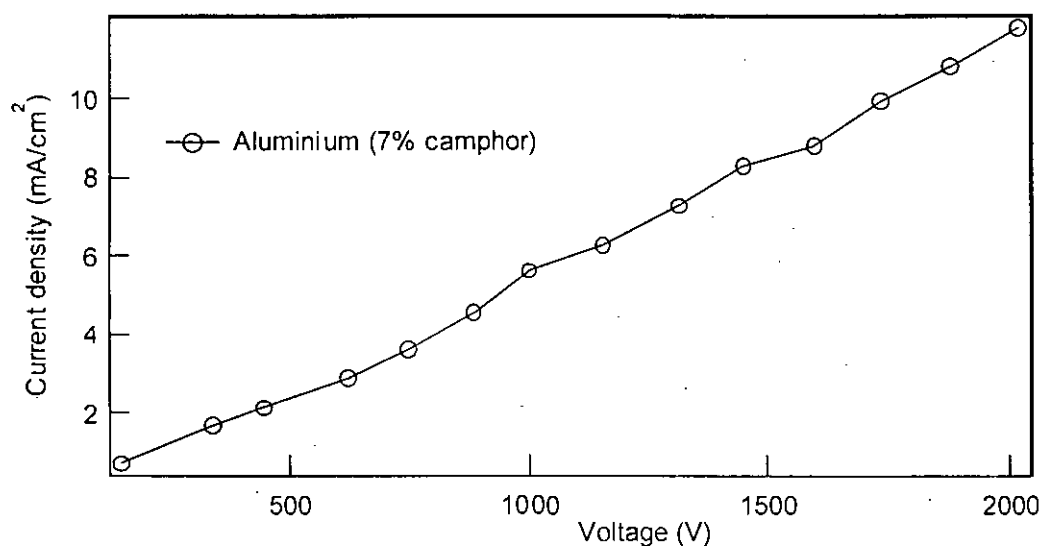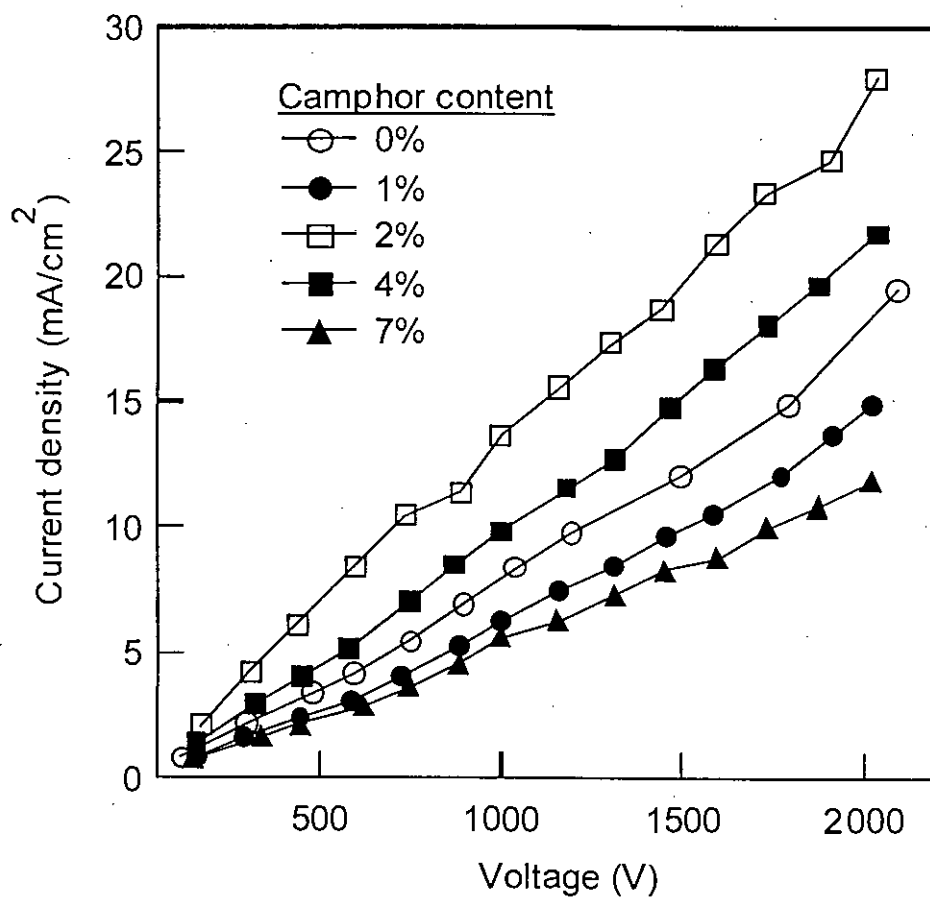
Figure 3.8: Current density of the aluminum substrate as a function of applied potential with respect to methanol with different percentage of camphor (0%, 1%, 2%, 4% and 7%)

Table 3.6: Methanol with 0% camphor solution and Cu substrate

Applied Voltage (Volts)	Current Density (mA/cm^2)	Temperature (^{0}C)
120.0	1.1	22
300.0	3.0	24
477.0	4.5	26
597.0	5.8	28
750.0	6.2	29
895.0	8.0	35
1038.0	9.2	38
1193.0	10.8	42
1491.0	15.0	51
1789.0	18.2	58
2087.0	23.0	61
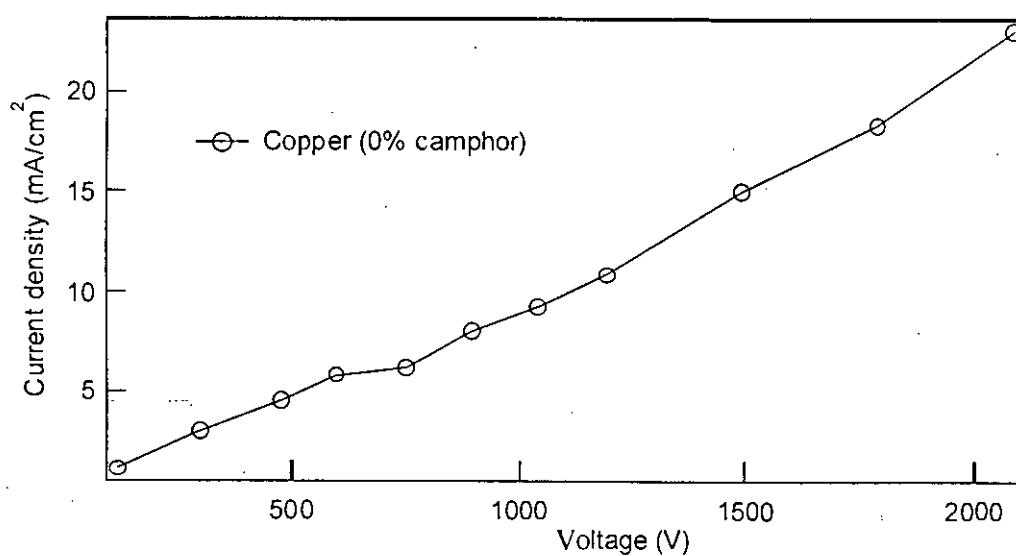
Figure 3.9: Current density of the copper substrate as a function of applied potential with respect to methanol with 0% camphor.

The data of table 3.6 in case of 0% camphor on Cu substrate is plotted in figure 3.9 and it is found that, by changing voltage from 0 V to 2087 V current density changes from 0 mA to 23 mA.

Table 3.7: Methanol with 1% camphor solution and Cu substrate

Applied Voltage (Volts)	Current Density (mA/cm^2)	Temperature (0^0c)
158.4	0.9	25
290.8	1.8	26
449.2	2.7	28
576.0	3.4	29
728.6	4.6	37
866.8	5.8	41
1000.0	7.1	45
1169.2	8.6	46
1298.8	9.7	58
1445.7	11.0	59
1604.1	12.4	61
1759.6	14.2	66
1923.8	16.0	66
2024.6	17.7	67

Figure 3.10: Current density of the Copper substrate as a function of applied potential with respect to methanol with 1% camphor.

The data of table 3.7 in case of 1% camphor on Cu substrate is plotted in figure 3.10 and it is found that, by changing voltage from 0 V to 2024.6 V current density changes from 0 mA to 17.7 mA.

Table 3.8: Methanol with 2% camphor solution and Cu substrate

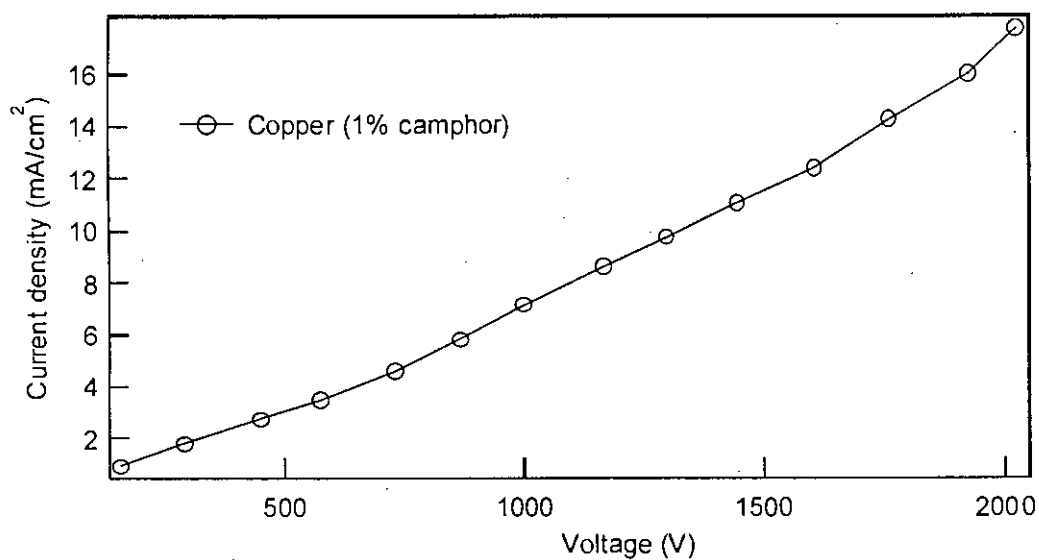| Applied Voltage (Volts)	Current density (mA/cm^2)	Temperature (^{0}C)
152.6	1.4	24
288.0	2.9	32
440.6	4.5	36
584.6	6.0	38
708.4	7.6	38
864.0	10.0	48
1000.0	12.0	58
1152.0	14.6	56
1298.8	17.3	56
1440.0	20.0	56
1584.0	22.0	56
1728.0	22.6	55
1863.3	24.6	55
2018.8	26.0	55

Figure 3.11: Current density of the copper substrate as a function of applied potential with respect to methanol with 2% camphor.

The data of table 3.8 in case of 2% camphor on Cu substrate is plotted in figure 3.11 and it is found that, by changing voltage from 0 V to 2018.8 V current density changes from 0 mA to 26 mA.

Table 3.9: Methanol with 4% camphor solution and Cu substrate

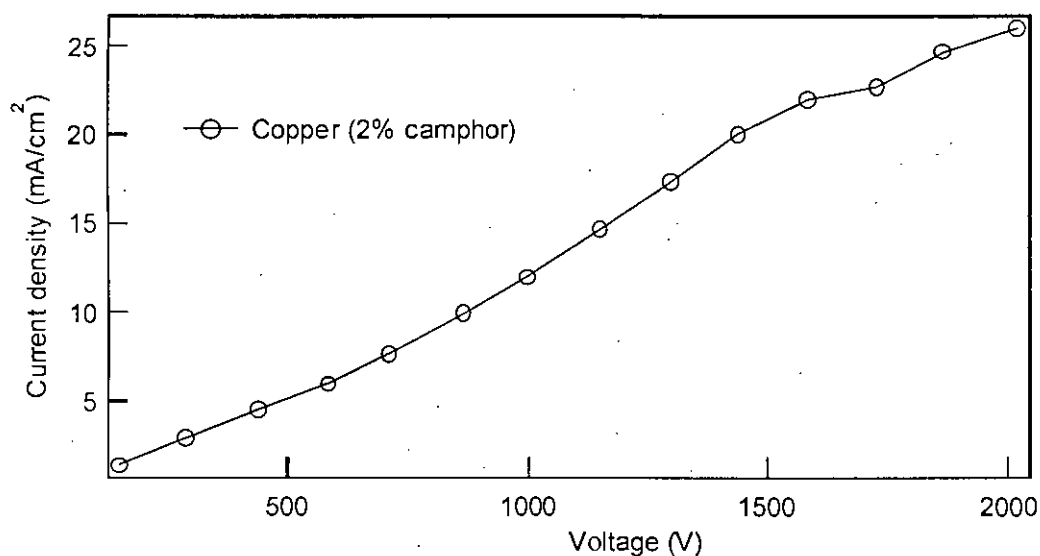| Applied Voltage (Volts)	Current density (mA/cm^2)	Temperature (0°C)
144.0	1.1	29
296.6	2.5	29
434.8	3.6	30
584.6	5.1	35
708.4	6.2	36
881.2	8.0	45
1000.0	9.3	51
1163.5	10.8	53
1301.7	13.4	55
1468.8	15.4	64
1592.6	17.6	66
1728.0	18.6	66
1869.1	19.6	67
2016.0	20.7	67
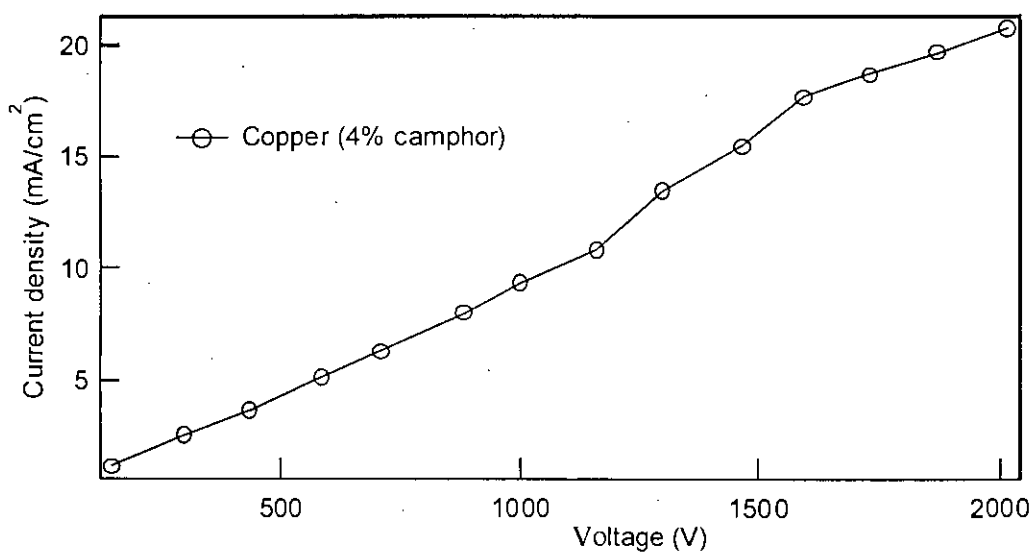
Figure 3.12: Current density of the Copper substrate as a function of applied potential with respect to methanol with 4% camphor.

The data of table 3.9 in case of 4% camphor on Cu substrate is plotted in figure 3.12 and it is found that, by changing voltage from 0 V to 2016 V current density changes from 0 mA to 20.7 mA.

Table 3.10: Methanol with 7% camphor solution and Cu substrate

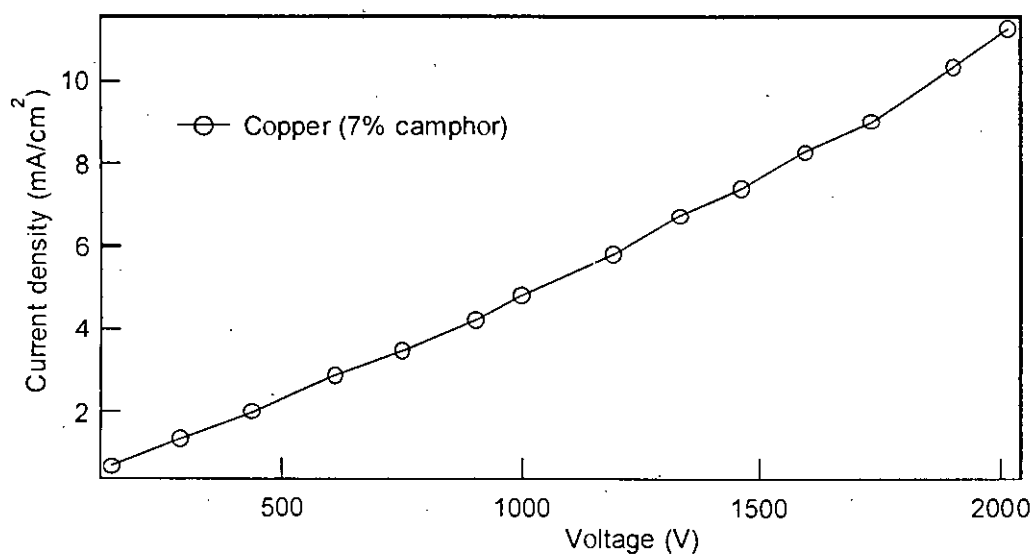| Applied Voltage (Volts)	Current Density (mA/cm^2)	Temperature (^{0}C)
146.8	0.6	26
288.0	1.3	26
437.7	2.0	26
613.4	2.8	29
751.6	3.4	32
904.3	4.2	34
1000.0	4.8	39
1192.3	5.8	49
1336.3	6.7	51
1463.0	7.4	61
1595.5	8.2	61
1730.8	9.0	62
1900.8	10.3	62
2016.0	11.2	65

Figure 3.13: Current density of the copper substrate as a function of applied potential with respect to methanol with 7% camphor.

The data of table 3.10 in case of 7% camphor on Cu substrate is plotted in figure 3.13 and it is found that, by changing voltage from 0 V to 2016 V current density changes from 0 mA to 11.2 mA.

The current density as a function of applied potential is also measured for Cu substrate. Variation of current density with applied potential for Cu substrate is almost similar to that obtained for Al substrate. The variation of current density with applied potential for Cu substrates is shown in figure 3.14. The current density is decreased initially with camphor (1%) and increased with camphor for 2% camphor in methanol solution. However, with further incorporation of camphor, the current density is decreased. Though the successive variation pattern of current densities for both Al and Cu are alike, they do not show the same magnitude of current densities for same condition.
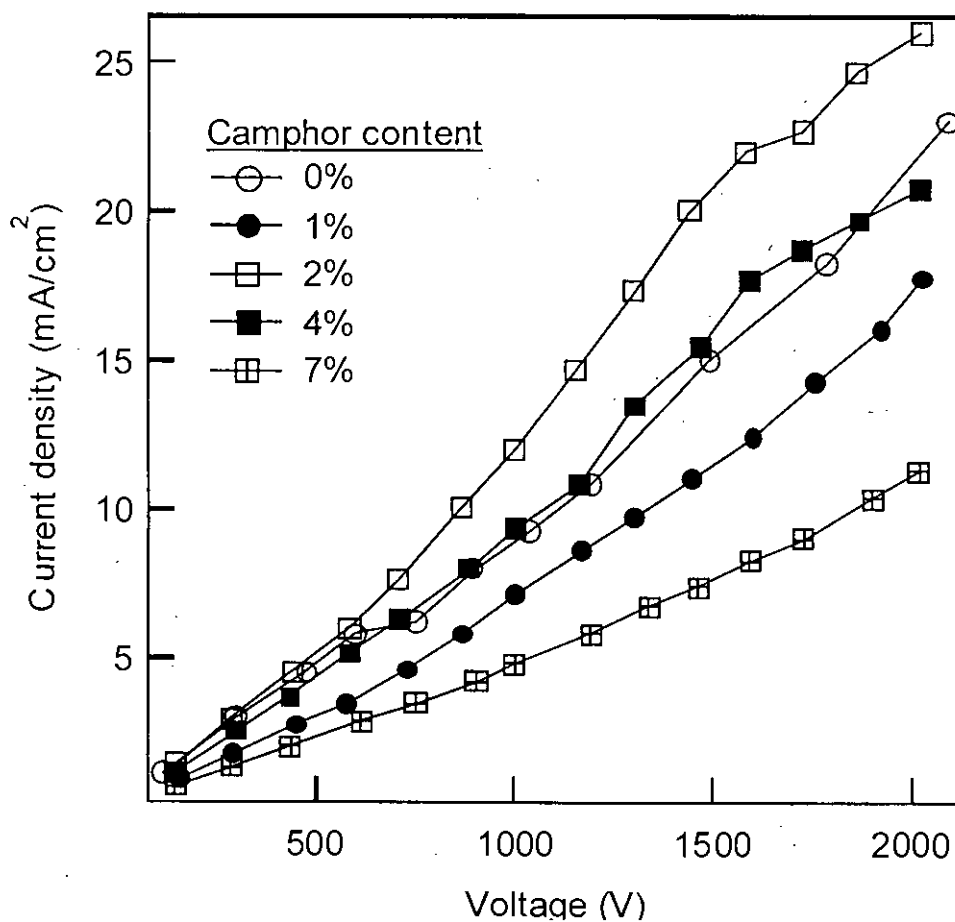

Figure 3.14: Current density of the copper substrate as a function of applied potential with respect to methanol with different percentage of camphor (0%, 1%, 2%, 4% and 7%)

Table 3.11: Methanol with 0% camphor solution and Si substrate

Applied Voltage (Volts)	Current Density (mA/cm^2)	Temperature (^{0}C)
161.3	2.7	25
311.0	4.3	25
443.5	6.3	26
578.9	8.3	28
737.3	11.5	29
864.0	13.7	35
999.4	16.0	39
1152.0	18.7	42
1324.8	21.5	48
1471.7	23.5	57
1595.5	25.5	57
1748.2	26.7	57
1889.3	28.0	57
2062.1	26.7	59
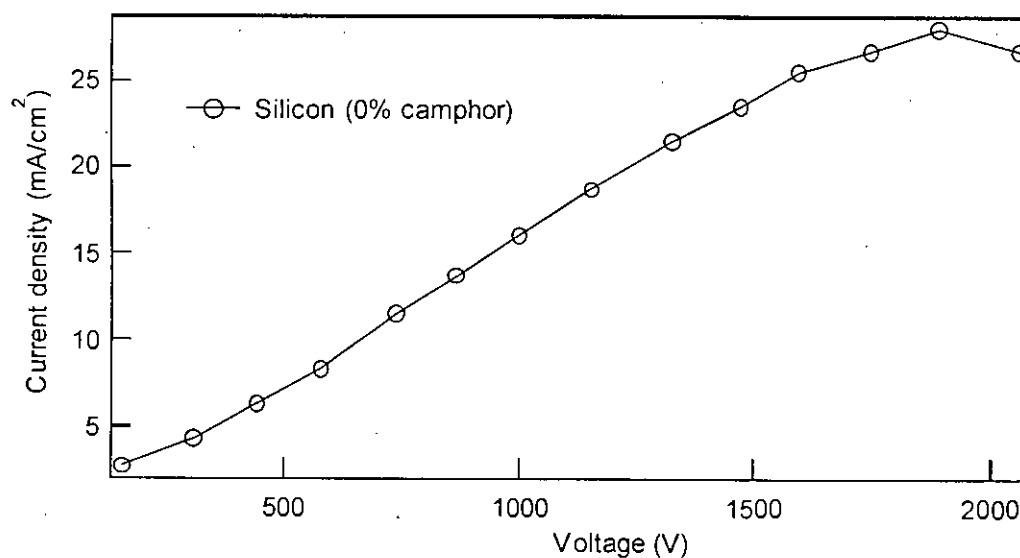
Figure 3.15: Current density of the Silicon substrate as a function of applied potential with respect to methanol with 0% camphor.

The data of table 3.11 in case of 0% camphor on Si substrate is plotted in figure 3.15 and it is found that, by changing voltage from 0 V to 2062.1 V current density changes from 0 mA to 26.7 mA.

Table 4.12: Methanol with 2 % camphor solution and Si substrate

| Applied Voltage (Volts)	Current density (mA/cm^2)	Temperature (^{0}C)
155.5	2.3	26
293.8	4.7	26
437.8	7.4	26
576.0	9.7	29
722.9	12.0	31
881.3	14.8	35
990.7	15.3	41
1152.0	17.3	45
1313.3	18.9	55
1442.9	18.9	57
1595.5	19.3	59
1728.0	20.7	62
1915.2	22.2	63
1993.0	23.6	63
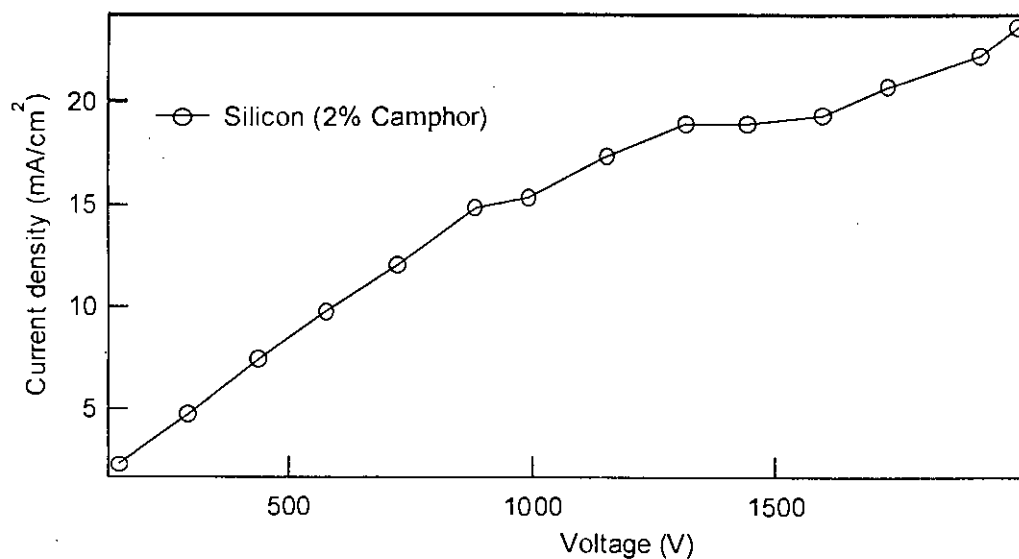
Figure 3.16: Current density of the Silicon substrate as a function of applied potential with respect to methanol with 2 % camphor

The data of table 3.12 in case of 2% camphor on Si substrate is plotted in figure 3.16 and it is found that, by changing voltage from 0 V to 1993 V current density changes from 0 mA to 23.6 mA.

Table 3.13: Methanol with 4 % camphor solution and Si substrate

| Applied Voltage (Volts)	Current Density (mA/cm^2)	Temperature (^{0}C)
158.4	2.5	26
313.9	4.7	26
443.5	6.3	26
590.4	8.2	29
720.0	9.3	33
892.8	12.2	35
1028.2	13.7	43
1195.2	16.5	45
1324.8	18.9	59
1440.0	20.3	61
1584.0	20.7	63
1728.0	22.7	64
1874.9	24.1	64
2018.9	26.1	64
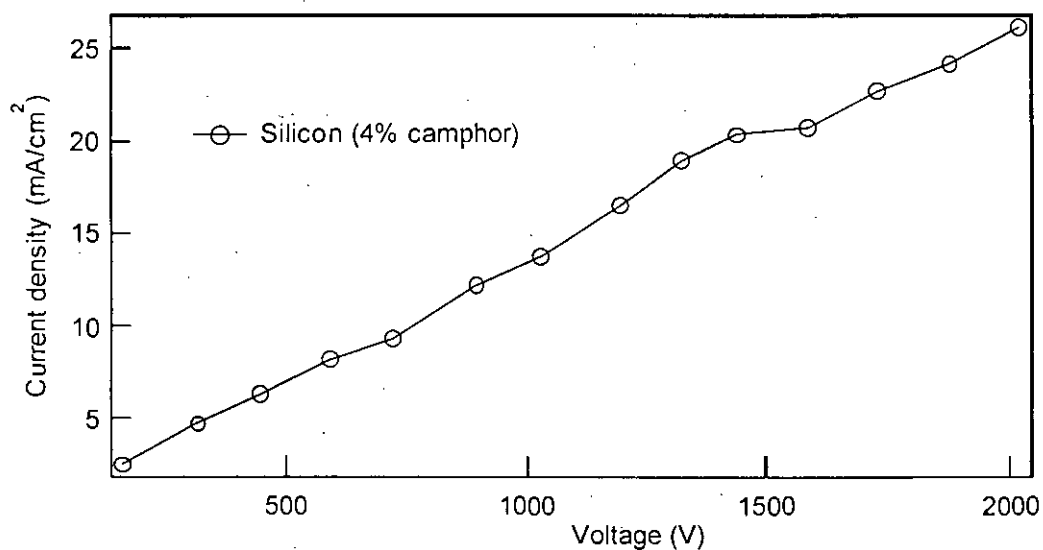
Figure 3.17: Current density of the Silicon substrate as a function of applied potential with respect to methanol with 4% camphor.

The data of table 3.13 in case of 4% camphor on Si substrate is plotted in figure 3.17 and it is found that, by changing voltage from 0 V to 2018.9 V current density changes from 0 mA to 26.1 mA.

Table 3.14: Methanol with 6 % camphor solution and Si substrate

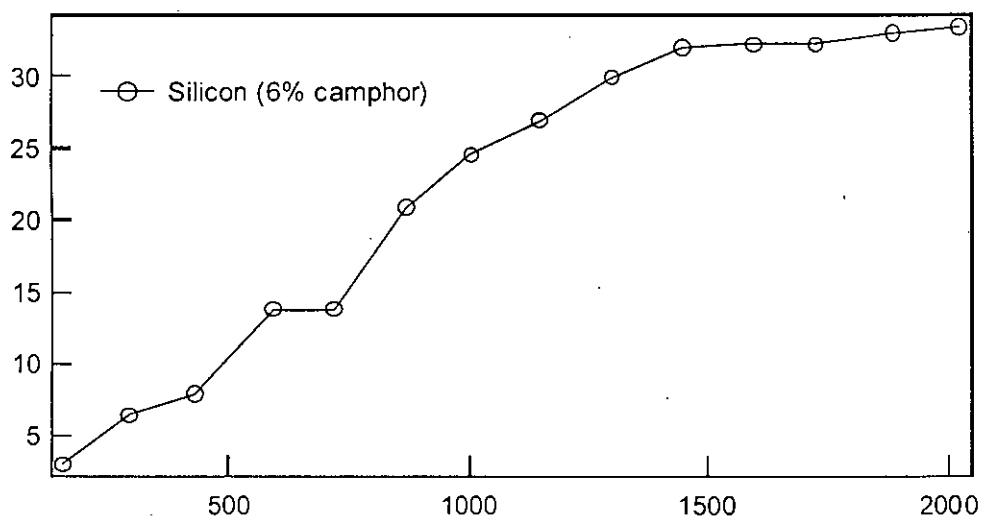| Applied Voltage (Volts)	Current density (mA/cm^2)	Temperature (^{0}C)
155.5	3.0	24
290.9	6.4	27
429.1	7.9	29
593.3	13.8	35
720.0	13.8	35
869.8	20.9	42
1005.1	24.5	44
1149.1	26.9	49
1301.8	29.9	57
1451.5	32.0	58
1598.4	32.2	66
1725.1	32.2	66
1883.5	33.0	66
2024.6	33.4	67

Figure 3.18: Current density of the Silicon substrate as a function of applied potential with respect to methanol with 6% camphor.

The data of table 3.14 in case of 6% camphor on Si substrate is plotted in figure 3.18 and it is found that, by changing voltage from 0 V to 2024.6 V current density changes from 0 mA to 33.4 mA.

Table 3.15: Methanol with 8% camphor solution and Si substrate

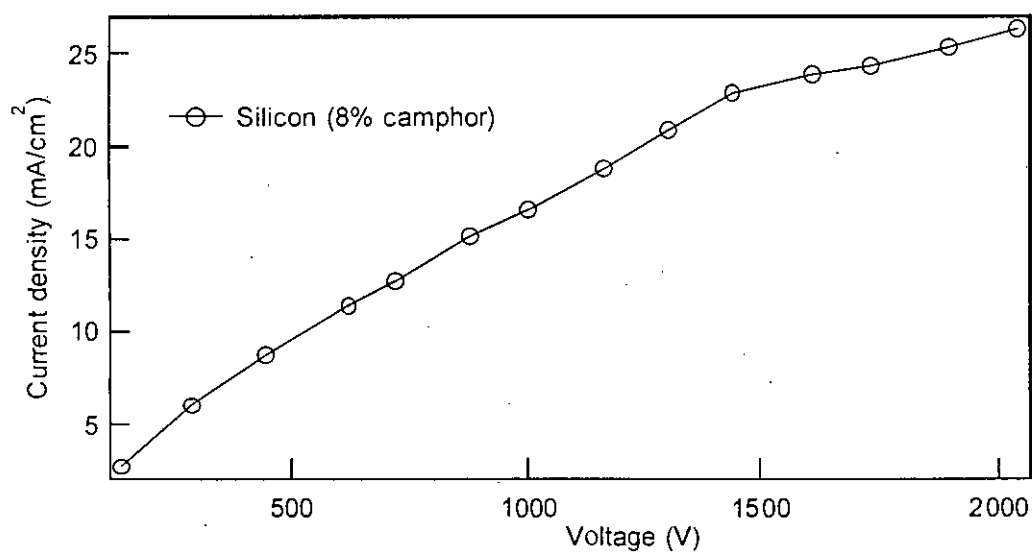| Applied Voltage (Volts)	Current density (mA/cm^2)	Temperature (^{0}C)
138.2	2.7	24
285.1	6.0	24
443.5	8.7	24
622.1	11.4	26
720.0	12.7	28
878.4	15.1	29
1000.0	16.6	39
1163.5	18.8	44
1304.0	20.9	49
1442.9	22.9	57
1609.9	23.9	66
1733.8	24.3	66
1897.9	25.3	66
2041.9	26.3	67

Figure 3.19: Current density of the Silicon substrate as a function of applied potential with respect to methanol with 8% camphor.

The data of table 3.15 in case of 8% camphor on Si substrate is plotted in figure 3.19 and it is found that, by changing voltage from 0 V to 2041.9 V current density changes from 0 mA to 26.3 mA.

Again the current density as a function of applied potential is measured for Si substrate. Variation of current density with applied potential for Si substrate is a little bit different to that obtained for Al and Cu substrate. It is shown in figure 3.20. The current densities are decreased initially with camphor (2%) and continue decreasing for 4% also. Then, with further incorporation of camphor (6%), the current density is increased and reaches to a maximum value, but again current density decreases for more camphor added (8% and above).
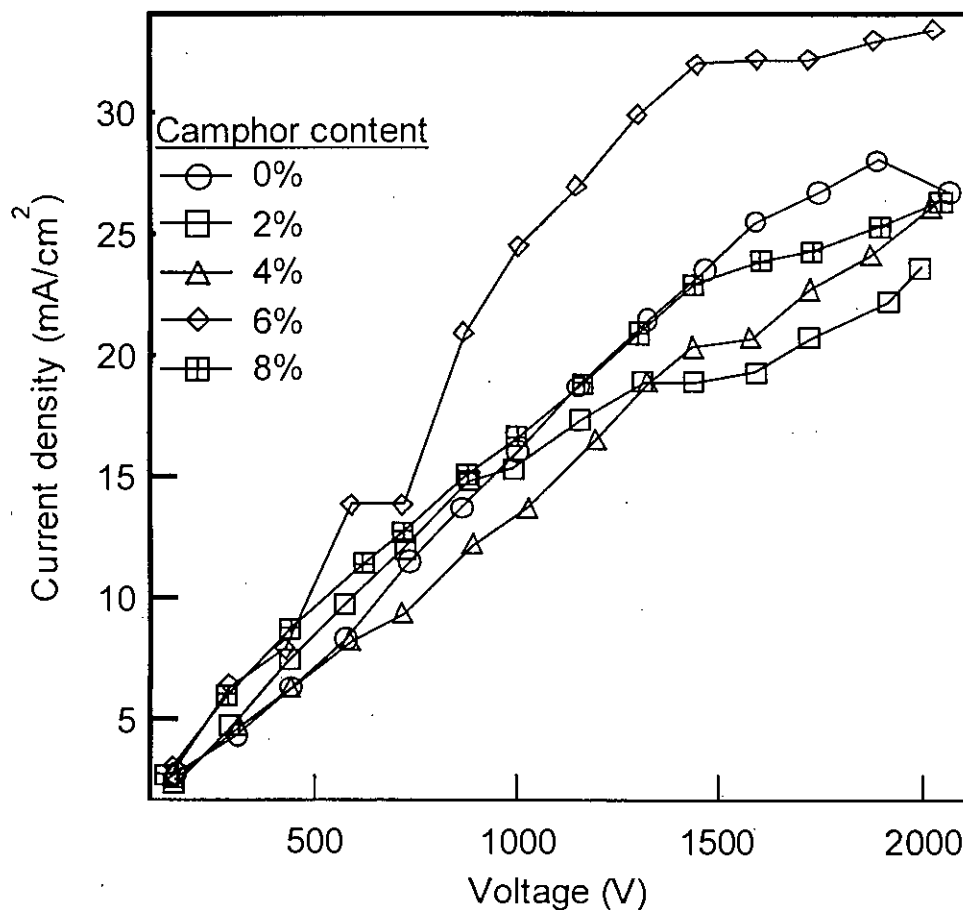

Figure 3.20: Current density of the silicon substrate as a function of applied potential with respect to methanol with different percentage of camphor (0%, 2%, 4%, 6% and 8%)

To compare the relative current density position of all the substrates the above three set of curves (each set contain five curves) are summarized in figure 3.21. It is found that current densities of Al and Cu are almost alike but those of Si substrate are totally different. So silicon has more affinity to camphor regarding current density.
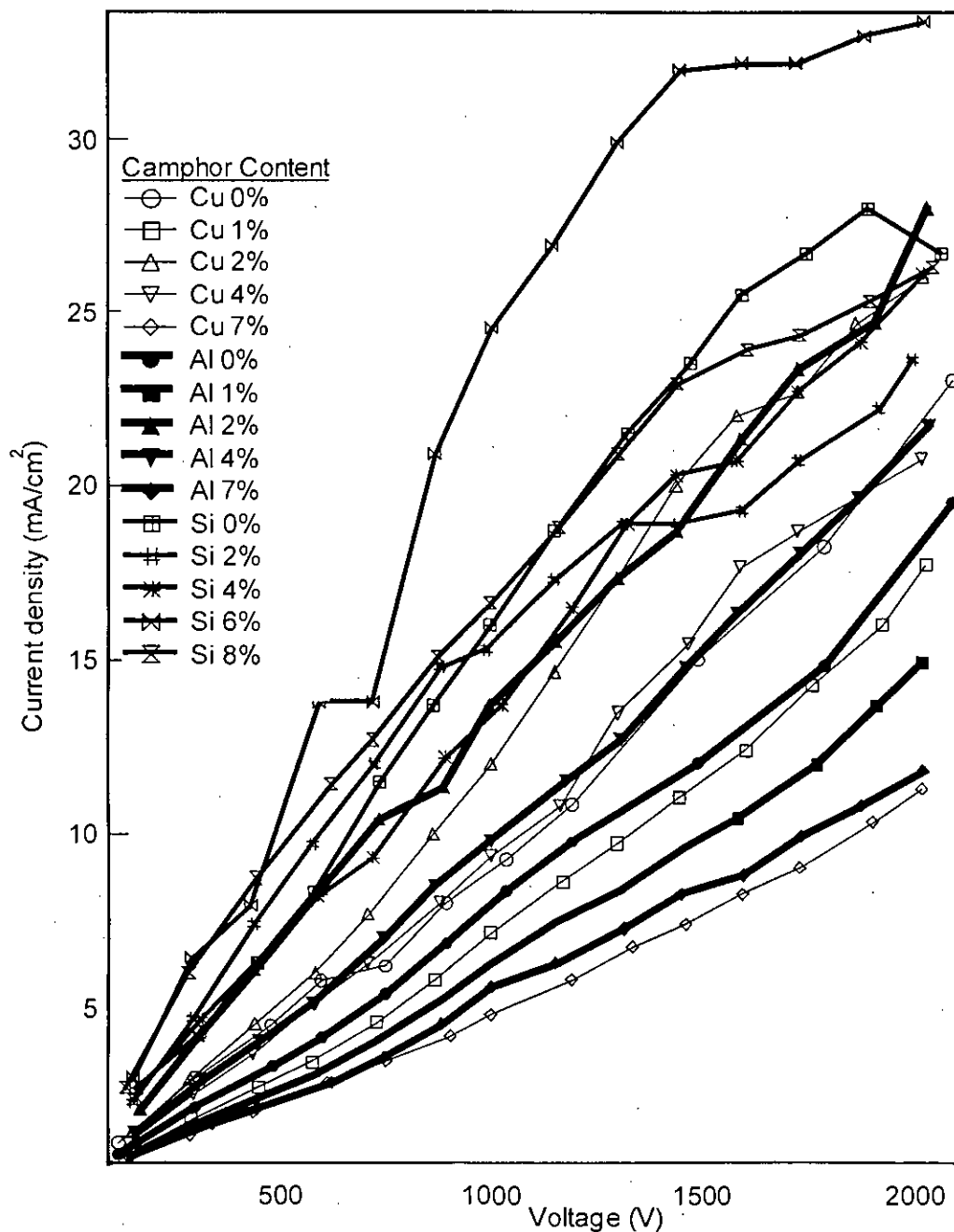
Figure 3.21: Current density of the three substrates (Al, Cu and Si) as a function of applied potential with respect to methanol with different percentage of camphor

For simplicity and easy assimilation current densities for applied potential of 1000V, 1500V and 2000V for all three substrates with camphor solution at room temperature are plotted. (Figure 3.22, 3.23 and 3.24) The same picture is found here. For all the

three cases Si shows much more current densities than the other two for all percentage of camphor. In between Al and Cu for some percentage of camphor, Cu shows higher current density and for other few cases it shows lower current densities. So same conclusion is that both Al and Cu have almost same affinity to camphor in case of carbon bonding but comparatively very low than that of Si.
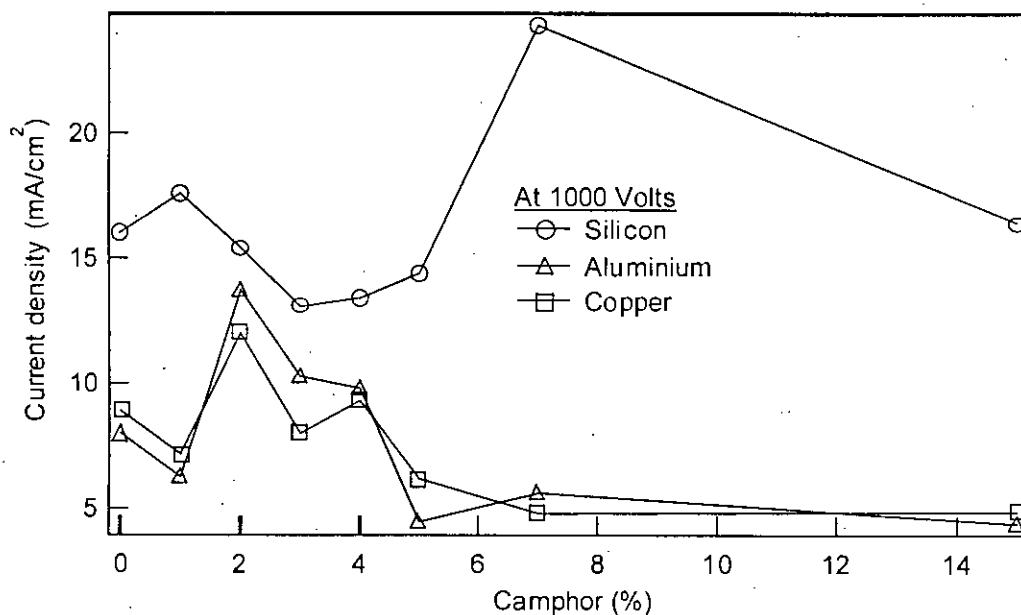

Figure 3.22: Current density as a function of % of camphor in methanol solution at 1000 V for Al, Cu and Si substrates
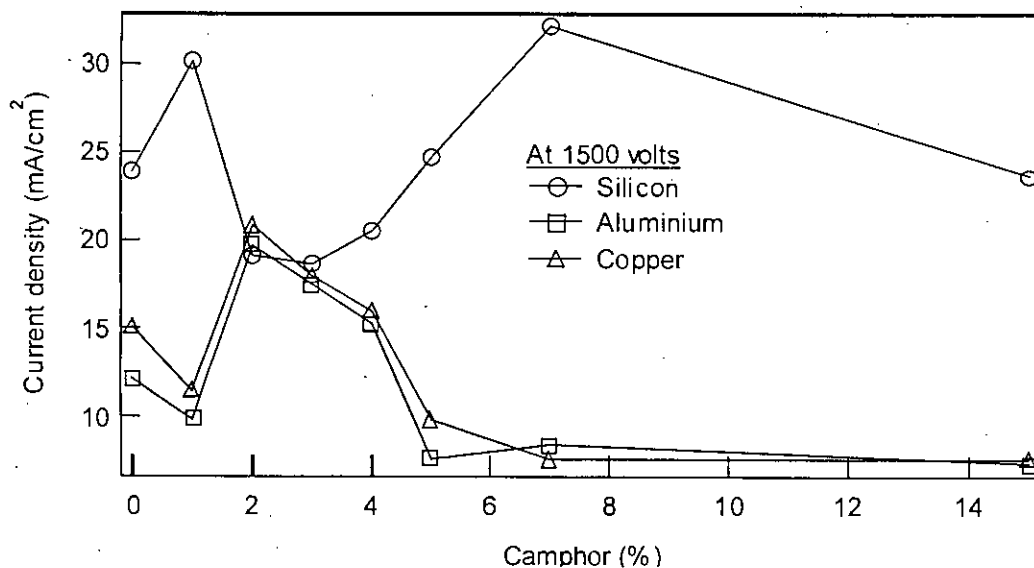

Figure 3.23: Current density as a function of % of camphor in methanol solution at 1500 V for Al, Cu and Si substrates
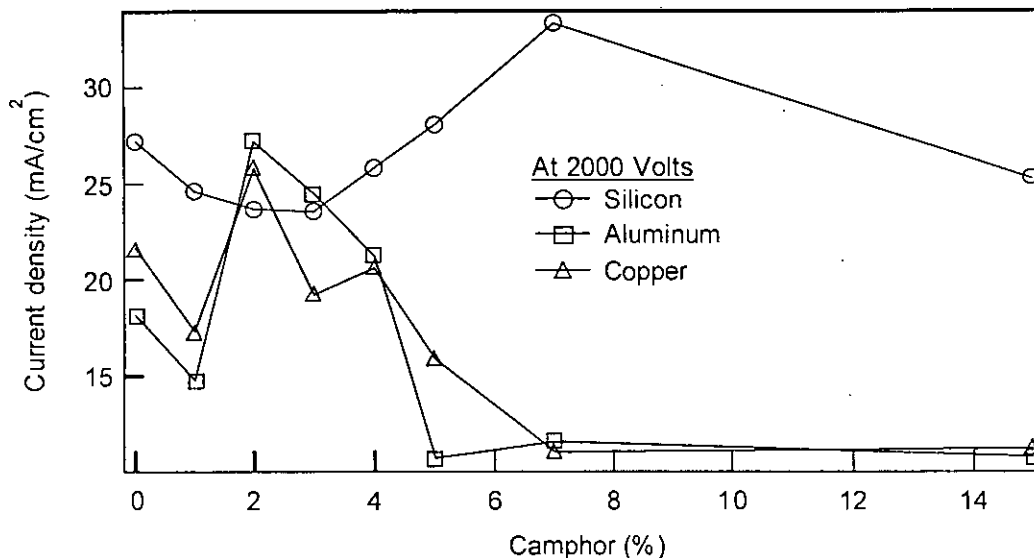
Figure 3.24: Current density as a function of % of camphor in methanol solution at 2000 V for Al, Cu and Si substrates

For the case of 1000 V current densities of Si is higher than those of Al and Cu for all percentage of camphor. But for the case of 1500 V and 2000 V current densities of Si is higher for all other percentage of camphor except the 2% of camphor, where current densities of Al and Cu are higher than those of Si.

3.3.2 Analyses of the role of camphor on current densities by P^H

The P^H plays an important role in film formation from an organic solution. The role of camphor on deposition rate can be understood from the curve of P^H as a function of camphor in methanol (figure 3.25). P^H of the solution increases with increasing the percentage of camphor in methanol. The P^H of the methanol containing 1% camphor is about 8. The P^H has increased with camphor content and for the methanol containing 20% camphor the P^H is 8.63. The variation of P^H with camphor content indicates the influence of camphor on deposition rate.

P^H of solution before and after deposition is measured. P^H of same solution is changed with deposition. For example during depositing on an Al substrate in a methanol

solution with 10% camphor the P^H of the solution was 8.26 before deposition and 7.37 after deposition. The difference in P^H before and after deposition indicates that films are grown from camphor incorporated methanol solution.
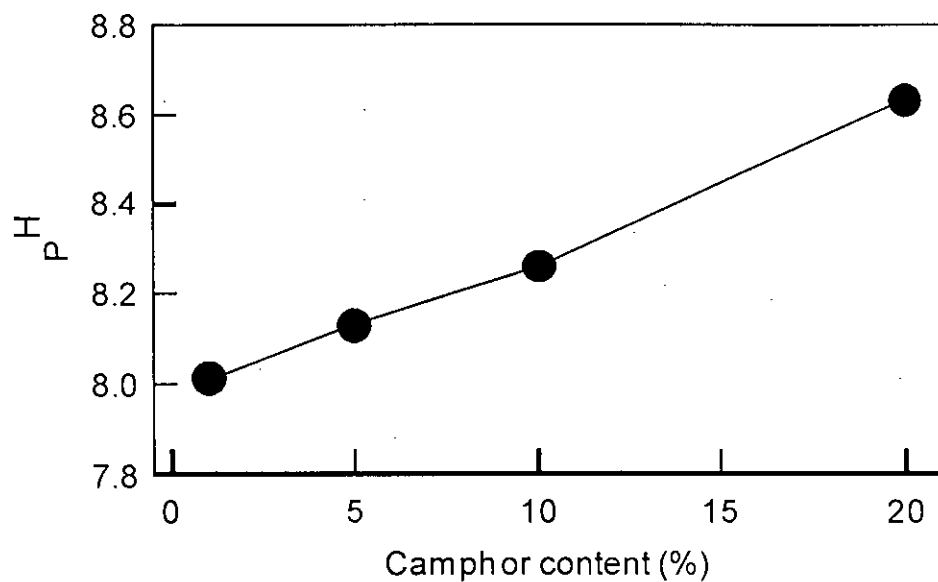
Figure 3.25: P^H as a function of camphor in methanol

3.3.3 Observations in Optical Microscope

Observing physically and by optical microscope it is found that the deposited layer of carbon thin film is different for three substrates. They are shown in figures 3.26 – figures 3.40.

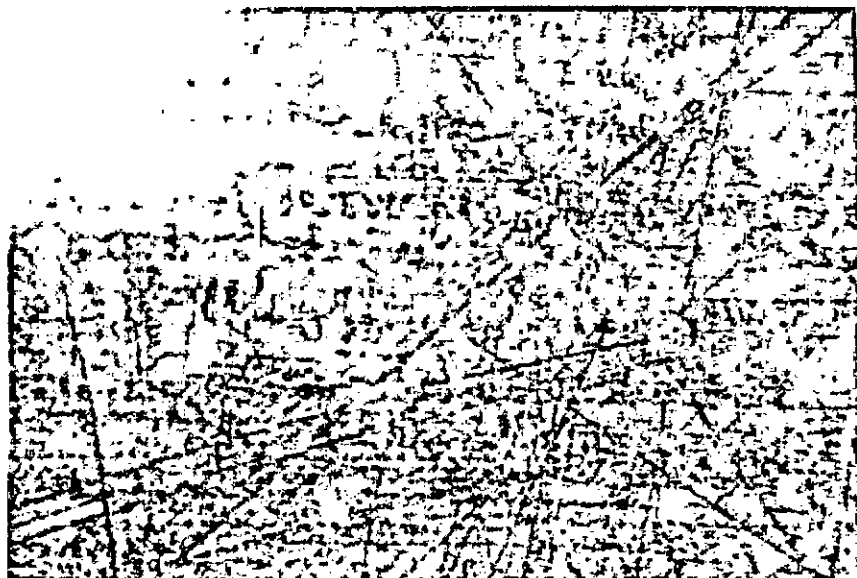Figure 3.26: Pure aluminum substrate observed in optical microscope.

Figure 3.27: Carbon thin film deposited in 0% methanol solution on Al substrate observed in optical microscope.

Figure 3.28: Carbon thin film deposited in 1% methanol solution on Al substrate observed in optical microscope.

Figure 3.29: Carbon thin film deposited in 2% methanol solution on Al substrate observed in optical microscope.

Figure 3.30: Carbon thin film deposited in 4% methanol solution on Al substrate observed in optical microscope.

Figure 3.31: Pure copper substrate observed in optical microscope.

Figure 3.32: Carbon thin film deposited in 0% methanol solution on Cu substrate observed in optical microscope.
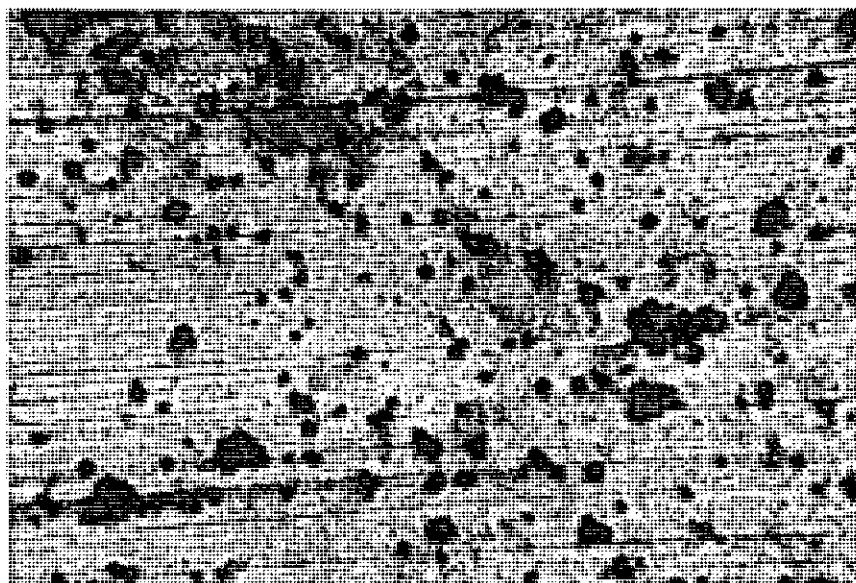
Figure 3.33: Carbon thin film deposited in 1% methanol solution on Cu substrate observed in optical microscope.
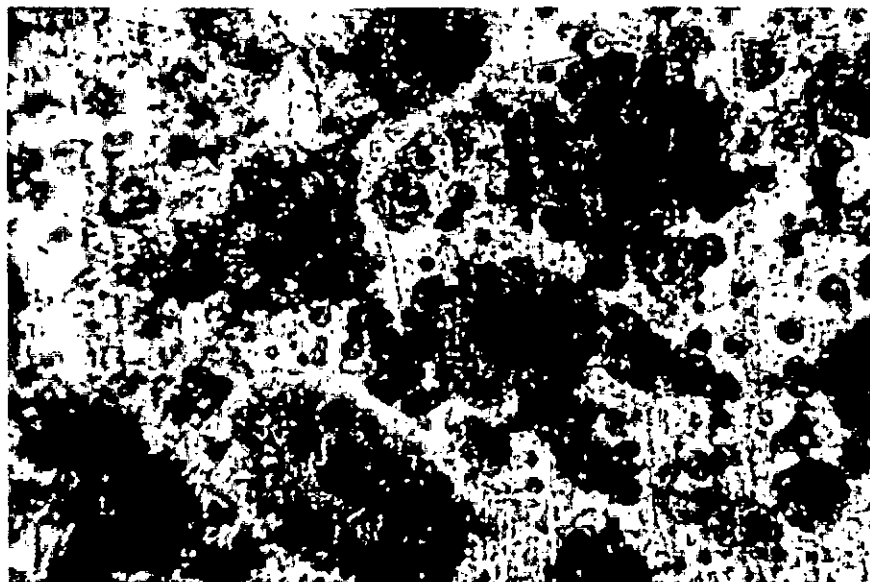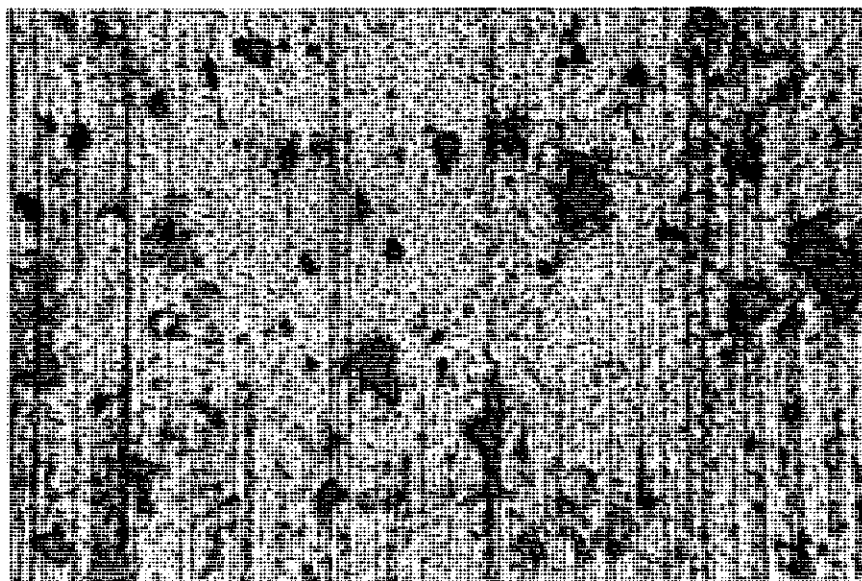
Figure 3.34: Carbon thin film deposited in 2% methanol solution on Cu substrate observed in optical microscope.
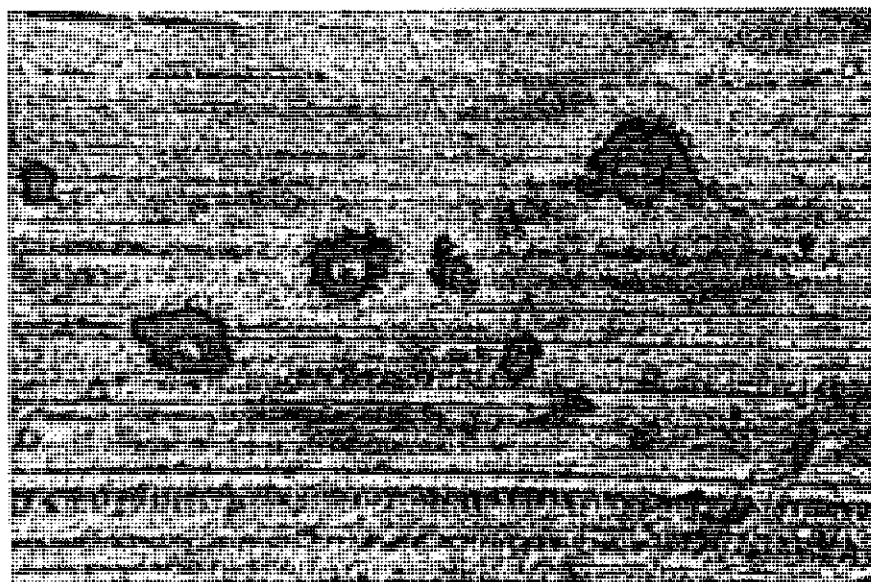
Figure 3.35: Carbon thin film deposited in 4% methanol solution on Cu substrate observed in optical microscope.
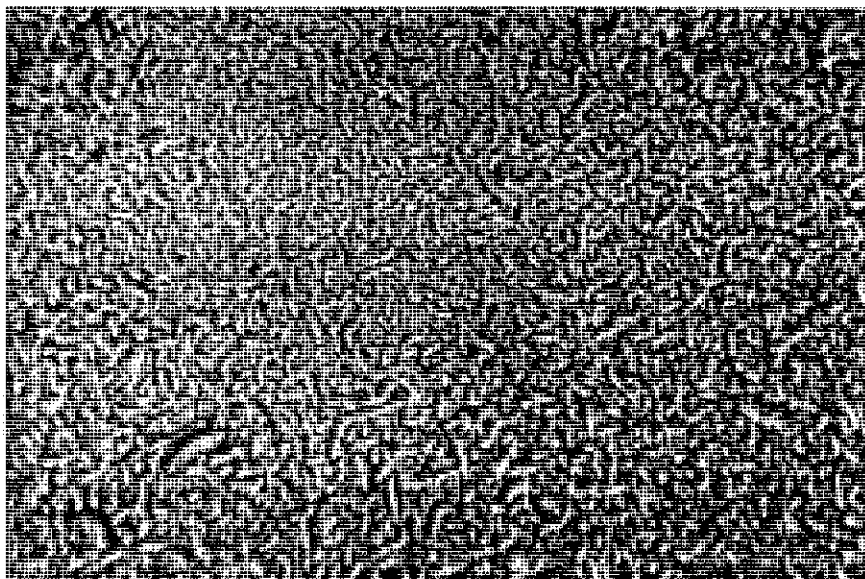
Figure 3.36: Pure silicon substrate observed in optical microscope.

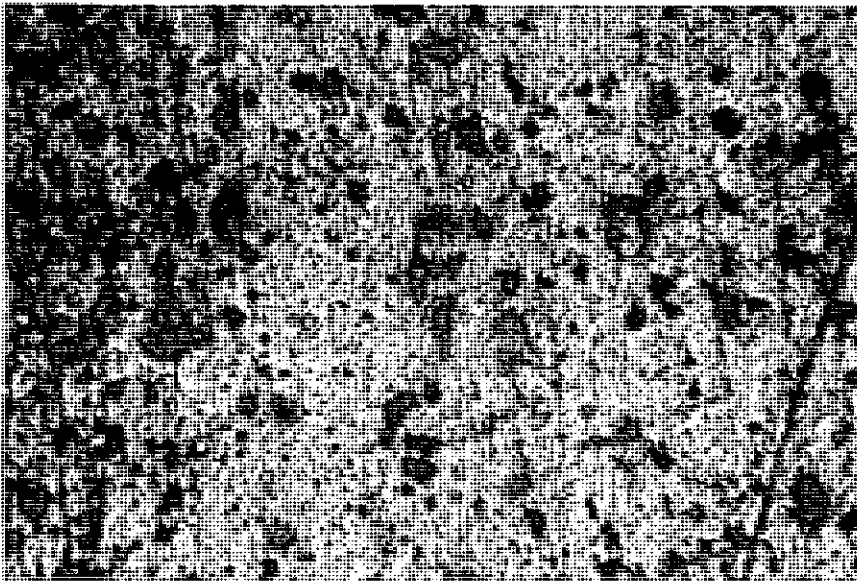Figure 3.37: Carbon thin film deposited in 0% methanol solution on Si substrate observed in optical microscope.
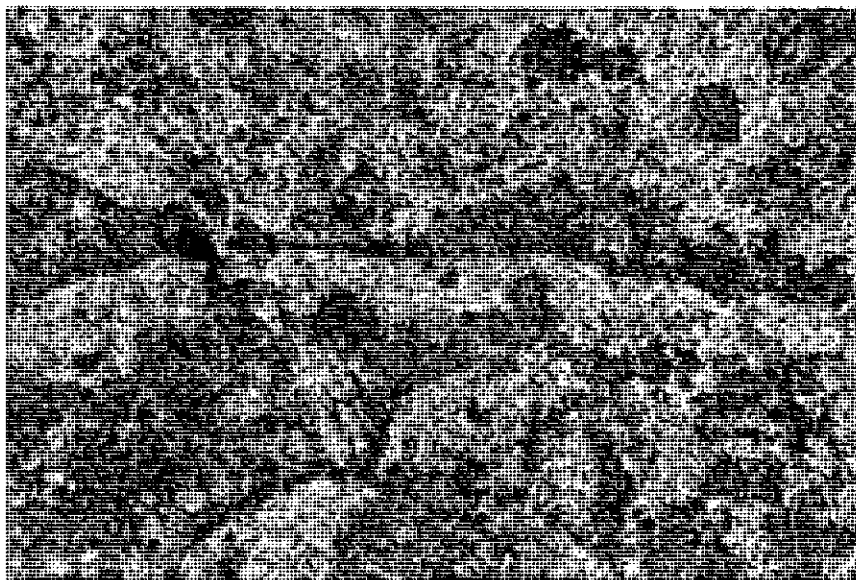
Figure 3.38: Carbon thin film deposited in 2% methanol solution on Si substrate observed in optical microscope.
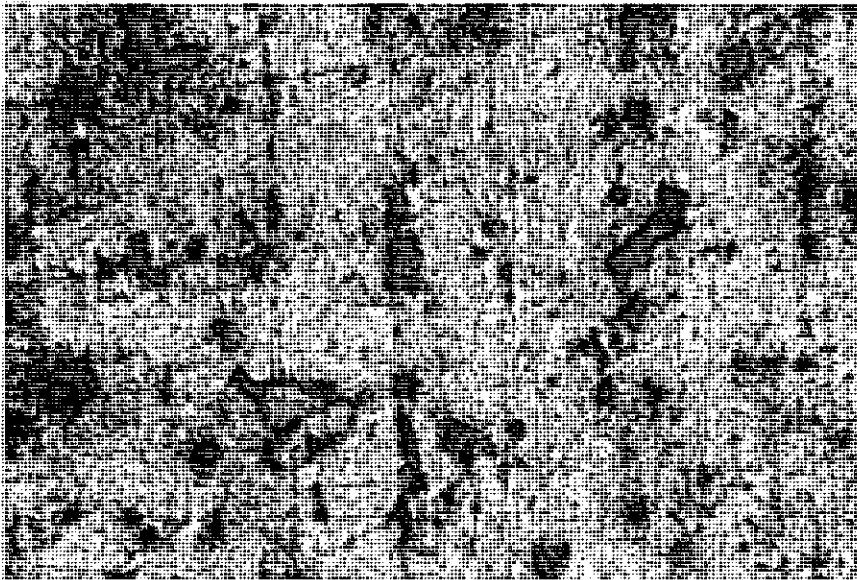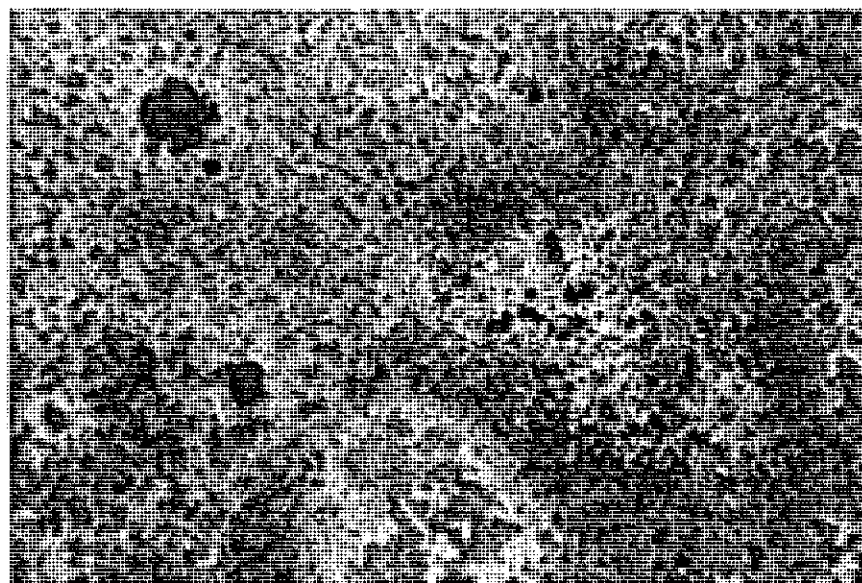

Figure 3.39: Carbon thin film deposited in 6% methanol solution on Si substrate observed in optical microscope.
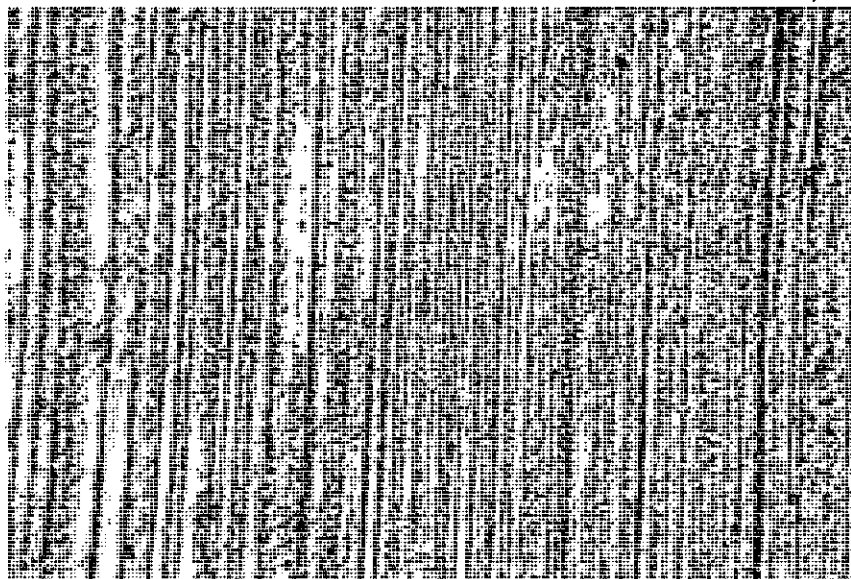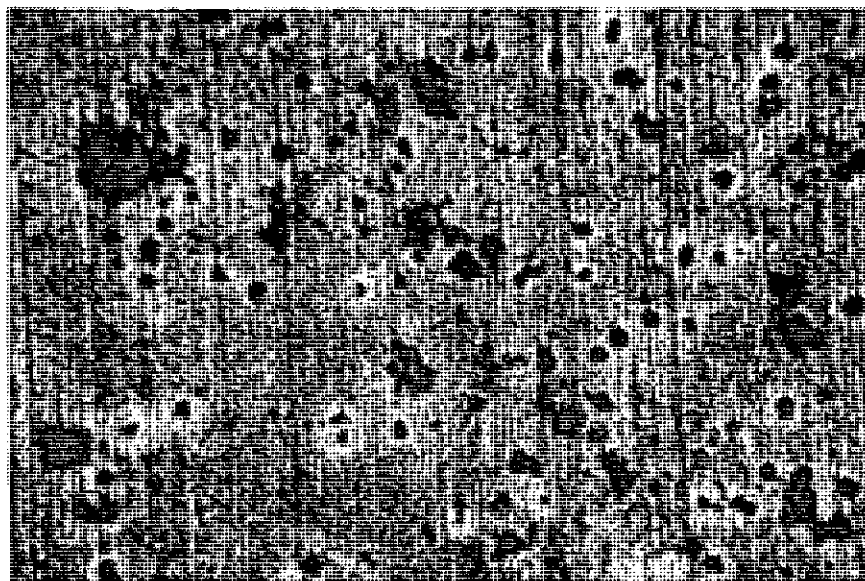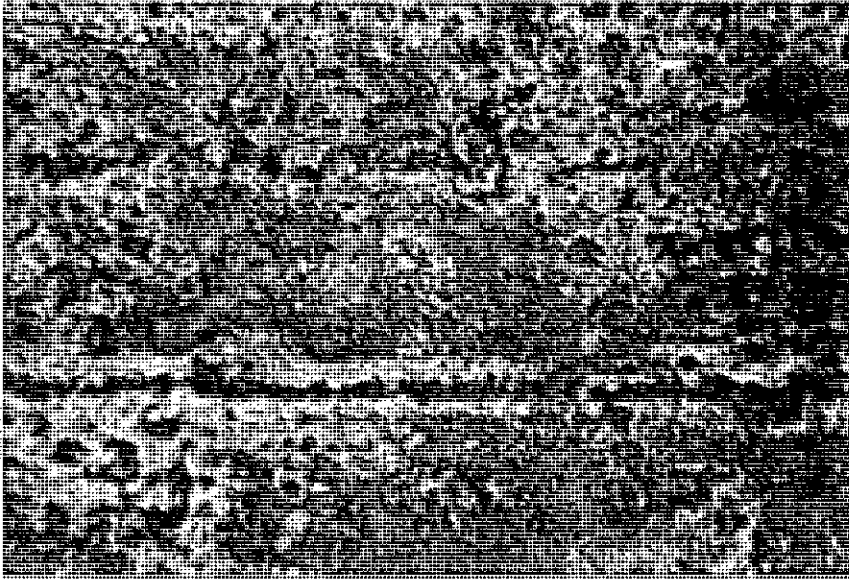
Figure 3.40: Carbon thin film deposited in 8% methanol solution on Si substrate observed in optical microscope.

Observing physically and optical microscope (400X) it is found that for every case there are sharp differences between electrodeposited substrates and pure substrates. These differences indicate formation of films. Again film pattern for different percentage of camphor is different. So camphor has a role on film formation.

3.3.4 SEM Analysis

3.3.4.1 Introduction

In this technology a beam of electrons is sharply focused upon the surface of the specimen and X-ray emitted from the surface are then analyzed spectrally or energetically by a crystal spectrometer or analyzed spectrally or energetically by a crystal spectrometer or proportion counter. The emitted X-ray is analyzed with a dispersive spectrometer, which employs an analyzing crystal to separate characteristic wavelengths from the emitted spectra for identification and measurements of the elements.

Specimen Stage

X-ray Analyzer

X-ray Method
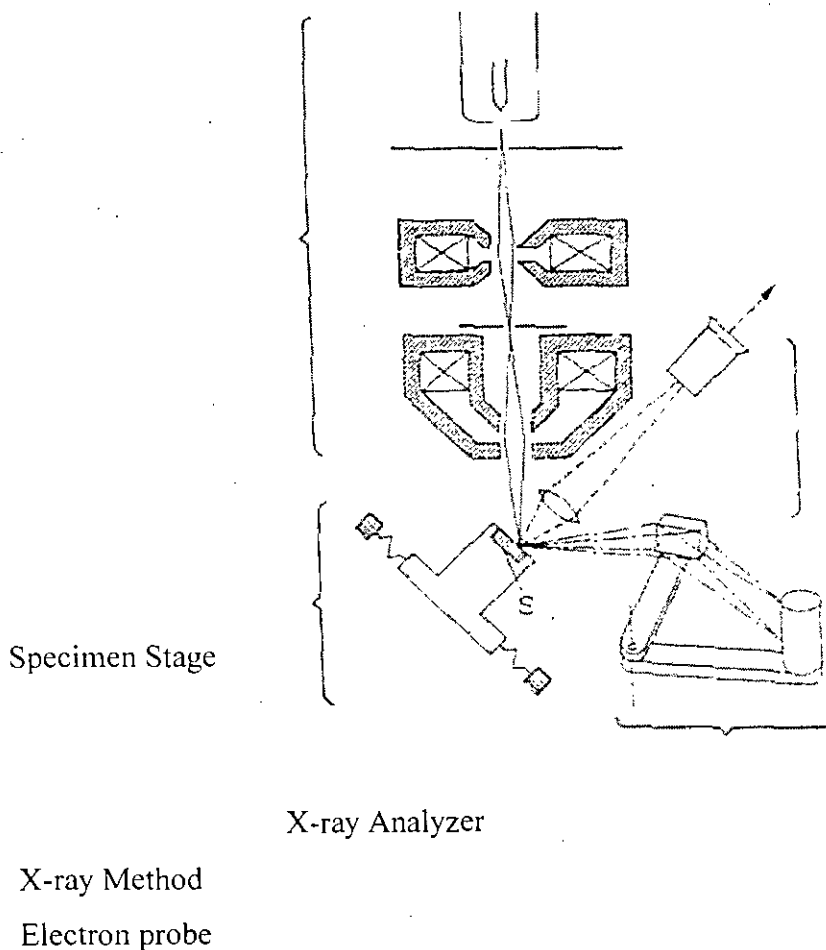
Electron probe

Figure 3.41: Electron Probe Micro Analyzer.

The excitation of the X-rays in the probe depends on a number of factors, such as the number of electrons absorbed, the number of electrons back scattered without energy loss because they do not contribute to X-ray excitation etc.

Samples are given a good flat metallurgical polish (to keep the same path length for emergent X-rays from all points of the surface) and perhaps a light etches to bring out surface features for examination.

3.3.4.2 Film Composition

The morphology of film deposited in methanol and different % camphoric solution in methanol for SEM observes Si, Al and Cu substrate are shown in figures 3.42, 3.43, 3.44, 3.45 and 3.46.
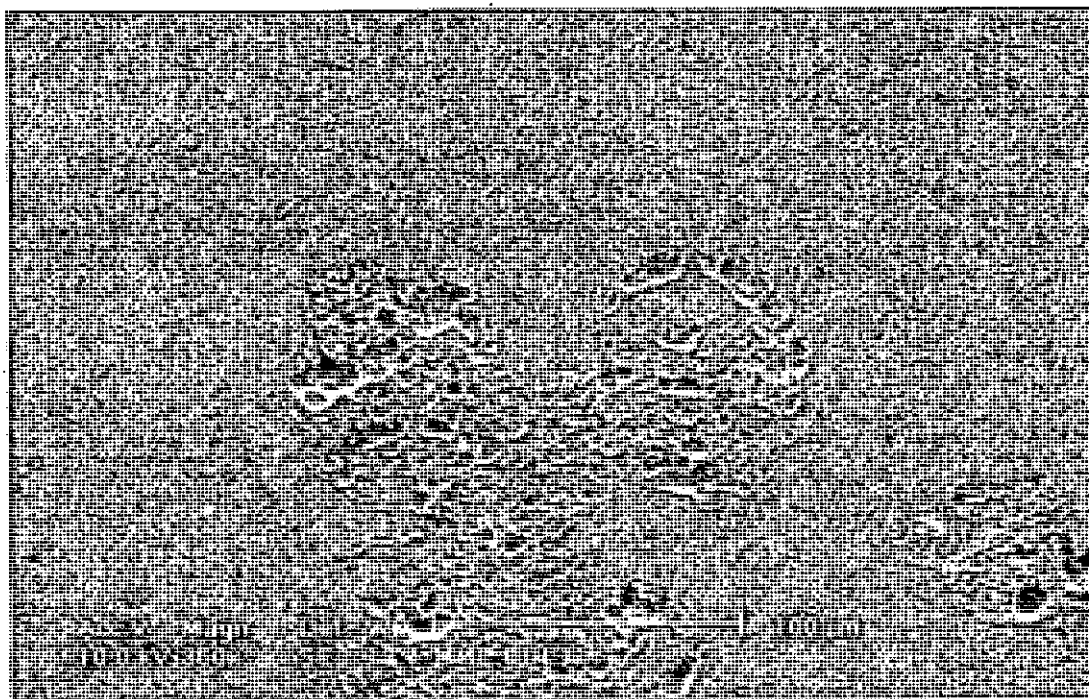
Figure 3.42: SEM micrograph of the film deposited in only methanol solution for 8 hrs and in Si substrate.
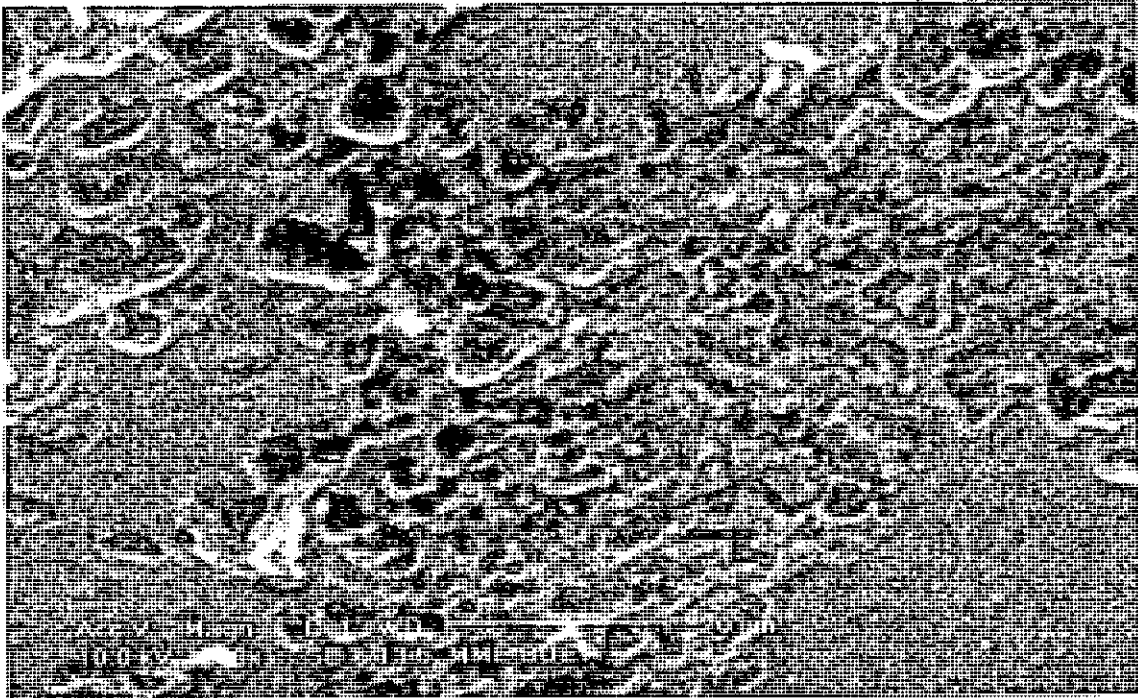
Figure 3.43: SEM micrograph of the film deposited in 6% camphor in methanol solution for 8 hrs and in Si substrate.
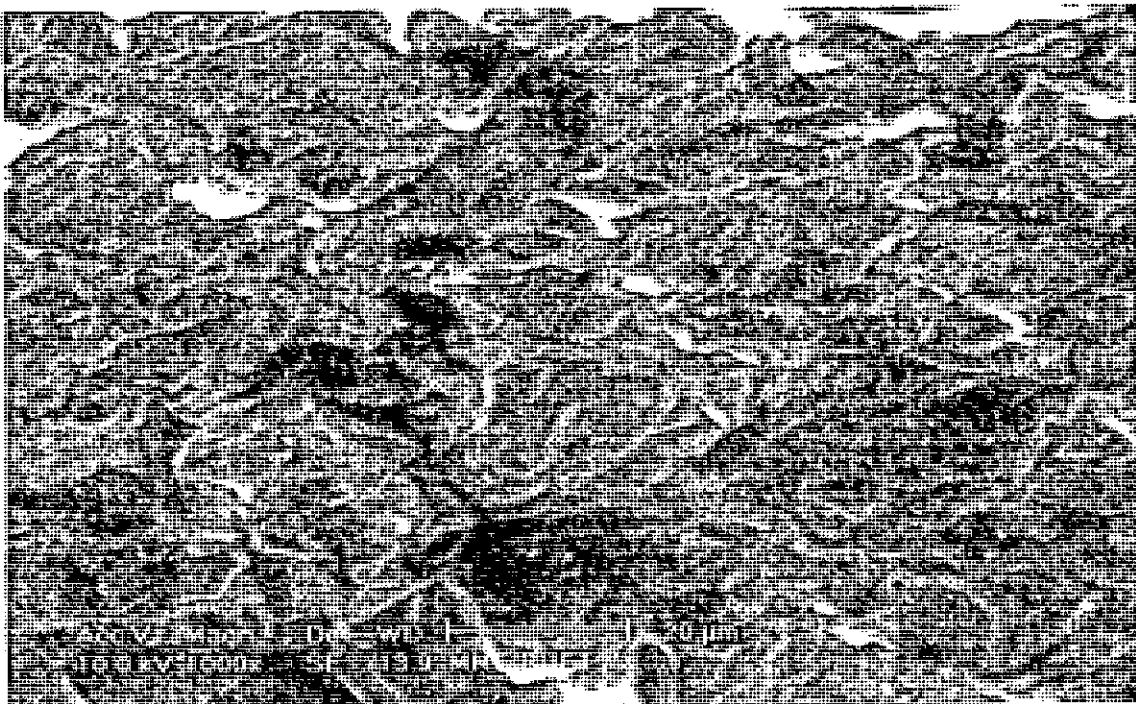
Figure 3.44: SEM micrograph of the film deposited in 2% camphor in methanol solution for 8 hrs and in Al substrate.
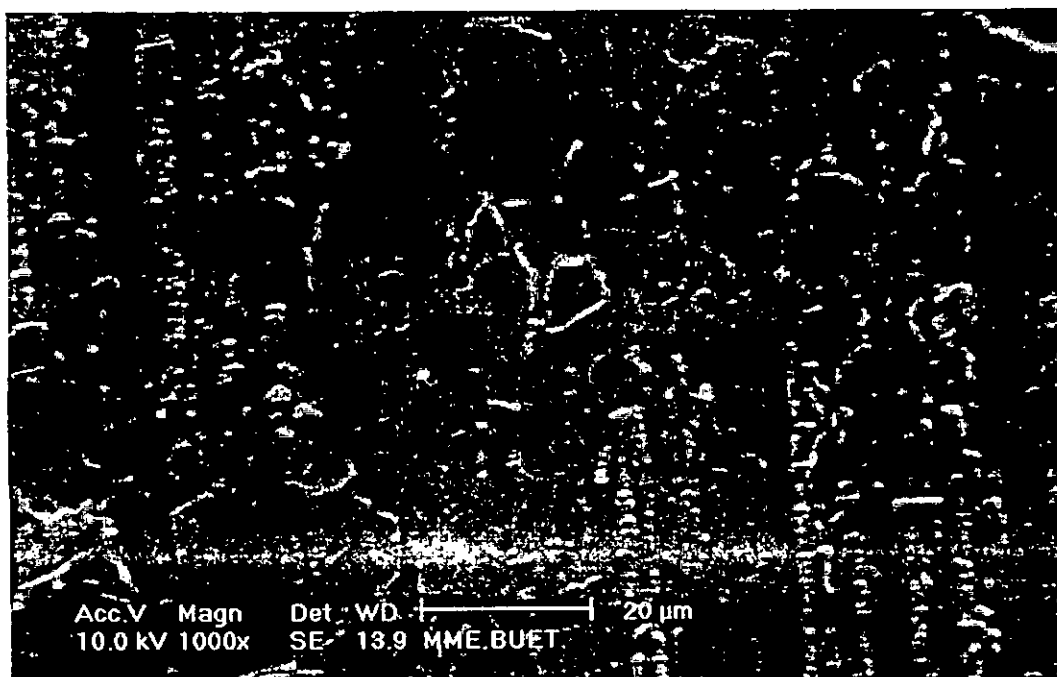
Figure 3.45: SEM micrograph of the film deposited in 2% camphor in methanol solution for 8 hrs and in Cu substrate (Magnification 1000x).
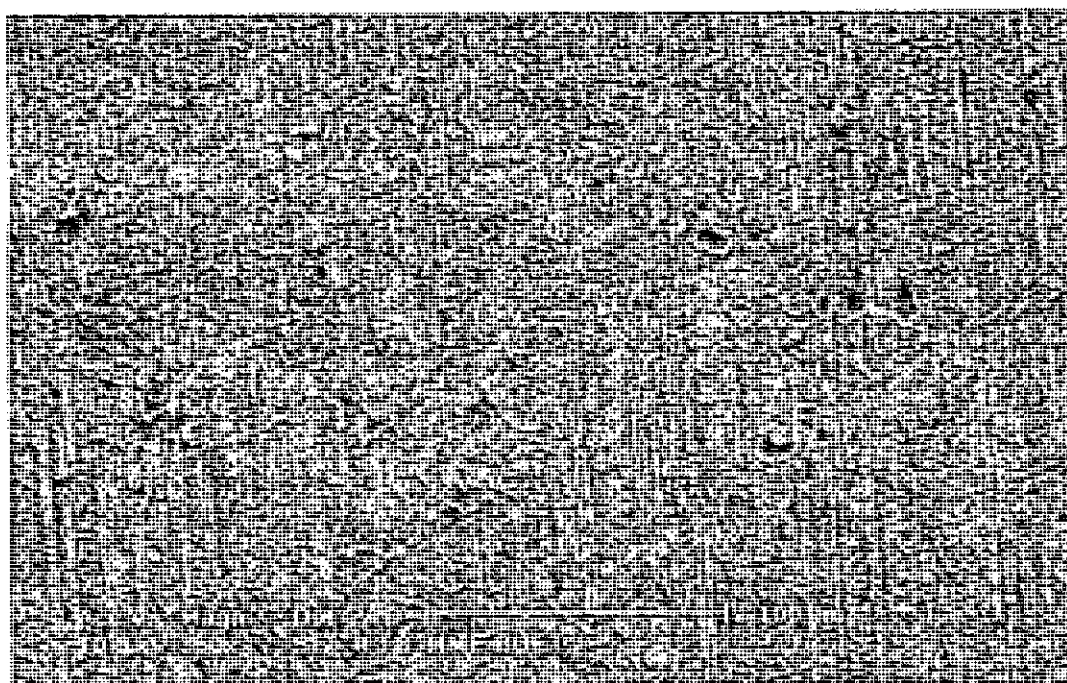
Figure 3.46: SEM micrograph of the film deposited in 2% camphor in methanol solution for 8 hrs and in Cu substrate (Magnification 350x).

Observing by SEM micrograph it is found that there are differences between the micrograph of the electrodeposited films on different substrates. Also changes are observed in micrographs of same electrodeposited substrates for different percentage of camphor. So substrate type and the camphor percentage have influences on carbon thin film formation.

3.3.5 EDS Analysis

1) The composition of the film deposited on Si substrate at three different points are tabulated below:

Table 3.16: Composition of Carbon and Silicon on the film (Si substrate)

Type	Weight %			Atomic %		
Position	1	2	3	1	2	3
C	20.56	13.44	21.15	32.50	22.19	33.37
Si	79.44	86.56	78.85	67.50	77.81	66.63
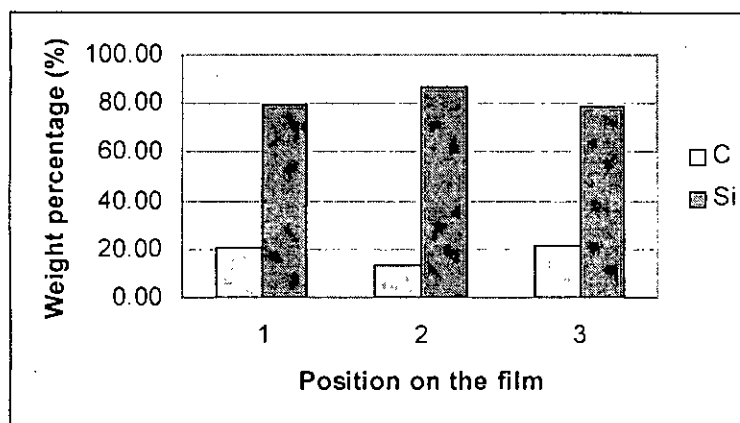
Figure 3.47 bar chart weight % of Carbon and Silicon of the film on Si substrate.
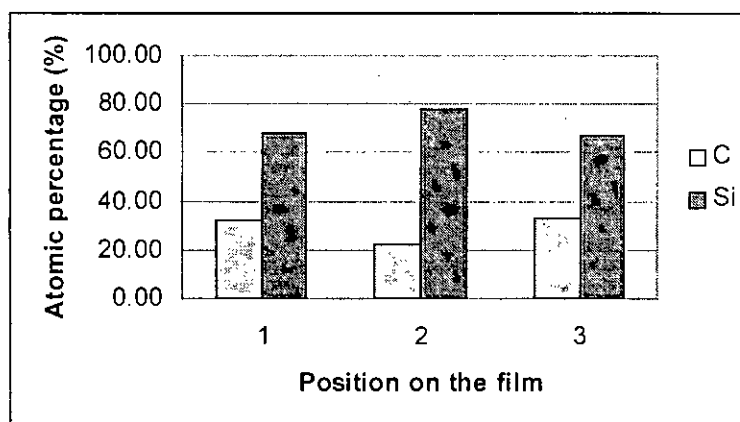
Figure 3.48: Bar chart atomic % of Carbon and Silicon of the film on Si substrate.

2) The composition of the film deposited on Cu substrate at two different points are tabulated below:

Table 3.17: Composition of Carbon and Copper on the film (Cu substrate)

Type	Weight %		Atomic %	
Position	1	2	1	2
C	12.91	13.24	26.76	28.35
Cu	87.09	86.76	73.24	71.65
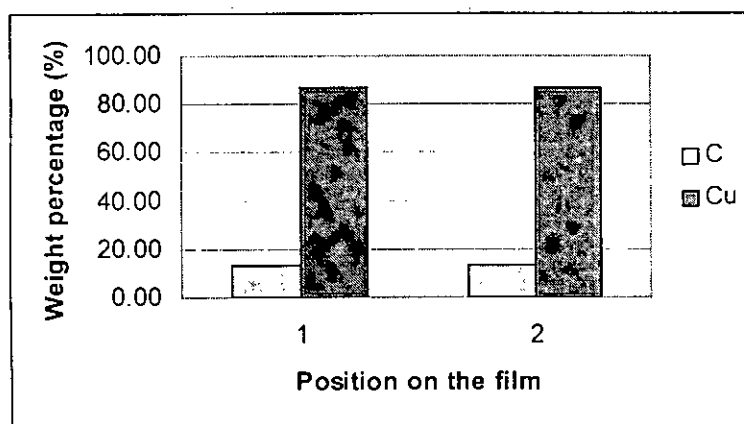
Figure 3.49: Bar chart weight % of Carbon and Copper of the film on Cu substrate.
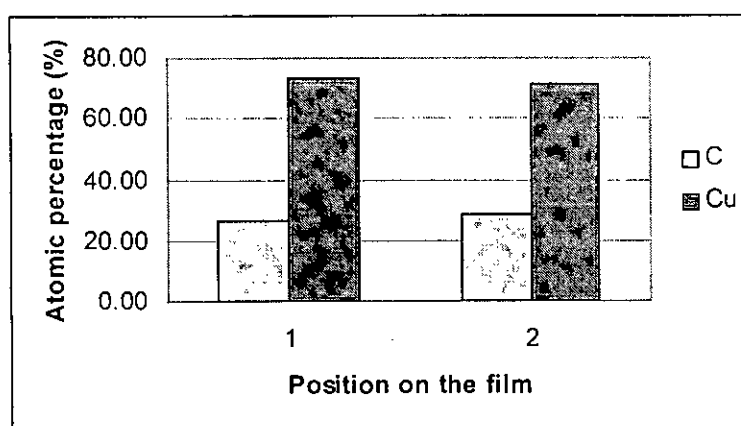
Figure 3.50: Bar chart atomic % of Carbon and Copper of the film on Cu substrate.

3) The composition of the film deposited on Al substrate at two different points are tabulated in table 3.18:

Table 3.18: Composition of Carbon and Aluminum on the film (Al substrate)

Type	Weight %		Atomic %	
Position	1	2	1	2
C	9.63	12.21	14.76	19.54
Al	90.37	87.79	85.24	80.46
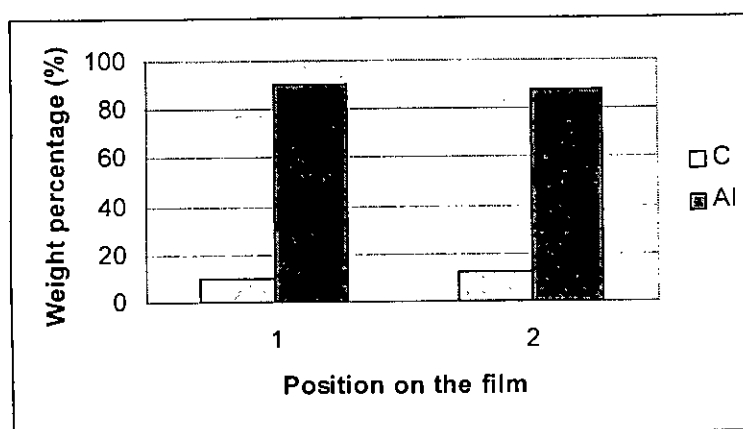
Figure 3.51: Bar chart weight % of Carbon and Aluminum of the film on Al substrate.
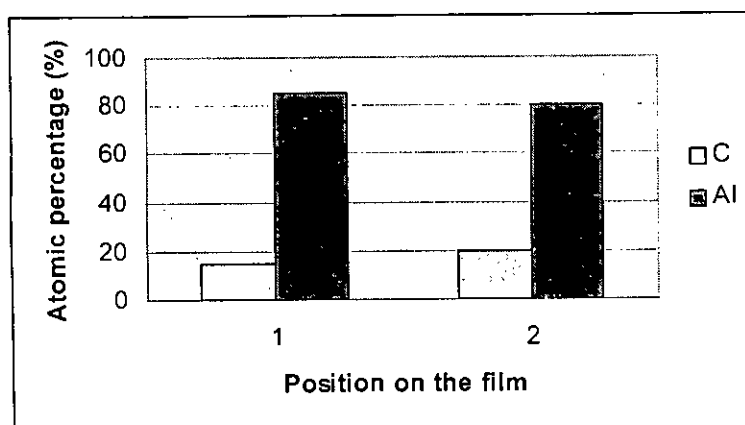
Figure 3.52: Bar chart atomic % of Carbon and Aluminum of the film on Al substrate.

From the above composition analysis and bar charts there are indications that certain carbon films are there. Also from the tables and related charts it is very clear to us that, percentage of carbon on the electrodeposited substrate is maximum for Si substrate.

The deposited layer of thin carbon film is different for three substrates. Si has got the most distinct and relative "thick" layer of thin film than Cu and Al substrates. Also from current density vs applied voltage characteristics, Silicon shows higher current density than Al and Cu. So the chemical affinity between C and Si is higher than Al and Cu. They form a compound Si_xC that accelerate carbon deposition over Si substrate.

3.3.6 FTIR Spectroscopy

3.3.6.1 C-H Vibrational Modes in FTIR

The C-H vibrational modes produce a series of infrared absorption peaks, which can provide very detailed information on the local C-H bonding [46]. It is possible to assign each peak to a different carbon configuration – sp^3, olefinic sp^2 or sp^1 – and the number of hydrogen neighbors. One may approximate that only the H moves in this modes, due to the large difference in C and H masses. Each configuration gives rise to one C-H stretching mode per H atom at around 3000 cm^{-1}, plus two further deformation modes per atom below 1500 cm^{-1}. All modes are FTIR sensitive except the A_2 twisting modes. Detail is listed in table 3.19 and table 3.20

According to the vibrational modes in infrared spectroscopy (table 3.19 and table 3.20) in case of FTIR spectroscopy measurement for percentage photon energy transmission (%T) against the inverse wavelength (cm^{-1}) a peak (minima) around 2850 cm^{-1} [40] indicates low relative percentage transmission of photon energy or prominent absorption of photon energy at that wavelength and it indicates existence of sp^3 C-H stretch.

Similarly in case of FTIR spectroscopy measurement for percentage photon energy transmission (%T) against the inverse wavelength (cm^{-1}) a peak (minima) around 2950 cm^{-1} [40] indicates low relative percentage transmission of photon energy or prominent absorption of photon energy at that wavelength and it indicates existence of sp^2 C-H stretch.

In case of FTIR spectroscopy measurement for percentage photon energy transmission (%T) against the inverse wavelength (cm^{-1}) very low relative percentage transmission of photon energy in the range of 1000 cm^{-1} to 2000 cm^{-1} indicates prominent absorption of photon energy [40] at that wave length range and it indicates existence of amorphous carbon (C-H) bond.

Table 3.19: C-H infrared vibrational mode assignments in a-C: H.

Line	Wave number, cm^{-1}		Dischler assignment		New assignment configuration
	Hard a-C: H	Soft a-C: H	Configuration	Symmetry	
1	3300	3300	sp^1 CH	A s	
2	3045	3060	Arom sp^2 CH	A s	
3		3025	Olef sp^2 CH$_2$	B$_1$ as	
4	3000	3000	Olef sp^2 CH	A s	
5		2970	sp^3 CH$_3$	E sd	
6		2945	Olef sp^2 CH$_2$	A$_1$ ss	
7	2920	2920	sp^3 CH$_2$	B$_1$ as	
8	2920		sp^3 CH	A$_1$ s	
9		2875	sp^3 CH$_3$	A$_1$ ss	
10	2850	2850	sp^3 CH$_2$	A$_1$ ss	
11		1490	sp^3 CH$_3$	E dd	
12		1450	Olef sp^2 CH$_2$	A$_1$ scissors	
13	1440	1450	sp^3 CH$_2$	A$_1$ scissors	
14	1435	1445	Arom sp^2 CH	A bend	
15	1370		sp^3 CH	E bend	Unassigned
16		1325	sp^3 CH$_3$	A$_1$ sd	sp^3 CH$_2$ B$_2$ wag
17	1290	1280	Olef sp^2 CH	A bend	
18	1170	1180	sp^3 CH$_2$	A$_2$ twist	sp^3 CH E bend
19		1110	Olef sp^2 CH$_2$	B$_2$ wag	
20		1075	sp^3 CH$_3$	E dd	
21	1030	1030	sp^3 CH$_2$	B$_2$ wag	sp^3 CH$_2$ B$_1$ rock
22	910	910	Olef sp^2 CH$_2$	A$_2$ twist	
23	840	840	Olef sp^2 CH	B bend	
24	755	755	Arom sp^2 CH	B bend	
25		700	sp^1 CH	E bend	
26		700	Olef sp^2 CH$_2$	B$_1$ rock	
27	700	700	sp^2 CH$_2$	B$_1$ rock	

Modes 1-10 are C-H stretch, lines 11-27 are C-H deformation. s = stretch, ss = symmetric stretch, as = antisymmetric stretch, sd = symmetric deformation, dd = degenerate deformation.

Table 3.20: C-H infrared vibrational mode assignments in a-C: H, after Dischler.

Line	Wave number, cm^{-1}	Assignment
1	2180	sp^1
2	1620-1600	Olef sp^2
3	1580	Arom sp^2
4	1515	Mixed sp^2/sp^3
5	1300-1270	Mixed sp^2/sp^3
6	1245	Mixed sp^2/sp^3
7	1160	sp^3
8	970	Olef sp^2
9	885-855	sp^3
10	840	Arom sp^2

3.3.6.2 FTIR Spectroscopy curves of few samples

Percentage optical transmittance for few electrodeposited substrates of Al, Cu and Si are measured against wave number by a FTIR spectrometer named "SHIMADZU FOURIER TRANSFORM INFRARED SPECTROPHOTOMETER".

Model no. FTIR - 8400 (P/N 206 - 71000)

     FTIR - 8900 (P/N 206 - 70900)

Flowing are the FTIR spectroscopy curves of few films of Al, Cu and Si (Figure 3.53 to Figure 3.56).

Figure: 3.53 FTIR spectroscopy curve for Si (with 0% camphor in methanol), Si (with 6% camphor in methanol) and Si (with 8% camphor in methanol) of 4.5 hour (Full Curve).

(a) Al with 4% camphor in methanol

(b) Cu with 4% camphor in methanol

Wave Number (cm⁻¹)
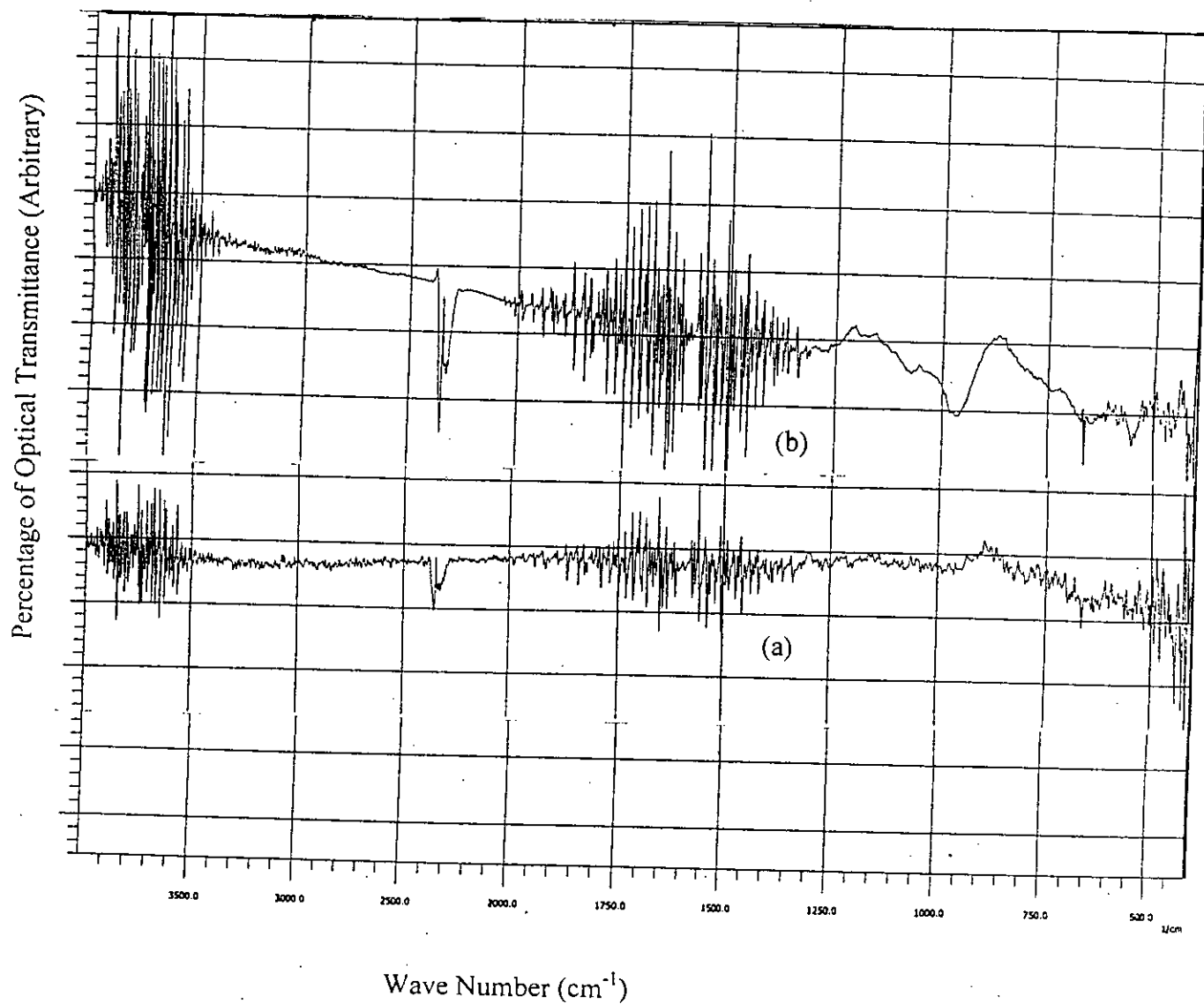
Figure: 3.54 FTIR spectroscopy curve for Al (with 4% camphor in methanol) and Cu (with 4% camphor in methanol) of 4.5 hour (Full Curve).

(a) Only methanol

(b) 6% camphor in methanol

(c) 8% camphor in methanol

Figure: 3.55 FTIR spectroscopy curve for Si (with 0% camphor in methanol), Si (with 6% camphor in methanol) and Si (with 8% camphor in methanol) of 4.5 hour (Magnified part from 2500 cm^{-1} to 3000 cm^{-1}).

(a) Only methanol

(b) 6% camphor in methanol
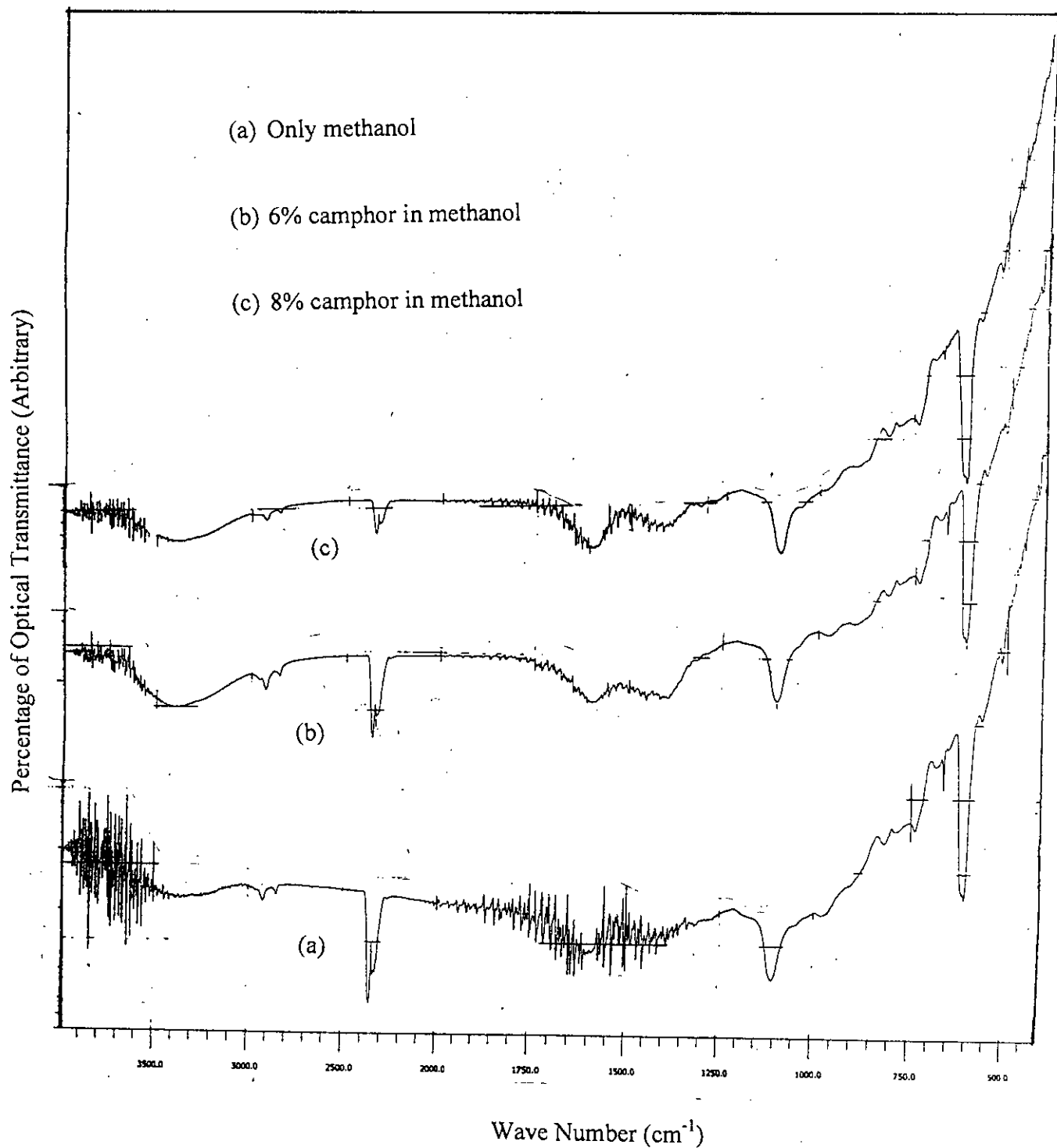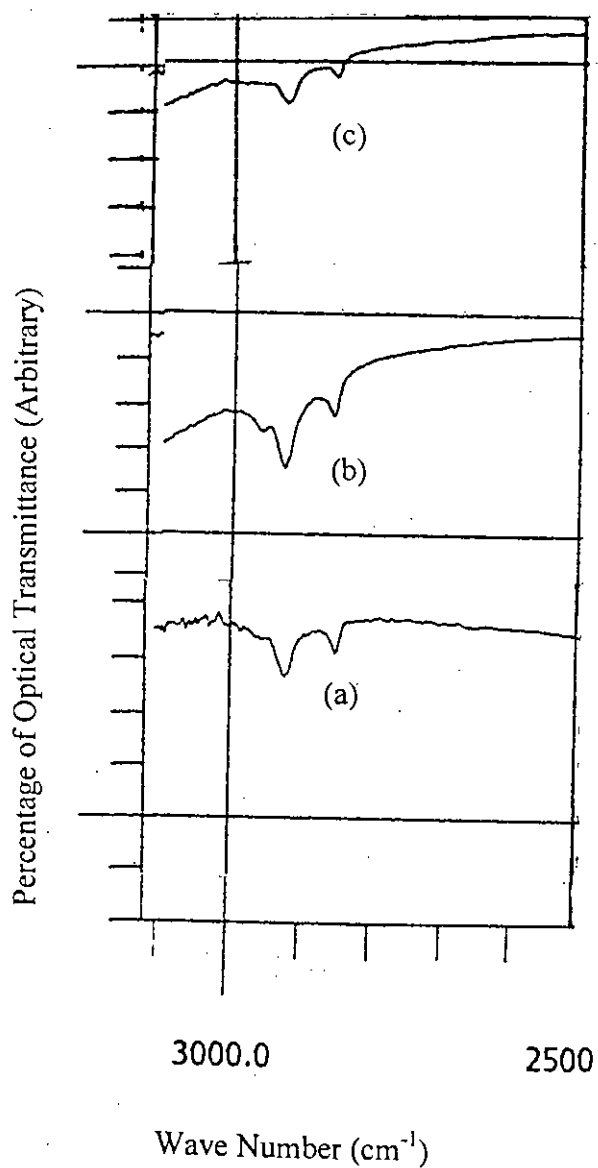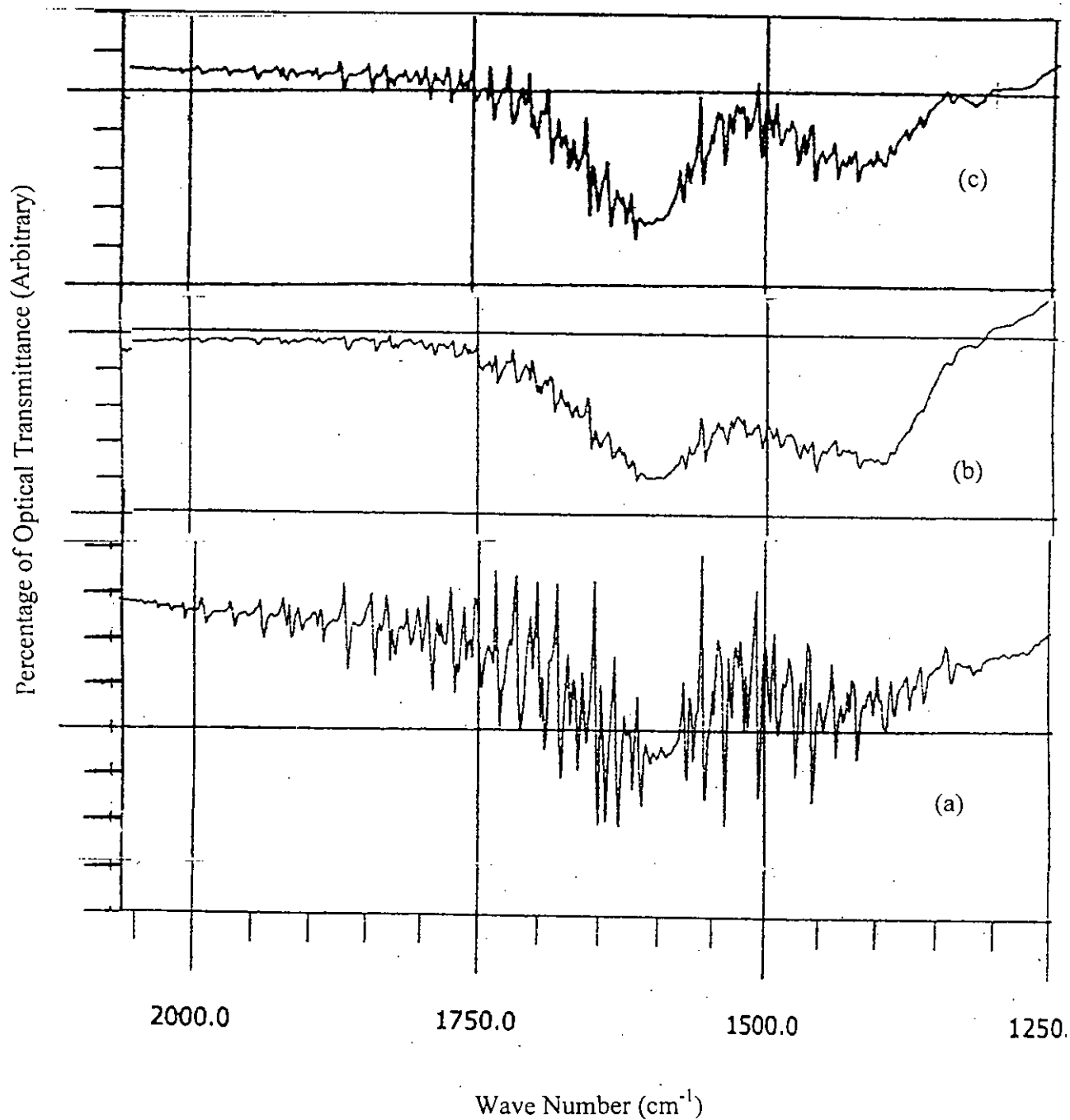
(c) 8% camphor in methanol

Figure: 3.56 FTIR spectroscopy curve for Si (with 0% camphor in methanol), Si (with 6% camphor in methanol) and Si (with 8% camphor in methanol) of 4.5 hour (Magnified part from 1250 cm^{-1} to 2000 cm^{-1})

Now in our analysis of the above figures (figure 3.53 to 3.56) of FTIR spectroscopy measurement it is observed that there are few indications of amorphous carbon and sp^2/sp^3 bonding in Si film, which is our main objective. But Al and Cu do not show such type of properties.

3.3.6.3 Measurement of the ratio of sp^3/sp^2 from the FTIR Spectroscopy measurement curves of few Si samples

In the figures of 3.53, 3.55 we observe that for each FTIR spectroscopy measurement of Si substrate there are two peaks (minima) along with a portion of bent curve in the region of 2500 cm^{-1} to 3000 cm^{-1}. If a straight line is drawn on each curve over the portion of sp^2 C-H stretch and sp^3 stretch ate area between the straight line and the curve will indicate the percentage of corresponding sp^2 or sp^3 bonding in the film. Using this technique we can calculate the ratio sp^3/sp^2 for any sample. The calculated areas, sp^3/sp^2 ratio and the corresponding camphor content in methanol for Si samples are listed in table 3.21.

Table 3.21 ratio of sp^3/sp^2 for different percentage of camphor in methanol for few Si substrate samples

% Of camphor with methanol solution on Si substrate	Area under sp^2 curve (no. of small squares in graph paper)	Area under sp^3 curve (no. of small squares in graph paper)	sp^3/sp^2 Ratio
0%	7.75	3.50	0.45
6%	8.00	5.25	0.66
8%	4.00	2.25	0.56

From the table 3.21 and the figure 3.57 it is very clear to us that the ratio sp^3/sp^2 can be controlled by camphor incorporation in methanol. And interestingly percentage of camphor for maximum sp^3/sp^2 ratio (0.66) is same as that for maximum current density (6% camphor). Initially by adding 6% camphor the ratio increases from 0.45 (0% camphor) to 0.66 again it decreases to 0.56 for 8% camphor. So by using this technique

we can vary the optical band gap by changing sp^3/sp^2 ratio and change carbon thin film characteristics.
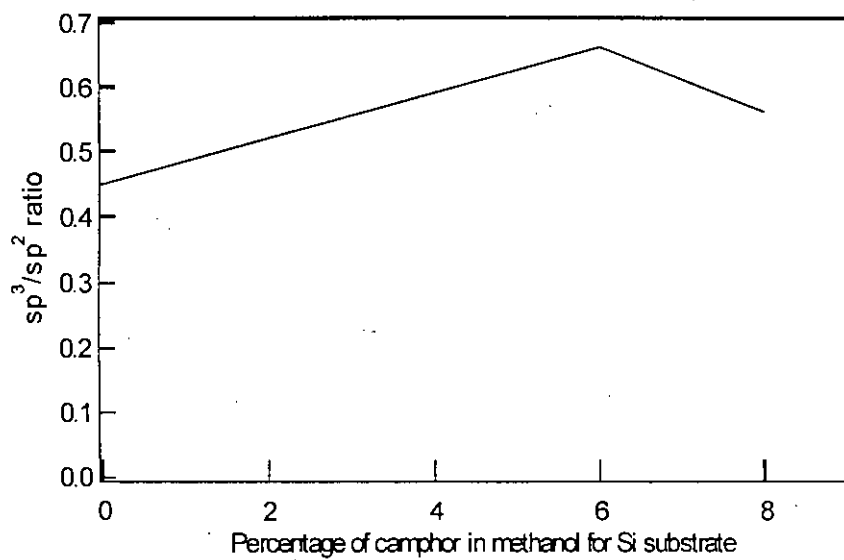
Figure: 3.57 sp^3/sp^2 ratio as a function of % camphor in methanol for Si substrate

3.3.7 Study of thin films by UV-VIS-NIR

When light energy is incident on a substrate, then whether the photon of energy incident will be absorbed or transmitted depends on the optical band gap (E_g) of the substrate and amount of photon energy (hv) incident.

$$E_g = E_c - E_v$$
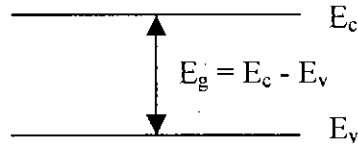
Figure 3.58: Energy band diagram of a substrate

The photon energy hv is found by the following equation

$$hv = (hc)/\lambda = 1243/\lambda \dots\dots\dots\dots\dots\dots\dots\dots\dots\dots\dots\dots [3.1]$$

Here, h = Plank's constant

v = Frequency of photon energy

c = Velocity of light wave

λ = Wavelength of photon energy in nanometer.

If the photon energy (hv) is greater than the band gap energy E_g then the energy will be absorbed by the substrate. If the photon energy (hv) is less than the band gap energy E_g then the energy will be transmitted through the substrate

3.3.7.1 Measurement of optical transmittance, reflectance and absorption for Si with 0% and 6% camphor using UV-VIS-NIR technique.

Two-carbon thin film of silicon substrate one with only methanol and one with 6% of camphor in methanol are deposited 4.5 hour maintaining same average current density. These are characterized through UV-VIS-NIR for percentage transmittance (%T), percentage reflectance (%R) and as well as for percentage absorption (%A) [%A is calculated from %T and %R] against light beam of several wavelengths ranging from 300 nanometer to 2500 nanometer.

The experiment is carried out in an instrument named "UV-VIS-NIR RECORDING SPECTROPHOTOMETER".

Model no. UV - 3100

Then few curves are plotted. % T vs wavelength for silicon with 0% camphor is plotted in figure 3.59. % T vs wavelength for silicon with 6% camphor is plotted in figure 3.60. The curve of figure 3.59 and 3.60 is summarized in figure 3.61. % R vs wavelength for silicon with 0% camphor is plotted in figure 3.62. % R vs wavelength for silicon with 6% camphor is plotted in figure 3.63. The curve of figure 3.62 and 3.63 is summarized in figure 3.64. % A vs wavelength for silicon with 0% camphor is plotted in figure 3.65. % A vs wavelength for silicon with 6% camphor is plotted in figure 3.66. The curve of figure 3.65, 3.66 is summarized in figure 3.67.
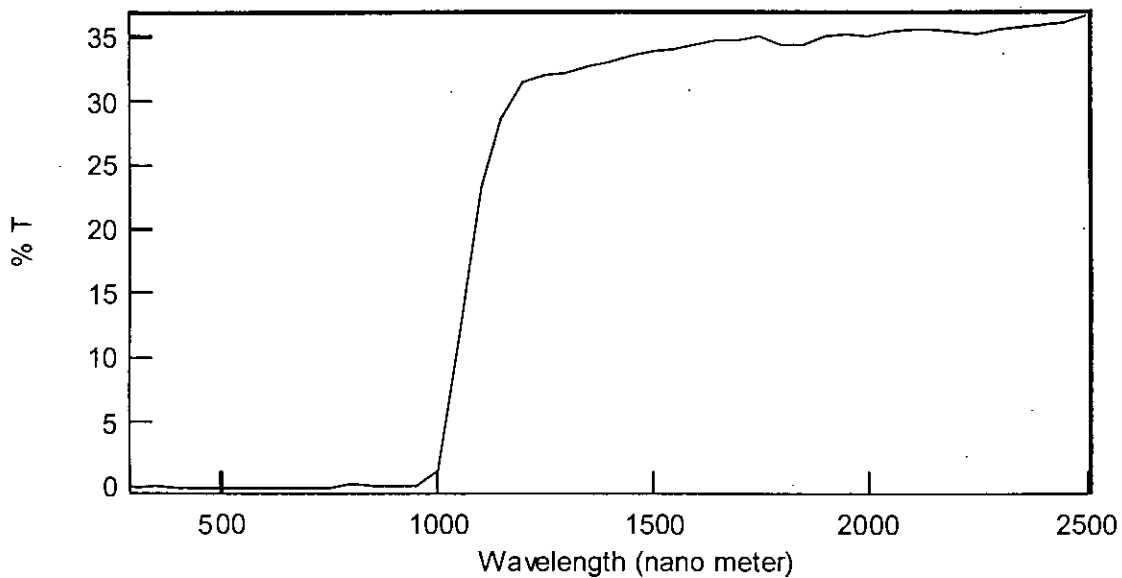
Figure: 3.59 % T vs wavelength (nanometer) for silicon with 0% camphor
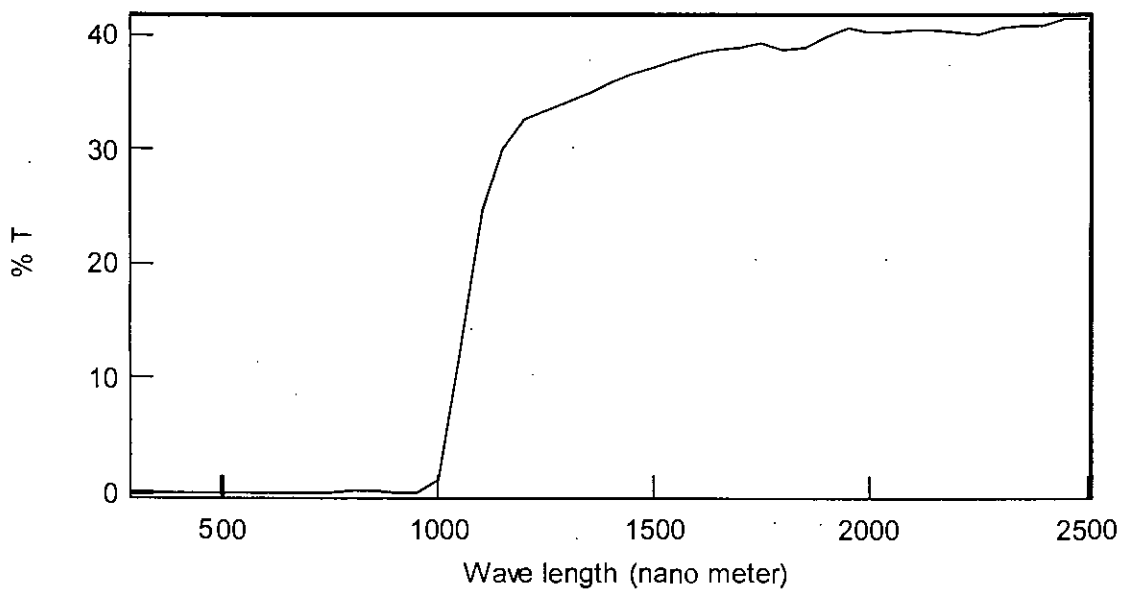
Figure: 3.60 % T vs wavelength (nanometer) for silicon with 6% camphor
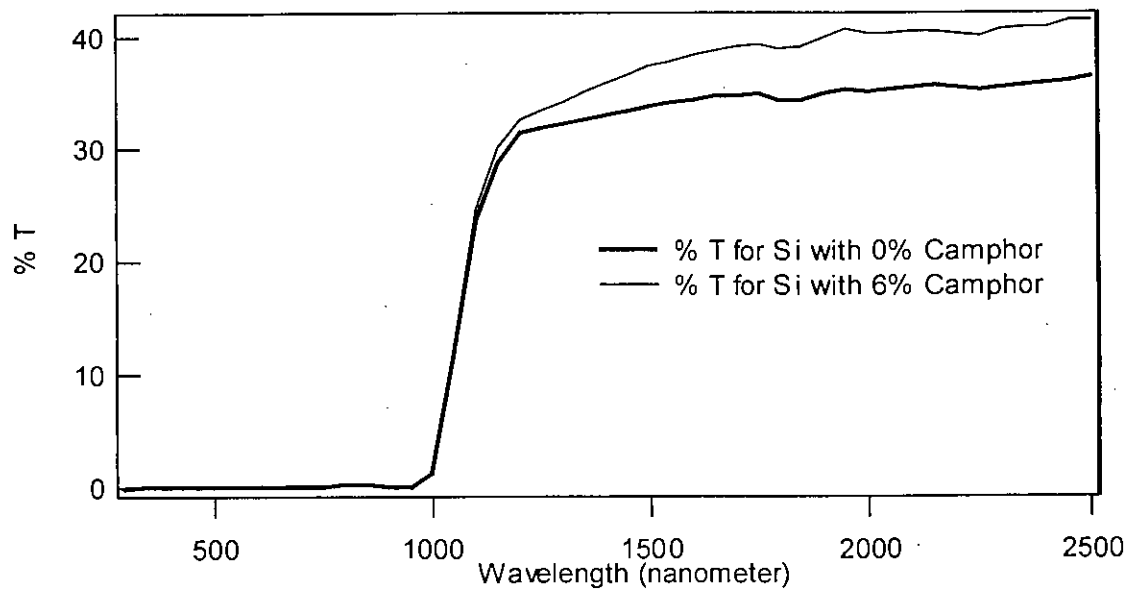
Figure: 3.61 % T vs wavelength (nanometer) for silicon with 0% and 6% camphor
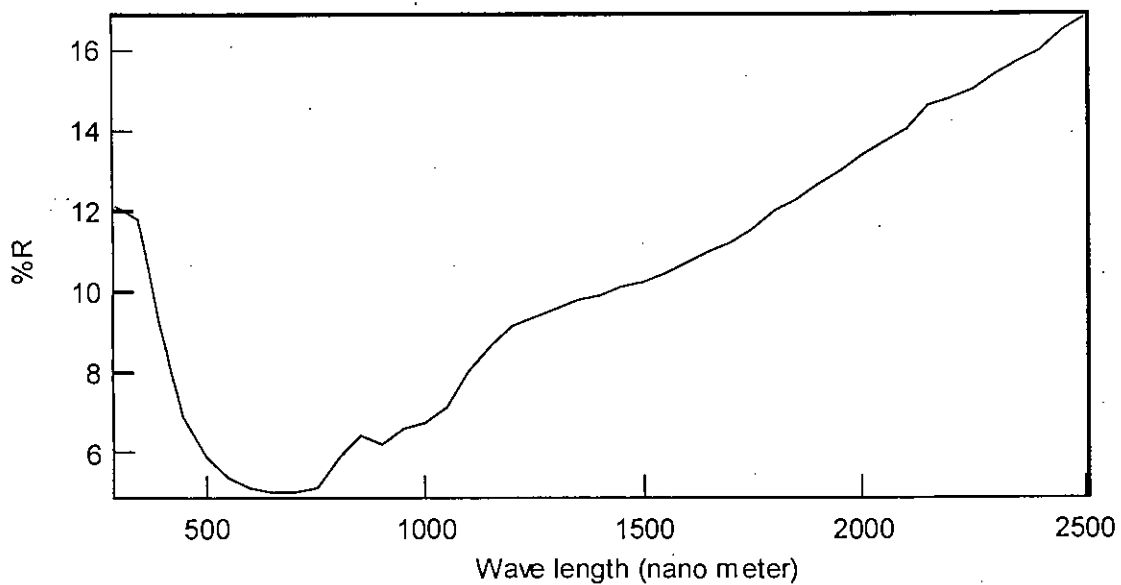
Figure: 3.62 %R vs wavelength (nanometer) for silicon with 0% camphor
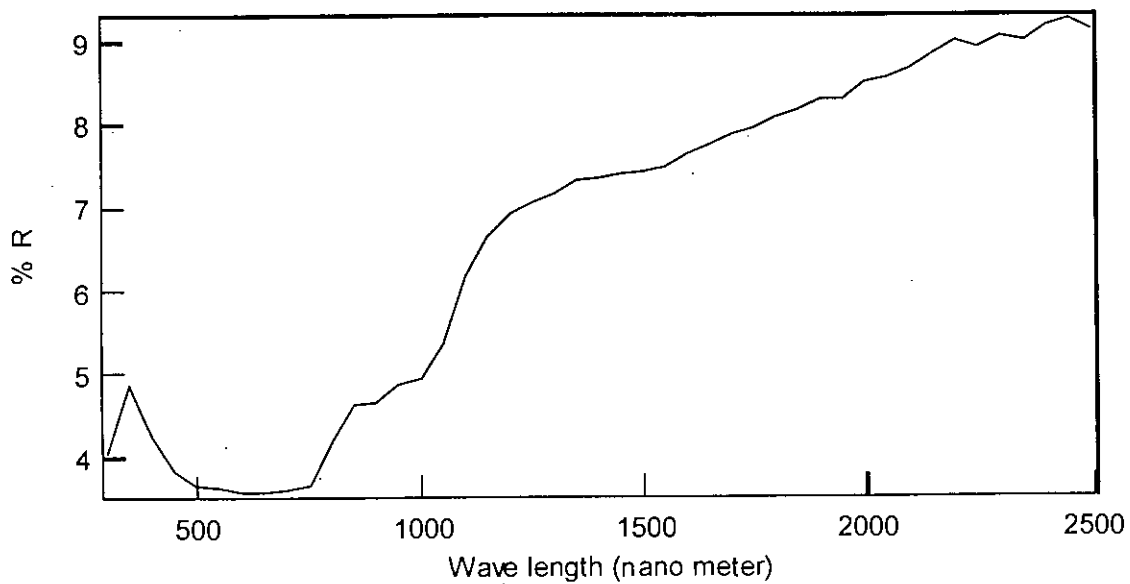
Figure: 3.63 % R vs wavelength (nanometer) for silicon with 6% camphor
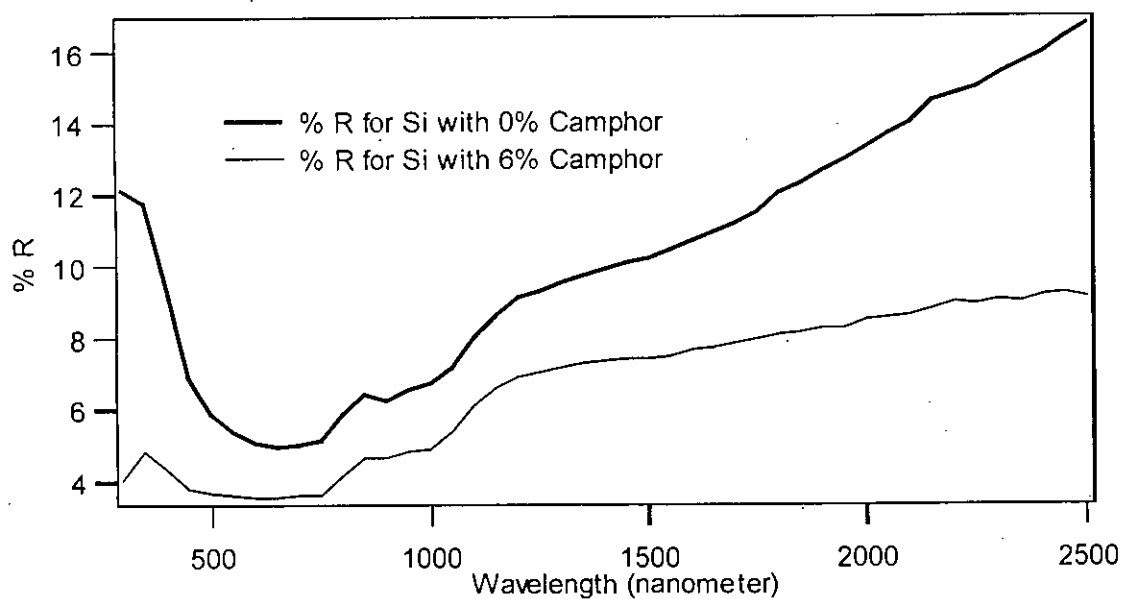
Figure: 3.64 % R vs wavelength (nanometer) for silicon with 0% and 6% camphor
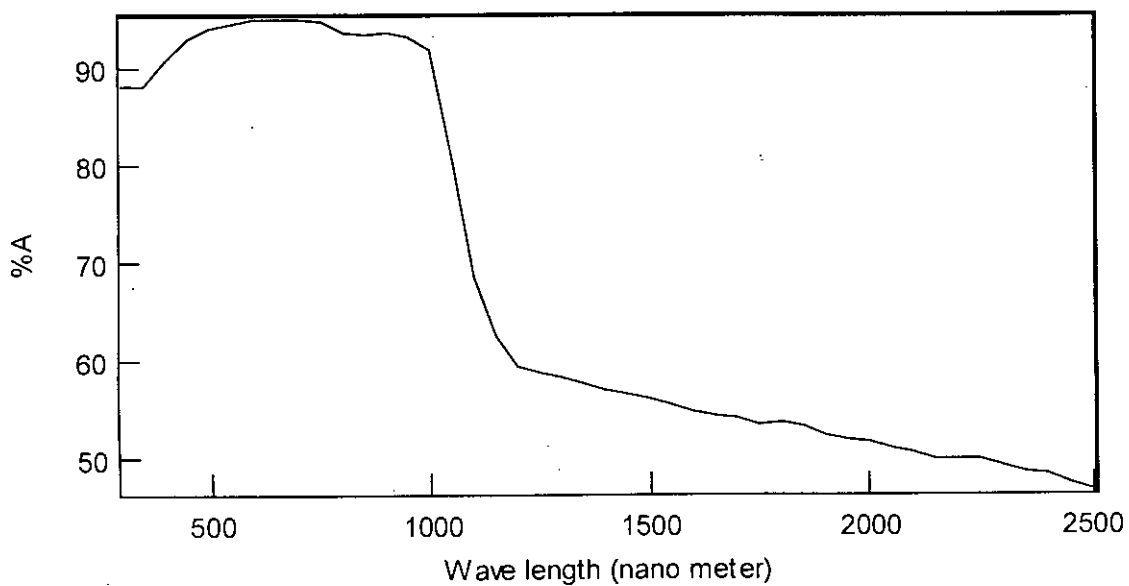
Figure: 3.65 % A vs wavelength (nanometer) for silicon with 0% camphor
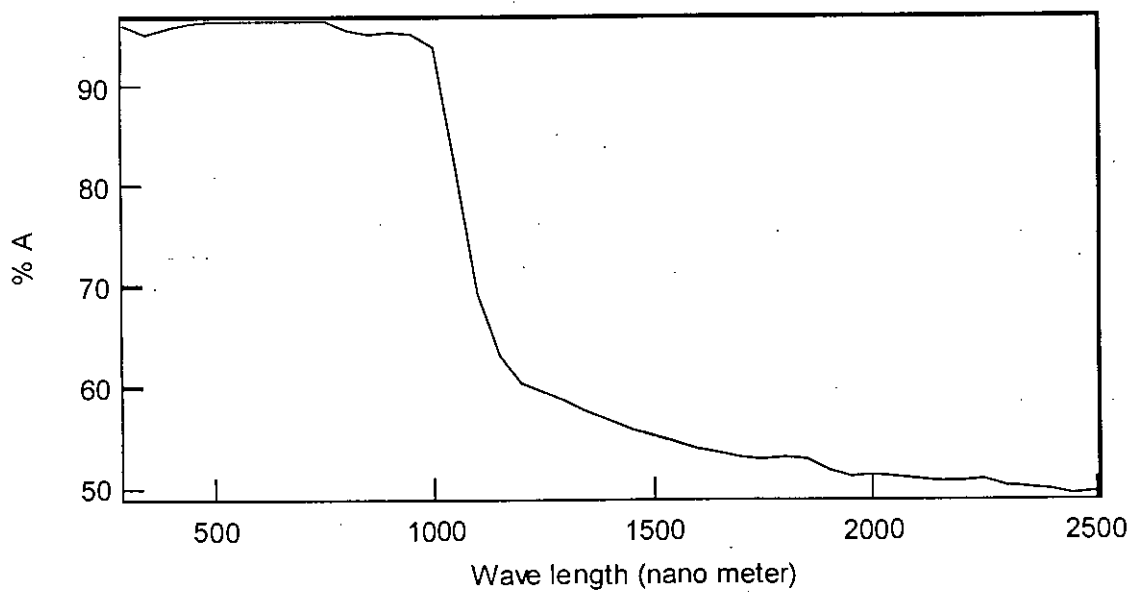
Figure: 3.66 % A vs wavelength (nanometer) for silicon with 6% camphor
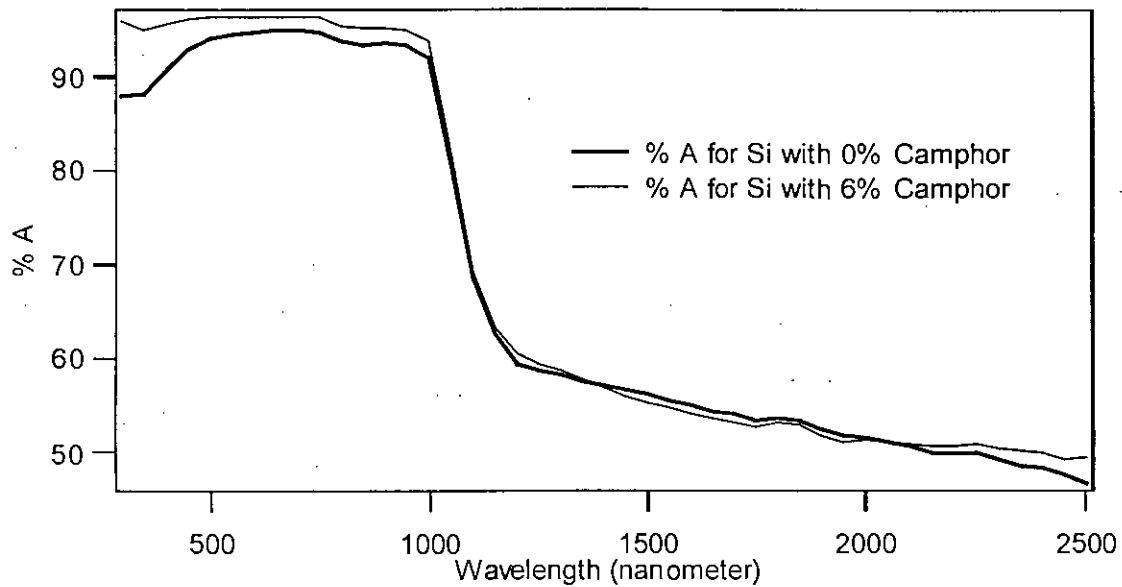
Figure: 3.67 % A vs wavelength (nanometer) for silicon with 0% and 6% camphor

From the individual curves and the comparative curves it is clear to us that the two samples have totally distinct character. % T for 0% camphor sample is relatively low than that of 6% camphor. Alternately % R for 0% camphor sample is relatively higher than that of 6% camphor so that sum of %T and % R for both cases are almost equal. Due to that their % A curves are almost coinciding. [As % A = 100 − (% T + % R)]. But in few region % A for 6% camphor is higher than that of 0% camphor. So we can conclude that optical properties of the above two samples are different. This is due to camphor incorporation.

3.3.7.2 Measurement of optical band gap for Si with 0% and 6% camphor in methanol

Now we want to measure the optical band gap of Si for o% and 6% camphor by using the above optical properties. Optical band gap depends on the optical absorption coefficient α (cm^{-1}) [41]. α can be calculated by the following equation.

$$\alpha = (1/X) \ln [(1-R)^2/T] \qquad\qquad [3.2]$$

Here, X = Thickness of the substrate

T = Photon energy transmitted through the substrate

R = Photon energy reflected from the substrate

In figure 3.68 optical absorption coefficient α (cm^{-1}) is plotted as a function of photon energy (eV)
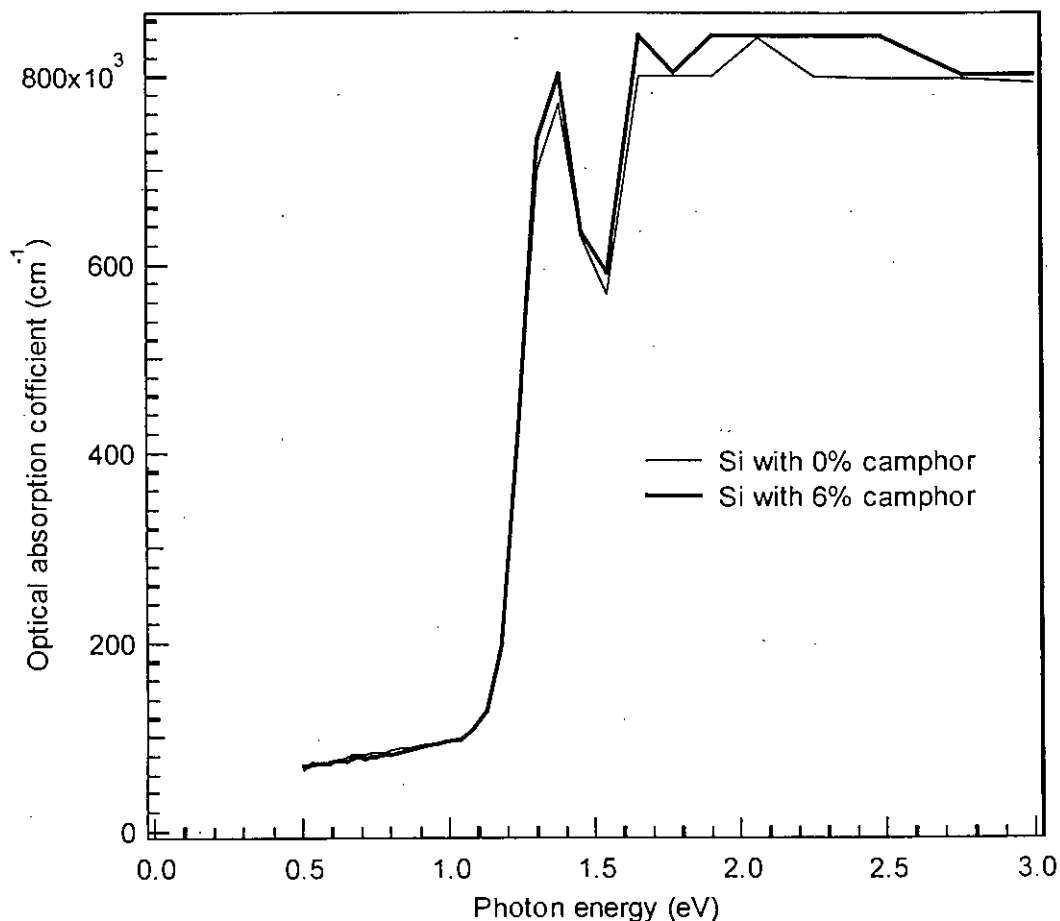
Figure: 3.68 Optical absorption coefficient α (cm⁻¹) as a function of photon energy (eV) for Si with 0% and 6% camphor

Here we observe that α drops abruptly in two region of photon energy one at around 1.2 eV and another at around 1.4 eV. So we get an indication two optical band gap here. One is perhaps for Si and another is for amorphous carbon. The two curves are coinciding in the first region and indicate the property of Si but they are different in the second straight-line region. So optical property for amorphous carbon is different for different percentage of camphor. As an indirect band gap material [41] the relation between the optical absorption coefficient (α) and the optical band gap (E_{opt}) for Si is as follows:

$$(\alpha h\nu)^{1/2} = B (E_{opt} - h\nu) \quad \dots\dots\dots\dots\dots\dots\dots\dots\dots\dots\dots\dots\dots\dots [3.3]$$

Here, h = Plank's constant

v = Frequency of photon energy

α = Optical absorption coefficient

h = Plank's constant

$E_{opt} = E_g$ = Optical band gap of the substrate

B = Density of the localized state constant

In the above equation E_{opt} = hv for α = 0. So by plotting $(\alpha h v)^{1/2}$ as a function of photon energy (hv) and extrapolating it towards x-axis we can find the optical band gap. $(\alpha h v)^{1/2}$ as a function of photon energy (hv) is plotted in figure 3.69 .
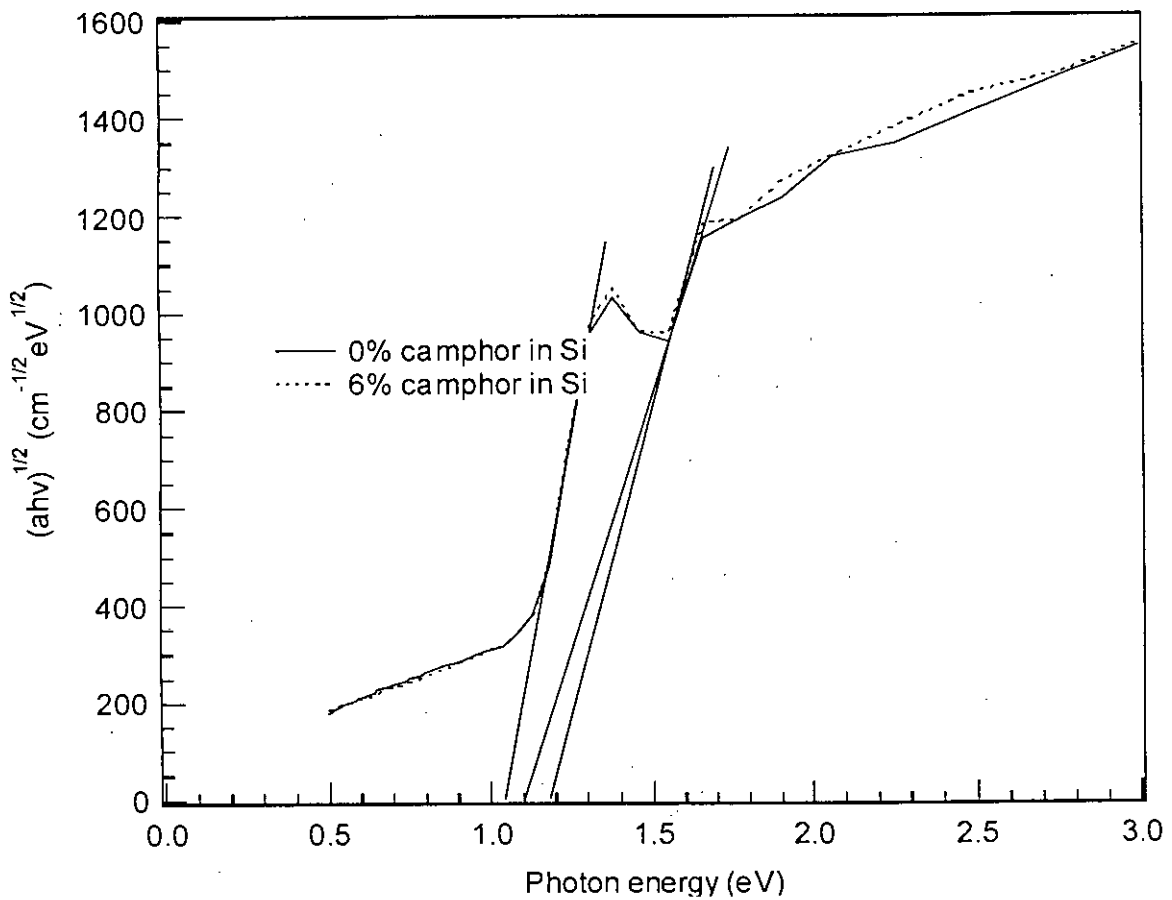
Figure: 3.69 $(\alpha h v)^{1/2}$ as a function of photon energy (eV)

As expected from the analysis of optical absorption coefficient we find here two straight-line portions of the curves thereby indicating two optical band gaps. One corresponds to Si and another corresponds to amorphous carbon bond. Like the absorption coefficient curve here also the two curves are coinciding in the first straight line region and indicate the property of Si and they are different in the second straight-line region and indicate the property of amorphous carbon. Now by extrapolating the above lines we get three-band gap indication as in the figure above. Those are optical band gap for Si is 1.05 eV, optical band gap for amorphous carbon with 0% camphor on Si is 1.1 eV and optical band gap for amorphous carbon with 6% camphor on Si is 1.2 eV. So it is possible to change the optical band gap by changing the percentage of camphor incorporation in methanol.

Now if we relate it with the ratio of sp^3/sp^2 found in FTIR the picture is as given in the table 3.22 below.

Table 3.22 Optical band gap for different condition

% Of camphor incorporation in methanol solution for Si	Ratio of sp^3/sp^2	Optical band gap (eV)
0%	0.45	1.1
6%	0.66	1.2

Chapter 4

Conclusions

4.1 Conclusions

Organic solution including methanol and different percentage of camphor (1%, 2%, 3%, 4%, 5%, 6%, 7% and 8%) in methanol has been used as electrolytes to deposit carbon thin films on Al, Cu and Si substrates. Conductivity of the electrolytes is studied by measuring the current density as a function of applied voltage. Role of camphor on electrodeposition was examined by measuring the P^H of the solution before and after deposition for different percentage of camphor.

The affinity of copper, aluminum and silicon to electro deposition is compared. The role of camphor on electro deposition is also observed. It is found that, for all the three substrates (Al, Cu and Si) the current density decreases initially with camphor from that of only methanol solution, and increases thereafter. However, there is a limit for camphor to add in methanol solution for increasing current density. We got maximum current density for Al and Cu substrate by using 2% of camphor in methanol solution. For Si maximum current density was maximum for 6% of camphor in methanol solution. Among the three substrates, silicon substrate shows

much more current density for same conditions than those of Al and Cu. With camphor incorporation in methanol the current density is varied and the deposition rate of the carbon film can be controlled.

P^H of the solution increases by increasing percentage of camphor in methanol. P^H of any solution decreases after deposition from that of before deposition. So camphor has an influence on carbon thin film deposition by electroplating through methanol solution.

The electrodeposited carbon thin films are characterized by optical microscopy, SEM micrograph, EDS analysis, FTIR spectroscopy and optical transmittance/reflectance measurement by UV-VIS-NIR techniques.

From the pictures of optical microscope and SEM micrograph, we investigate that certain films are there on all the three substrates. We got differences in film pictures for any particular substrate due to changes in camphor incorporation with methanol. So camphor has a role on film formation. EDS analysis shows that a certain percentage of carbon films are there on Al, Cu and Si. But percentage of carbon on Si substrate is much more higher than those of Al and Cu. Therefore Si has more affinity to carbon than the other two substrate. They form a compound Si_xC that accelerate carbon deposition over Si substrate.

From the FTIR spectroscopy measurement we observe that, there are certain sp^3 and sp^2 C-H stretch and existence of amorphous carbon bond on Si substrates. But Al and Cu do not show such type of property. Also we calculate the ratio of sp^3/sp^2 from FTIR curves of Si samples deposited using different percentage of camphor in methanol. We observed that for 0% camphor we got a moderate ratio of sp^3/sp^2 (0.45) then this ratio increases (0.66) for adding 6% of camphor into methanol but again it decreases (0.56) due to increase in camphor content (8%) into methanol. So ratio of sp^3/sp^2 can be controlled by camphor incorporation in methanol. It is also possible to tune the properties of the carbon film with camphor addition.

From the transmittance/reflectance measurement of Si substrate samples for different percentage of camphor in methanol (0% and 6%) using UV-VIS-NIR technique we found that the optical properties like optical transmittance, reflectance and absorption are different for different samples (due to change in camphor incorporation with methanol). And it is found that the optical band gap for Si substrate using only methanol solution is 1.1 eV then by adding 6% camphor into the solution it increases to 1.2 eV.

So the band gap of Si substrates can be varied by camphor incorporation in methanol.

By adding camphor in methanol solution we can get high in film quality than only methanol. The role of camphor as a precursor material for good quality film deposition in electroplating techniques is experimentally proved.

We believe that semiconductor carbon films with controllable characteristics may be obtained by electroplating technique.

4.2 Future Development and Suggestions for Future Work

In our laboratory work, we have used the metal (Al, Cu and Si) substrates only. In future P and N type silicon can be used to prepare C/Si heterojunction. It is needed to prepare films on glass substrate to characterize the films for proper understanding. Therefore need to find suitable way to deposit on glass.

To study the change of the electrolyte during electrolysis FTIR spectroscopy can be carried out on the electrolyte solution and original solution. Raman spectroscopy can be performed on deposited samples. If helps to know the structure and quality of deposited films.

Some arrangements can be carried out to measure the current density with respect to applied potential at constant temperature.

In our thesis un-doped carbon films are deposited. It is supposed to be P type, but no experimental evidence is carried out here. So suitable methods may be used to identify the doping type. For device applications, it is necessary to dope. Therefore it is needed to find suitable materials that can be used for P and N type doping.

References:

[1]   M. S. Dresselhaus, G. Dresselhaus and P. C. Eklund, "Science of fullerenes and carbons," *Academic Press. Inc.*, 1996.

[2]   S. M. Mominuzzaman, T. Soga, T. Jimbo, and M. Umeno, "Camphoric carbon soot: a new target for deposition of diamond-like carbon films by pulsed laser ablation," *Thin Solid Films*, vol. 376, pp. 1-4, 2000.

[3]   H. A. Yu, Y. Kaneko, S. Yoshimura and S. Otani, "Photovoltaic cell of carbonaceous film/n-type silicon," *Appl. Phys. Lett.,* vol. 68, no. 4, pp. 547-549, 1996.

[4]   M. Weiler, S. Sattel, T. Giessen, K. Jung, H. Ehrhardt, V. S. Veerasamy and J. Robertson, "Preparation and properties of highly tetrahedral hydrogenated amorphous carbon," *Physical Review B,* vol. 53, pp. 1594-1608, 1996.

[5]   Sunil Kumar, "Characteristics of bonding structures of diamond-like carbon films deposited by radio frequency," *Appl. Phys.,* vol. 58, pp. 1836-1838, 1991.

[6]   S. M. Mominuzzaman, K. M. Krishna, T. Soga, T. Jimbo and M. Umeno, "Raman Spectra of Ion Beam Sputtered Amorphous Camphoric Carbon Thin Films", *Carbon,* vol. 38, 2000, pp. 127-131.

[7]   M. Rusop, S. M. Mominuzzaman, T. Soga, T. Jimbo and M. Umeno, "Characterization of Phosphorus-Doped Amorphous Carbon and Construction of n-Carbon/p-Silicon Heterojunction Solar Cells", *Jpn. J. Appl. Phys.,* vol. 42, 2003, pp.2339-2344.

[8]   L. L. Maissel, and R. Giang, *Handbook of Thin Film Technology*, Chap. 5, p. 5, New York: McGraw-Hill, 1970.

[9]   Y. Namba, "Attempt to grow diamond phase carbon films from an organic solution," *J. Vac. Sci. Technol. A*, vol. 10, pp. 3368-3370, 1992.

[10]   T. Suzuki, Y. Marita, T. Yamazaki, S. Wada, and T. Noma, "Deposition of carbon films by electrolysis of a water-ethylene glycol solution," *J. Mater. Sci.*, vol. 30, pp. 2067-2069, 1995.

[11] Hao wang, Ming-Rong Shen, Zhao-Yuan Ning, and Chao Ye, "Deposition of diamond-like carbon films by electrolysis of methanol solution," *Appl. Phys. Lett.* vol. 69, pp. 1074-1076, 1996.

[12] Mominuzzaman, S.M., Krishna, K. M., Soga, T., Jimbo, T. and Umeno, M. "Optical Absorption and Electrical Conductivity of Amorphous Carbon Thin Films from Camphor: a Natural Source", *Jpn. J. Appl. Phys.*, vol. 38(2A), pp. 658-663, 1999.

[13] S. M. Mominuzzaman, M. Rusop, T. Soga, T. Jimbo and M. Umeno, " Nitrogen Doping in Camphoric Carbon Films and its Application to Photovoltaic Cell", 14th International Photovoltaic Science and Engineering Conference (PVSEC-14), Bangkok, Thailand, January 26 – 30, 2004.

[14] J E Field, Properties of Diamond (*Academic Press*, 1979).

[15] B. T. Kelly, *Physics of Graphite, Applied Science*, London, 1981.

[16] T. Motri and Y. Namba, "Surface Acoustic Wave Properties of Diamond-like Carbon Thin Films," *J. Vac. Sci. Technol. A1*, vol. 23, pp. 5, 1983.

[17] N. Savvides and B. Window, *J. Vac. Sci. Techonl. A3*, 2386 (1985).

[18] B. Dischler, in Amorphous Hydrogenated Carbon Films P Koidl and Oelhafen, *Proc Euro. Mat. Rcs. Soc.* 17 189 (Les Editions De Physique, Paris, 1987).

[19] D R Mckenzie, D. Muller, P. D.Swift, D. Segal, A.Saeed, P B Lukins and P J, "Microscopic structure of tetrahedral amorphous carbon", *Martin Diamond and Related Materials,* vol. 1 pp. 51, 1991.

[20] P. Koidl, C. Wild, B. Dischler, J. Wagner, and M. Ramsteiner, "Preparation and mechanical properties of composite diamond-like carbon thin films", *Mater. Sci. Forum,* vol. 1, pp. 52-53, 1989.

[21] M F Ashby, D R H Jones, *Engineering Material (Pegamon, 1980, 1980)* P 58, 78.

[22] S M Mominuzzaman, H Ebishu, T Soga, T Jimbo and M Umeno, "Phosphorus Doping and Defeat Studies of Diamond Like Carbon Films by Pulsed Laser Deposition Using Camphoric Carbon Target, *Diamond And Related Materials*, Vol. 10, pp 948-988, 2000.

[23] J C Angus, P Koidl and S Domiz in Plasma Deposited Thin Films, *Ed. J. Mort.* (Crc Ss, 1986)

[24] Y Catherine in Diamond and Diamond Like Carbon Filmed R E Clausinget Al (Plenum 1991) P 193

[25] Aisenberg and R. Chabot, "New radio frequency technique for deposition of hard carbon films", *J. Appl. Phys.* Vol. 42, pp. 2953, 1971.

[26] EG Sansalont, "TEM observations of diamond films produced by hot filement thermal CVD," *App. Phys.*, vol. 29, pp. 7, 1976.

[27] H Vora, T J Moravee, "Plasma deposition and etching of diamond-like carbon films", *J. App. Phys.* Vol. 52, pp. 6151, 1981.

[28] HR Kaufman, "Technology of ion beam sources used in sputtering," *J. Vac. Sci. Technol.*, vol. 15, pp. 272, 1978.

[29] C. B. Collins, F. Davanloo, F. R. Jandeer, T. J. Lee an C. B. Collins, *J. App. Phys.* 67 2081 (1990); *J. Matres* 5 298(1990).

[30] J Cuomo, J P Doyle, J Bruley, J C Liu, *App. Phys.* Lett. 58 466 (1991)

[31] N Savvides, *Jap. Ahys.* 55 4232 (1984).

[32] L Holland and S M Ojha, *Thin Solid Films* 58, 107(1979)

[33] C Weissmantel Etat, *Thin Solid Films* 63 315 (1979).

[34] S Matsumoto, Y Sato, M Tsutsumi and N Setakka, *J. Mater. Sci.* 17,310 (1982); S Matsumoto *J. Mater. Sci. Lett.* 4600 (1985).

[35] J Hauser, *J. Non Crrs. Solids* 23,21 9(977)

[36] B A Banks and S K Rutledge, *J. Vac. Sci. Technol.* 21,807, (1982).

[37] T J Moravec and T W Orent, *J. Vac. Sci. Technol.*, 18226 (1981).

[38] A Wangendristel and Y Wang' An Introduction to Physics and Technology of Thin Films,' *World Scientific Publishing Co.* Singapore.

[39] Md. Shafiqul Islam, "Spectral Photo Response Characteristics of N Carbon / P Silicon Heterostructure," M. Sc. Thesis Department Of Electrical and Electronic Engineering, BUET, Dhaka, Bangladesh, 2002.

[40] H.C. Barshilia, Somna Sah, B.R. Mehta, V.D. Vankar, D.K. Avasthi, Jaipal and G.K. Mehta, "Microstructural modification in diamond-like carbon thin films caused by high energy ion irradiation," *Thin Solid Films*, vol. 258, pp. 123-127, 1995.

[41]   Sharif Md. Mominuzzaman, Kalaga Murali Krishna, Tetsuo Soga, Takashi Jimbo and Masayoshi Umeno, "Optical Absorption and Electrical Conductivy of Amorphous Carbon Thin Films from Camphor: A Natural Source," *Jpn. J. Appl. Phys.*, vol. 38, pp. 658-663, 1999.

[42]   R F Curl, R E Smalley, *Scientific American* pp. 32 (Oct 1991)

[43]   Hsiac –Chu Tsai and D B Bogy, American Vacuum Society, *J. Vac. Sci. Technol A.* Vol. 5, No. 6, Nov/Dec, pp. 3287-3313, 1987

[44]   C B Collins, F Davanloo, D R Jander, T J Lee, H Park, J H You, *J. App. Phys.* 69 862 (1991);

[45]   McKenzie, DR, Muller, D. & Pailthrope, "Hard elastic carbon thin films from linking of carbon nanoparticles", *BA Phys. Rev.* vol. 67, pp. 773-776, 1991.

[46]   B Dischler, A Bubenzer and P Koidl, "Microwave plasma deposition of diamond like carbon coatings", *Solid State Common.* Vol. 48, pp. 105, 1983.